2018-12

SMALL SATELLITE SWARM THEORY FOR SPARSE APERTURE RADAR APPLICATIONS

Yungbluth, John C., III

Monterey, CA; Naval Postgraduate School

NAVAL POSTGRADUATE SCHOOL

MONTEREY, CALIFORNIA

THESIS

SMALL SATELLITE SWARM THEORY FOR SPARSE APERTURE RADAR APPLICATIONS

by

John C. Yungbluth III

December 2018

Thesis Advisor: James H. Newman
Second Reader: Giovanni Minelli

THIS PAGE INTENTIONALLY LEFT BLANK

REPORT DOCUMENTATION PAGE			*Form Approved OMB No. 0704-0188*

1. AGENCY USE ONLY *(Leave blank)*	**2. REPORT DATE** December 2018	**3. REPORT TYPE AND DATES COVERED** Master's thesis

4. TITLE AND SUBTITLE SMALL SATELLITE SWARM THEORY FOR SPARSE APERTURE RADAR APPLICATIONS	**5. FUNDING NUMBERS**
6. AUTHOR(S) John C. Yungbluth III	
7. PERFORMING ORGANIZATION NAME(S) AND ADDRESS(ES) Naval Postgraduate School Monterey, CA 93943-5000	**8. PERFORMING ORGANIZATION REPORT NUMBER**
9. SPONSORING / MONITORING AGENCY NAME(S) AND ADDRESS(ES) N/A	**10. SPONSORING / MONITORING AGENCY REPORT NUMBER**

11. SUPPLEMENTARY NOTES The views expressed in this thesis are those of the author and do not reflect the official policy or position of the Department of Defense or the U.S. Government.

12a. DISTRIBUTION / AVAILABILITY STATEMENT Approved for public release. Distribution is unlimited.	**12b. DISTRIBUTION CODE** A

13. ABSTRACT (maximum 200 words)

In the next few years, the Space Systems Academic Group (SSAG) and the Small Satellite Laboratory at the Naval Postgraduate School (NPS) may begin work on a small satellite swarm constellation. This thesis introduces flight operations concepts for small satellite formations conducting sparse aperture radar missions to inform decision makers at NPS of possible flight operations options. An orbital modeling program called Systems Tool Kit was used to simulate combinations of flight patterns and orbits, including a pendulum and a helix inline hybrid model, and a cartwheel hybrid model. The MATLAB software package was used to plot the simulated orbits, calculating the flight formation stability, and for calculating the relative effects of sensor separation on the system resolution. Findings include a stable dispersion pattern for the satellites to conduct their mission and an ability to maintain safe, collision-free flight operations.

14. SUBJECT TERMS Satellite Swarm Theory	**15. NUMBER OF PAGES** 121
	16. PRICE CODE

17. SECURITY CLASSIFICATION OF REPORT	**18. SECURITY CLASSIFICATION OF THIS PAGE**	**19. SECURITY CLASSIFICATION OF ABSTRACT**	**20. LIMITATION OF ABSTRACT**
Unclassified	Unclassified	Unclassified	UU

NSN 7540-01-280-5500 Standard Form 298 (Rev. 2-89) Prescribed by ANSI Std. 239-18

THIS PAGE INTENTIONALLY LEFT BLANK

Approved for public release. Distribution is unlimited.

SMALL SATELLITE SWARM THEORY
FOR SPARSE APERTURE RADAR APPLICATIONS

John C. Yungbluth III
Major, United States Army
B, Xavier University, 2002

Submitted in partial fulfillment of the
requirements for the degree of

MASTER OF SCIENCE IN SPACE SYSTEMS OPERATIONS

from the

NAVAL POSTGRADUATE SCHOOL
December 2018

Approved by: James H. Newman
Advisor

Giovanni Minelli
Second Reader

James H. Newman
Chair, Department of Space Systems Academic Group

THIS PAGE INTENTIONALLY LEFT BLANK

ABSTRACT

In the next few years, the Space Systems Academic Group (SSAG) and the Small Satellite Laboratory at the Naval Postgraduate School (NPS) may begin work on a small satellite swarm constellation. This thesis introduces flight operations concepts for small satellite formations conducting sparse aperture radar missions to inform decision makers at NPS of possible flight operations options. An orbital modeling program called Systems Tool Kit was used to simulate combinations of flight patterns and orbits, including a pendulum and a helix inline hybrid model, and a cartwheel hybrid model. The MATLAB software package was used to plot the simulated orbits, calculating the flight formation stability, and for calculating the relative effects of sensor separation on the system resolution. Findings include a stable dispersion pattern for the satellites to conduct their mission and an ability to maintain safe, collision-free flight operations.

THIS PAGE INTENTIONALLY LEFT BLANK

TABLE OF CONTENTS

LIST OF FIGURES

LIST OF ACRONYMS AND ABBREVIATIONS

2D	two dimensional
3D	three dimensional
AGI	Analytical Graphics Incorporated
COE	Classical Orbital Elements
COF	Center of Formation
CONOP	concept of operation
DEM	digital elevation modeling
ECI	Earth-centered inertial
EO	electro-optical
GEO	geostationary orbit
GPS	global positioning satellites
IR	infrared
JPL	Jet Propulsion Lab
ISS	International Space Station
LEO	low Earth orbit
L/F	Lead/Follow
MEO	medium Earth orbit
MIT	Massachusetts Institute of Technology
MSI	multi spectral images
NASA	National Aeronautics and Space Administration
NPS	Naval Postgraduate School
Pan	panchromatic
PPI	plan-position indicator
RAAN	right ascension of the ascending node
RF	radio frequency
SAA	South Atlantic Anomaly
SAR	synthetic aperture radar
SLR	side looking radar
SNR	signal-to-noise ratio
SSAG	Space Systems Academic Group

STK	Systems Tool Kit
TT&C	telemetry, tracking, and command

ACKNOWLEDGMENTS

First, I would like to thank Dr. Jim Newman for his guidance, support, and help throughout the thesis process. I would also like to thank Mr. Giovanni Minelli for countless hours of assistance and patience while working with coding in MATLAB. Next, I want to thank Professor RC Olsen for his discussions and guidance regarding radar imaging. I would also like to thank the Space Systems Academic Group staff, faculty, and students for the education and experiences that allowed me to complete this thesis. Finally, I would like to thank the Graduate Writing Center and Thesis Processing Office staff here at NPS for assisting me in transferring my research into a comprehensive thesis paper.

THIS PAGE INTENTIONALLY LEFT BLANK

I. INTRODUCTION

Currently, synthetic aperture radar (SAR) is a well-developed and flight proven technology while small satellite swarm technology is purely theoretical. In the next few years, the Space Systems Academic Group (SSAG) and the Small Satellite Laboratory at the Naval Postgraduate School (NPS) proposes to begin building a small satellite swarm constellation architecture. To support that effort, this thesis demonstrates that there is a manageable flight formation for a small satellite swarm. Using a program called Systems Tool Kit (STK), this research demonstrates different combinations of flight patterns and orbits, as well as optimizing the ideal SAR mission that will help inform the NPS "way ahead" for its small satellite swarm constellation.

A. WHY SAR, SWARMS, AND SMALL SATELLITES

SAR is an electro-optical (EO) imaging capability that operates in the radio frequency (RF) spectrum without the need for visible light. As a result, SAR imaging satellites are not restricted to operate in an orbit that keeps targets in daylight at all times, greatly increasing the options for the types of orbits available for analysis, including altitude and inclination. SAR is neither affected by light nor cloud cover. The phased array used to collect radar data to be processed into an image is a much simpler, smaller, and lighter design than the cameras that produce panchromatic (Pan), infrared (IR), or multi-spectral images (MSI) at comparative resolutions [1].

Small satellites, as discussed in Chapter II, were chosen for this research because they currently appear to be very important for future space operations. As technology allows us to miniaturize, we are able to build much smaller and more capable satellites than even a few years ago. Since a SAR phased array payload was chosen for this thesis, a smaller bus (support structure) is required. Companies that build large satellites rarely reach the maximum size or weight limits of the payload compartment on top of the launch vehicles they use. In order to save money, the companies launching primary payloads sometimes sell the excess space to smaller secondary payloads.

Launching as a secondary payload is a much more economical way to launch a small satellite into space, rather than paying for the entire launch as a primary payload. As a result, developing launch strategies catering to small satellite payloads has become an emerging and booming market for companies like Rocket Lab and Virgin Orbit [2]. Given that launch opportunities may be plentiful; it is reasonable to look at creative uses of multiple small satellites. Given the success of synthetic aperture radar using larger satellites, interest is being generated to see whether swarms of small satellites can perform the functions of larger satellites.

Swarm technology is a relatively new concept for conducting small satellite operations and, to date, is also completely theoretical. The idea, and the core of this research, is to fly multiple small satellites in formation to conduct a similar mission a much larger satellite currently does. In simple terms, the larger a phased array is, the better the real aperture resolution of our radar image will be. If the small satellites are close enough together, it should be possible for them to act as a much larger real aperture phased array called sparse aperture radar. This thesis explores the sparse aperture SAR concept as a specific example. If two or more swarms are flown at different inclinations, as explained in Chapter II, and image the same target at the same time, the target can be viewed as a 3D image. Figure 1 is an example of a bi-static radar image.

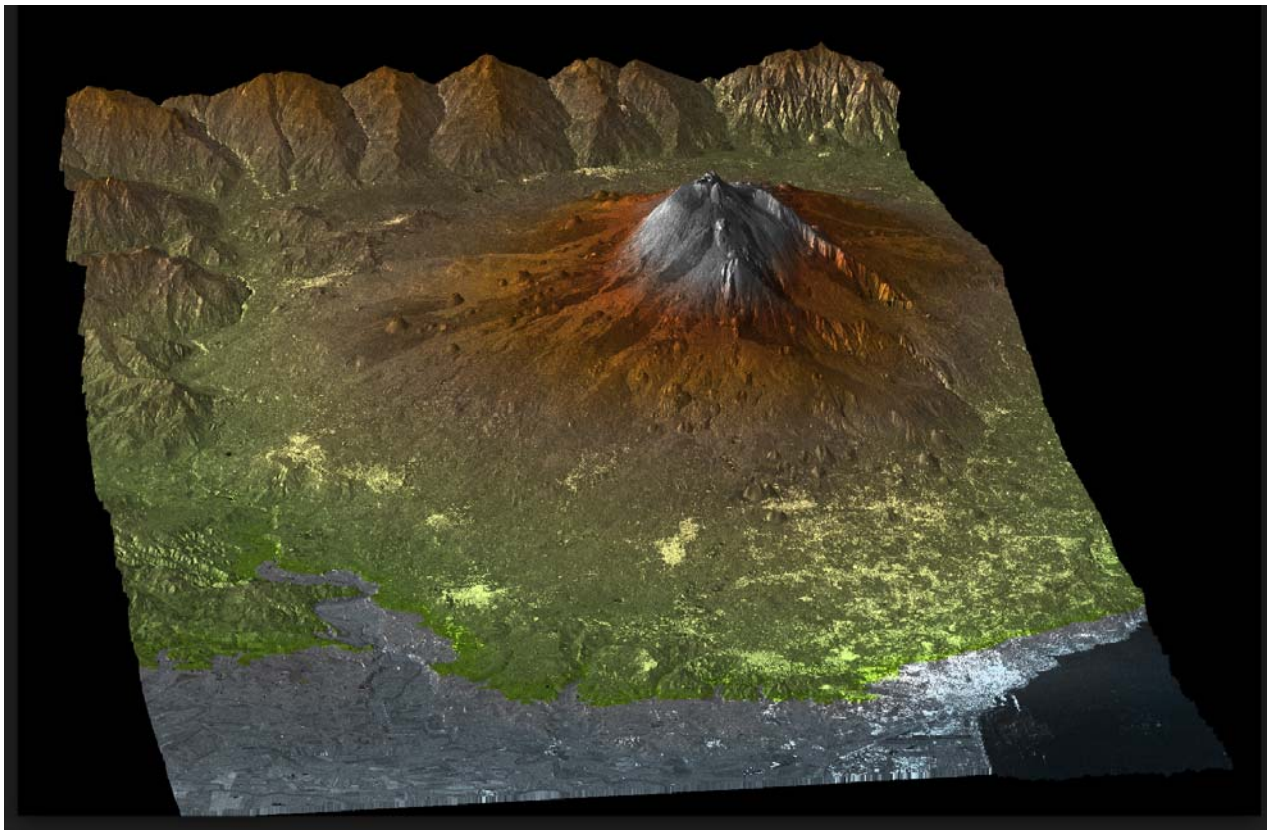

Figure 1. First TereSAR-X and TanDEM-X bi-static imagery acquired. Source: [3].

B. FRAMING THE PROBLEM

This research will highlight the extremely complex issues involved in flying multiple satellites that range from the size of a coffee thermos to a large copy machine traveling at approximately 7.8 km/s and only a few feet apart. It is very important that these flight patterns be precise. Failure to avoid collisions could damage other satellites in the formation and cause hazardous space debris as discussed in Chapter II, Section J.

Next, we must identify a mission, or payload, to complement the small satellites swarm capabilities. A SAR payload will be used in order to demonstrate flight operations. As with any camera or imaging device, the closer to Earth that the swarm flies, the better the resolution and the sooner the satellites will deorbit once their mission has ended, reducing the amount of inoperable objects in space. The higher the orbit, the longer the swarms' life expectancy will be but the longer it will take to deorbit once complete, as

discussed in more detail in Chapter II. Several other orbital conditions include; at what altitude, how often, and at what times of the day we want to effectively image specific targets. There is a detailed explanation of some required tradeoffs between these considerations made in Chapter III of this thesis.

C. RESEARCH QUESTIONS

The primary research question is: "What is the most effective and efficient formation for a small satellite swarm to support a sparse aperture radar mission with regards to collision avoidance for future NPS satellite operations?"

Secondary questions explored were as follows:

- What is an acceptable balance between effectiveness and efficiency?
- How long can a small satellite swarm remain stable in each chosen formation before major station keeping operations are required to avoid a collision or loss of the swarm's required relative positions?
- What are the assumptions required in order to model the simulations in STK?
- What are the assumptions required in order to analyze resolution estimates in MATLAB?
- What specific areas of engineering and/or operations are relevant but outside of the scope for this thesis?
- What are some additional research opportunities for future study?

As research progressed, additional questions were added. "What is the distance between each satellite at different intervals throughout an average swarm orbit?" "How does the distance between each satellite affect an imaging mission?"

D. HYPOTHESIS

The hypothesis is that smaller and less complex small satellite swarm formations will prove to be safer due to a sturdy flight formation which will provide the best possible stability. The initial proof of concept launches for small satellite swarms will have to focus

on conducting sustainable proximity operations at very close ranges. As a result, the pioneers in this field will have to use very simple formations with a small number of spacecraft flying in uncomplicated formations. However, as the small satellite community continues to improve in technology and techniques, more intricate formations will be achieved. After the risks of failure have been mitigated, more intricate flight patterns are expected to become standard for satellites operating in formations.

THIS PAGE INTENTIONALLY LEFT BLANK

II. TECHNICAL OVERVIEW AND LITERATURE REVIEW

A. BACKGROUND

Before developing orbital strategies for small satellites, it is important to understand the underlying principles. This chapter explains radar technical basics and why radar is the sensor of choice for flight. It also defines small satellites, provides several examples of swarm theories, and explains the orbital mechanics of the flight formation as well as the implications of failure if the wrong choices are made. This chapter also introduces the subject matter experts and discussions of previous contributors.

B. RADAR OVERVIEW

Radar is an active sensor that provides the energy required to be collected, called microwaves and Paul [1] emphasizes that infrared and optical imaging sensors are passive systems that collect radiated or reflected energy. Microwaves exist at approximately the 1-1000 GHz range on the electromagnetic spectrum, as shown in Figure 2 [1].

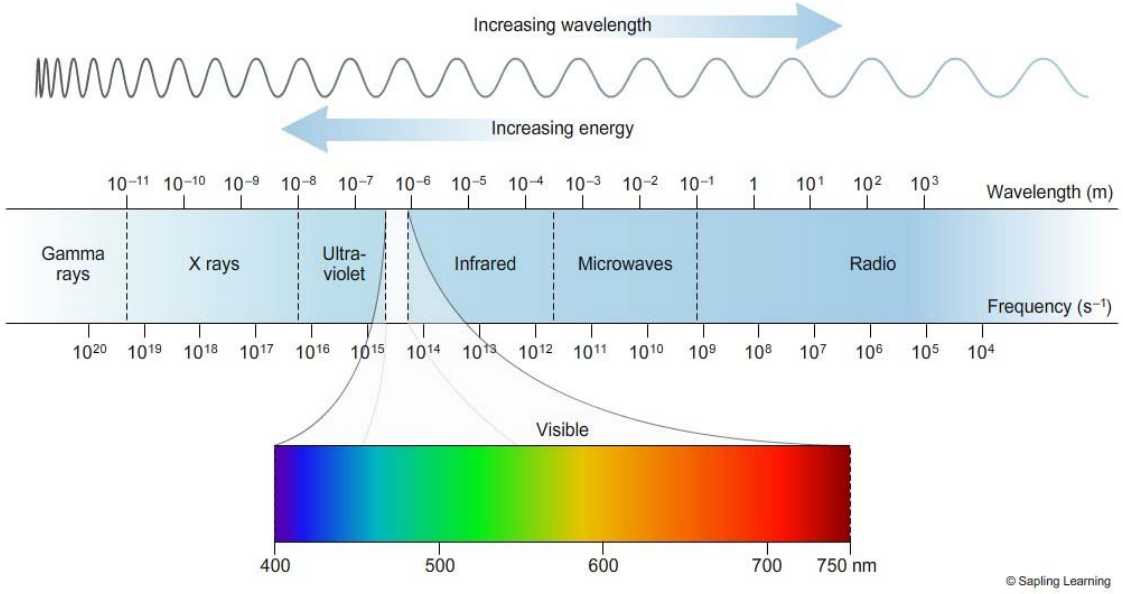

Figure 2. The electromagnetic spectrum. Source: [4].

Paul [1] establishes two primary types of radar: plan-position indicator and real aperture. The plan-position indicator (PPI) is a circular scanner used to monitor naval and air traffic, while real aperture radar is used to develop the most common types of imagery products. There are two types of imaging radar: side looking radar (SLR), which is a type of real aperture radar and uses a long, straight antenna and emits microwaves perpendicular to the flight path of the ground, and synthetic aperture radar (SAR), which uses the Doppler spread of the returning microwaves to synthesize a much larger aperture. The Doppler effect occurs when the receiver is moving with respect to the emitted microwaves as shown in Figure 3, causing a shift in frequencies like the change in pitch of a car honking its horn as it comes towards an observer and again as it moves away.

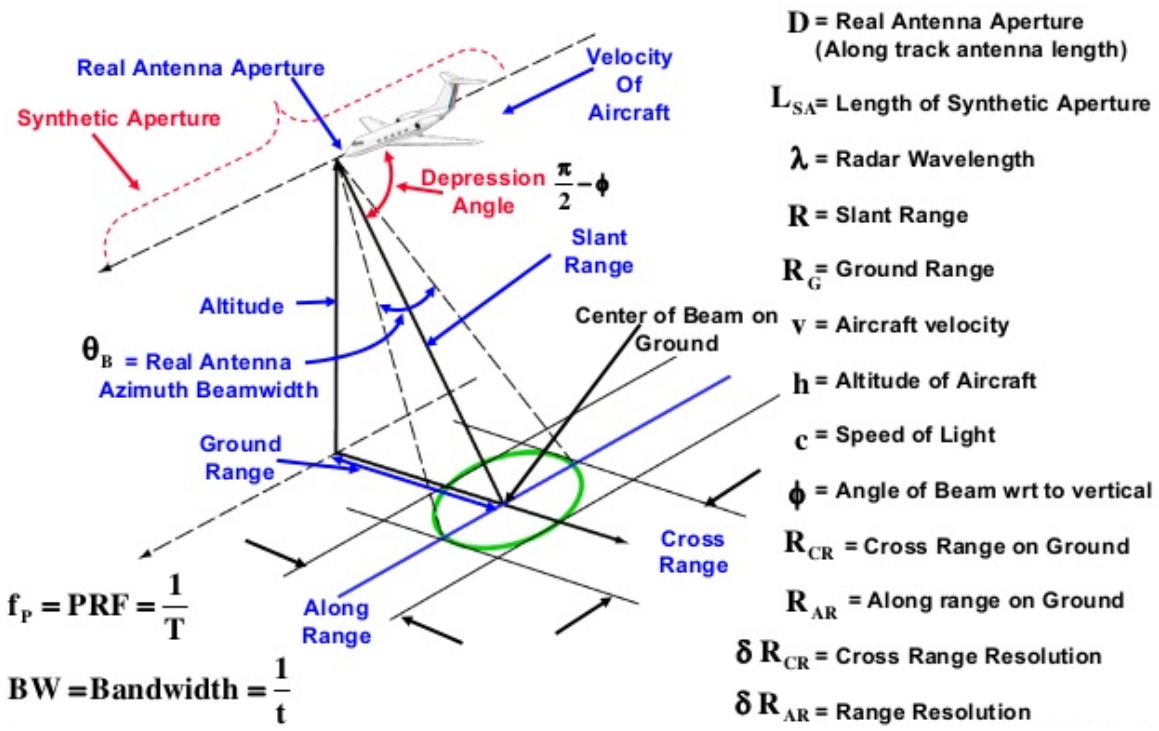

Figure 3. SAR geometry for calculating Doppler frequency shift for a point target. Source: [5].

Radar has two primary types of resolution: azimuthal and range. Azimuth resolution is determined by the size of the aperture; a larger aperture reduces the angular spreading of the microwaves, allowing a longer antenna to produce a tighter beam. The

length of the radiated pulse determines range resolution. If a pulse hits two objects on the ground, with one in front of the other, and the distances between them are half or more of the pulse length, then radar can resolve them [1].

The three forms of radar are mono-static, bi-static, and multi-static. A mono-static radar is a single platform that both transmits and receives its own microwave signals as described by Gerhard Krieger's "Advanced bi-static and multi-static SAR concepts and applications" briefing to the European Conference on Synthetic Aperture Radar in 2006 [6]. A bi-static radar system has spatial separation between the receiver and the transmitter and is the preferred system type because it provides a 2D image rather than a 1D. A multi-static radar system has at least one transmitter and multiple separated receiver platforms. Multi-static SAR receivers increase resolution using super-resolution techniques focusing on range and azimuth, 3D imaging, high quality and cost efficient digital elevation modeling (DEM), and high quality oceanography models [6].

SAR missions are usually conducted in one of three modes: scan, strip, and spot. The latter two are shown in Figure 4. Pang, Kumar, Goh, and Le [7] detail how scan mode currently requires too much energy to be considered for small satellite operations. Strip mode is when the antenna points in a fixed direction and images in unconnected swaths. In spot mode, the antenna is steered to stare at a single target, increasing the synthetic aperture as the sensor passes by the target, which increases the resolution of the image [8].

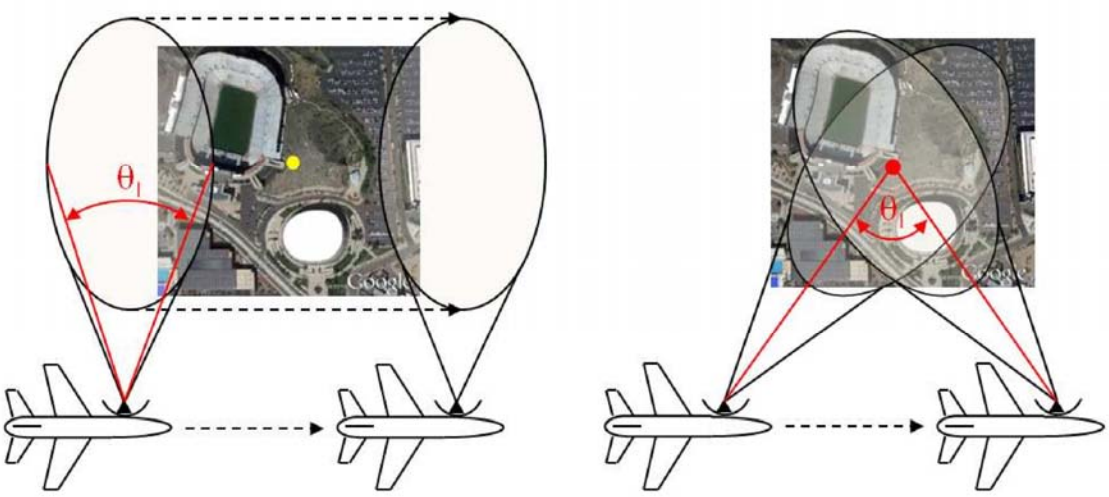

Figure 4. SAR strip mode and spot mode examples. Source: [8].

Sparse aperture radar can also be used to improve resolution. Sean Sundey summarizes that the "basic concept of sparse aperture is to replace the single large monolithic mirror with smaller collectors" [9]. In the case of radar, the mirror is replaced with an array. In his PhD dissertation, Nicholas Werth [8] notes that his "simulations … demonstrate that, when the image content is suitably sparse and the signal-to-noise ratio (SNR) is not too low, sparse decomposition algorithms are able to identify the location of 2D line spectral components accurately with high probability". Chung, Soon-Jo, and Hadaegh's "Swarms of femtosats for synthetic aperture applications" note that Rayleigh's criterion, $\Theta_r = 1.22\ \lambda / D$, gives the angular resolution (Θ_r) where D is the diameter of the aperture and λ is the wavelength [10]. Multiple receivers collect data within a communications frequency and then compile the individually collected information at a central location to correlate the data like pieces of a puzzle. Through one example of algorithms detailed by Krieger [6] and Miller, Dierking, and Duncan [11], the data is reconstructed to resemble a radar image from a more conventional single array source.

C. SMALL SATELLITES

Satellites come in all shapes and sizes, from the International Space Station (ISS) to satellites that can be held in one hand. This thesis refers to the spacecraft in our modelling as small satellites, commonly referred to as SmallSats. According to the National

Aeronautics and Space Administration (NASA) there are five classes of small satellites, designated by weight: minisatellites are 100-180 kilograms, microsatellites are 10-100 kilograms, nanosatellites are 1-10 kilograms, picosatellites are 0.01-1 kilograms, and femtosatellites are 0.001-0.01 kilograms [12]. The most popular type of satellite in recent years is a version of the nanosatellite called CubeSats. They are measured in multiples of 10x10x10 centimeters, known as a "unit" or U. CubeSats range in size from 1U to 12U, as shown in Figure 5 [9]. Unlike most CubeSat designs, however, satellites conducting coordinated flight operations require propulsion to achieve and maintain formation. As payload design and configuration extends beyond the scope of this thesis, spacecraft are generically referred to as small satellites in order to allow for the most latitude for future work.

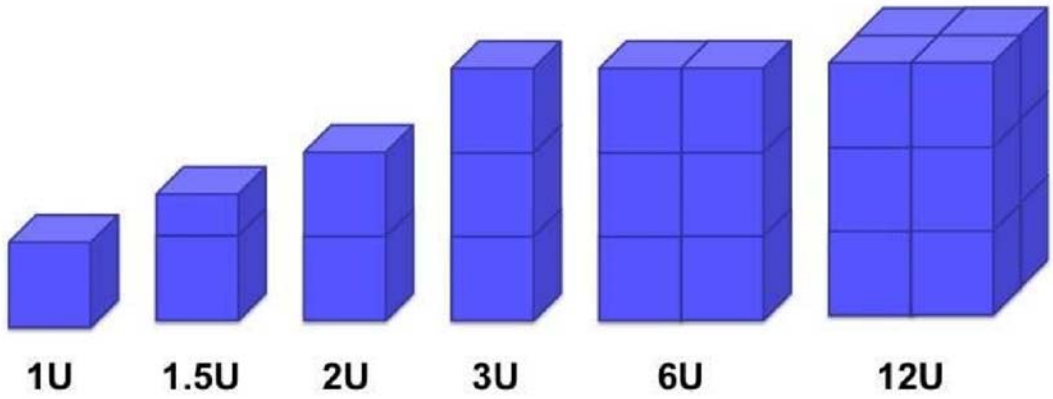

Figure 5. Typical CubeSat configurations. Source: [9].

D. SWARM THEORY

Sandau, Brieß, and D'Errico [13] bring to light the limitations and restrictions of small satellite missions compared to the more traditional, larger satellites. Small spacecraft have a limited capacity for high-data and high-power instruments; stability and size limitations prohibit large transmitters; and the limited power and size of a small satellite reduces the options for multifunctional instrumentation [13].

However, swarm technology may allow for a very interesting paradigm shift from the use of a single large, expensive, and multi-functional spacecraft to flights of smaller, much less expensive, and individually tasked spacecraft. Swarms permit simpler satellite designs that require less time to develop and launch. Modular designs can also be upgraded as the individual small satellites begin to reach the end of their lifespan and the swarm is repopulated.

E. SPARSE APERTURE RADAR USING A SWARM

Sparse aperture radar is interesting because it combines the benefits of SAR, multi-static radar and swarm theory. First, the Doppler Effect from SAR negates the need for a large array to be mounted on a satellite. Next, multi-static radar creates a 2D image by using the same concept as human depth perception. Finally, by using a swarm the differing angles of range and azimuth sampling with multiple receivers helps reduce some image processing errors and acts as a larger disaggregated receiver. Sparse aperture radar uses one wavelength (microwaves) to produce a pixilated mapping of heights and distances based on timing of the return signal. On the other hand, optical imaging cameras detect multiple wavelengths and require large numbers of pixels to produce images. As a result, optical imaging cameras are large and heavy. Unlike radar, optical imaging cameras cannot yet operate in a disaggregated manner.

F. ORBITAL MECHANICS OVERVIEW

Satellites today use many types of orbits. The three most relevant orbits for a possible swarm include geostationary orbit (GEO), medium Earth orbit (MEO), and low Earth orbit (LEO). The orbit chosen for this thesis is a low Earth orbit (LEO) which can be accessed more easily and cheaply.

A geostationary (GEO) satellite, as shown in Figure 6, orbits above the Earth at an altitude of approximately 35,800 kilometers, has no inclination and remains above the equator, and has an orbital period of 24 hours [14]. Inclination represents the tilt of the orbital plane with respect to the equator. Because the orbital period is the same as the Earth's rotation, these satellites are synchronized to create the appearance of hovering over the same place on the Earth. The best example of a GEO satellite is a telecommunications

satellite. A large and expensive rocket with a large amount of fuel is required to get a satellite to GEO. In addition, from such distance, radar imagery resolution is extremely poor.

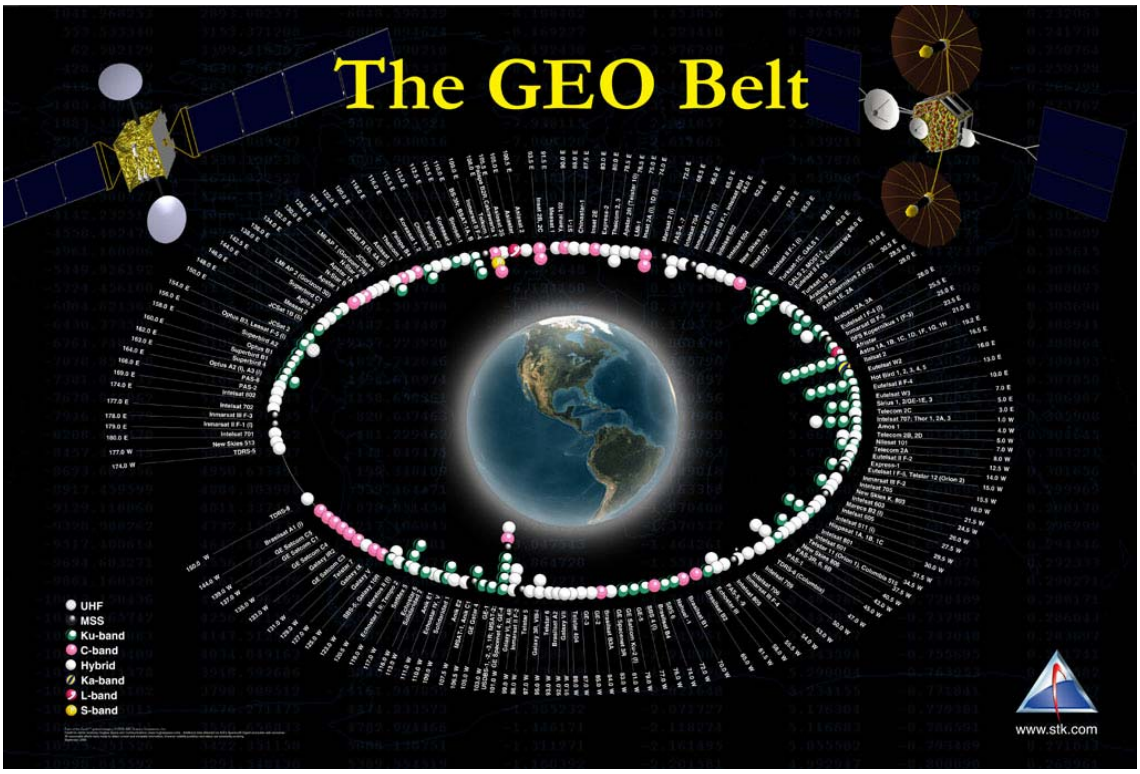

Figure 6. Geostationary Orbit. Source: [15].

Medium Earth orbit (MEO), shown in Figure 7, refers to the space between GEO and LEO. A MEO satellite, like the global positioning satellites (GPS), most commonly orbits above the Earth at about 20,200 kilometers, is inclined at 55 degrees, and has an orbital period of 12 hours [14]. MEO satellites require nearly the same amount of fuel and launch capability as GEO to attain orbit. As with GEO, at such distance, radar imagery resolution is very poor.

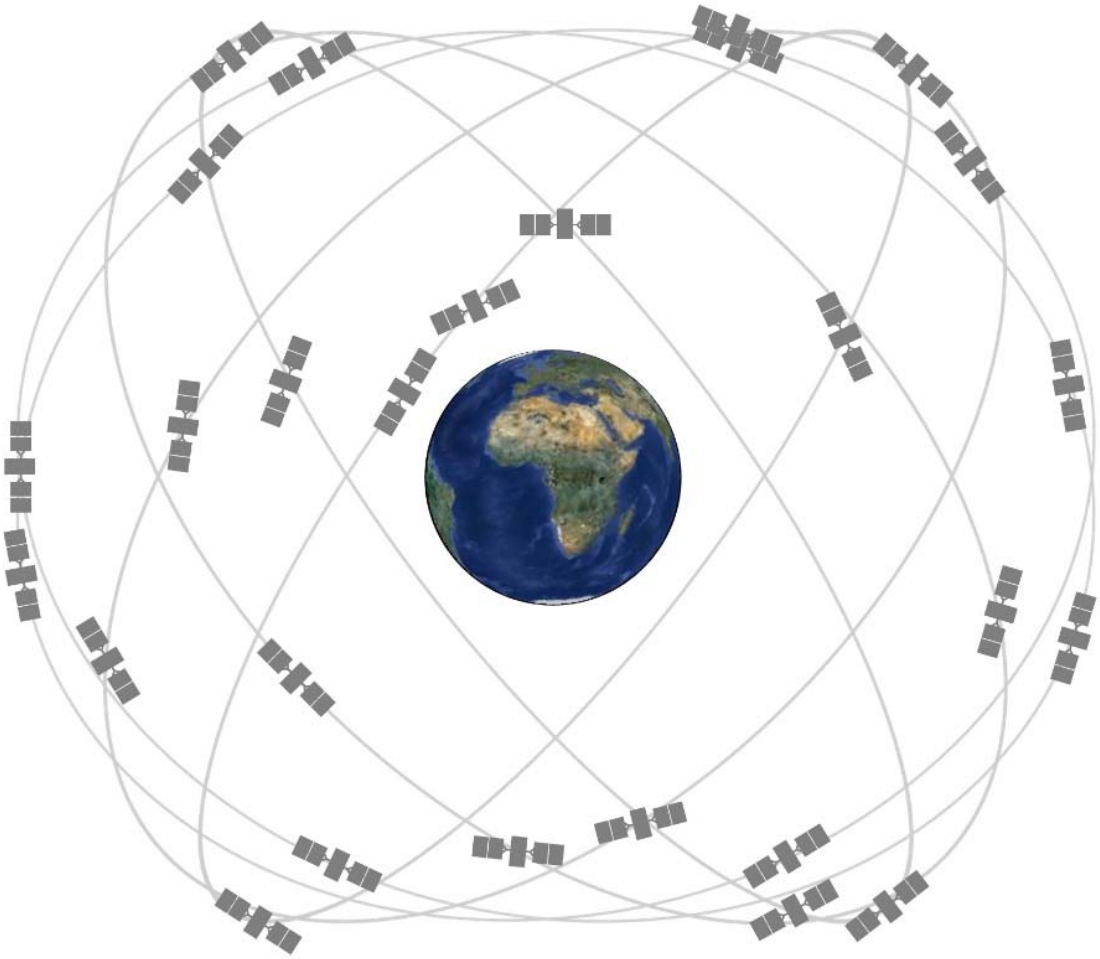

Figure 7. GPS Medium Earth Orbit. Source: [16].

Low Earth orbit (LEO) generally identifies an altitude between 200 km and 900 km that can have any inclination, shown in Figure 8. The orbital period of LEO satellites is about 90 minutes [14]. A good example of a LEO imagery satellite is the Worldview satellite. Several radar satellites operate in this orbit as well, like the German TerraSAR-X satellite. LEO orbits are the closest to Earth, cost the least amount of money to insert a satellite into and provide the best radar resolution.

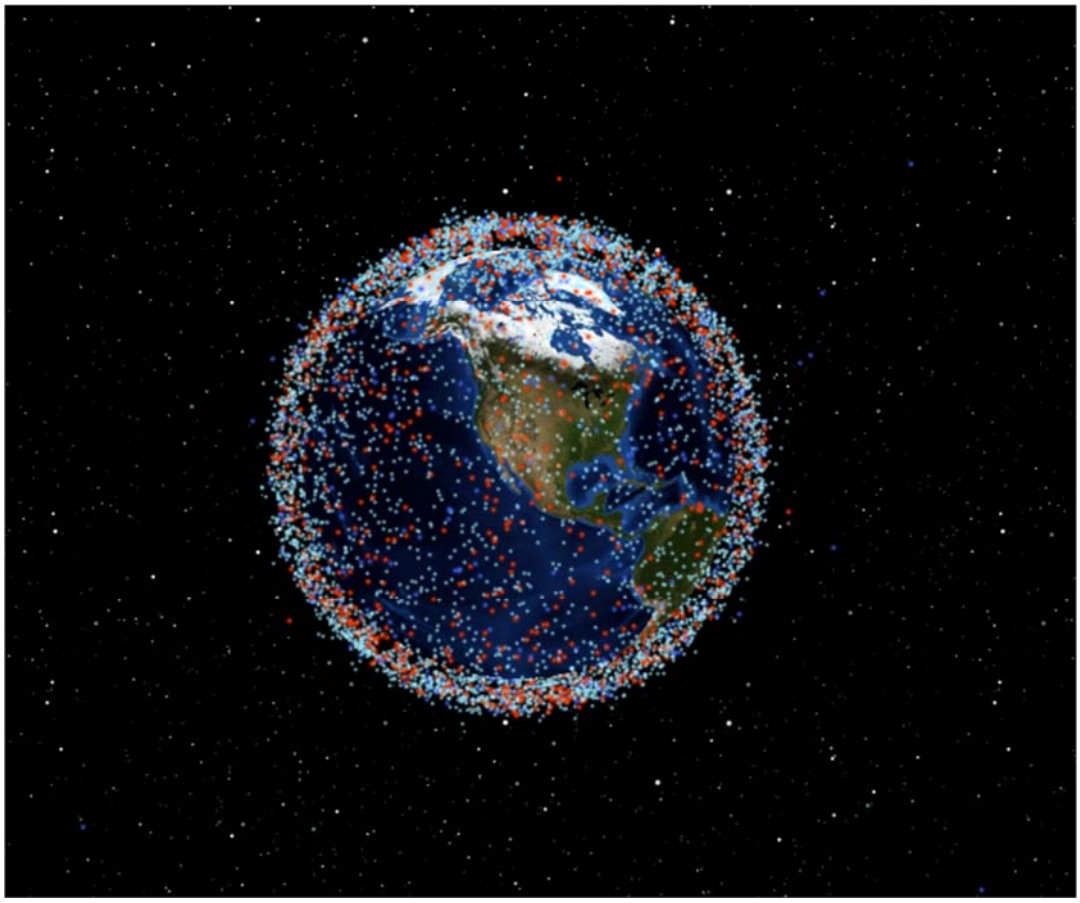

Figure 8. Low Earth Orbit. Source: [17].

Each type of orbit provides unique challenges. For LEO, the consideration that the Earth is not a perfect sphere (J2 perturbation) is important. The Earth is oblate, or fatter around the equator than at the poles, which results in gravitational effects on satellites in LEO. Furthermore, because of the lower altitude of a LEO orbit, the atmosphere causes drag for LEO satellites, traveling nearly 30,000 kph. This effect is both positive and negative. It is good because the spacecraft, at lower altitudes, will deorbit over time without requiring the use of fuel, allowing more space on the satellite to be used for its primary mission. However, to keep a satellite in its intended orbit for longer than a matter of months, it must carry fuel to occasionally boost itself from a decaying orbit. Also, at different altitudes, there are radiation particle considerations at the poles, along the Van Allen Radiation Belts, in the South Atlantic Anomaly (SAA) over Brazil, and during solar events like solar storms. Lastly, the least significant perturbation is the gravitational pull

on a satellite from the Earth's moon, the sun, and all other celestial bodies with a large mass.

The methods used in modeling involve altering the basic orbital elements to achieve a desired effect. Classical Orbital Elements (COEs) are parameters used to describe a specific orbit of a satellite orbiting the earth according to Kepler's laws of physics. An object's three-dimensional position and velocity, a total of six numbers or elements, correspond to the COEs: the semi-major axis, eccentricity, inclination, right ascension of the ascending node (RAAN), argument of perigee, and true anomaly [18].

The semi-major axis is one half the distance across the long axis of an ellipse as shown in Figure 9 [14]. Eccentricity defines an orbit's shape as shown in Figure 10 [14].

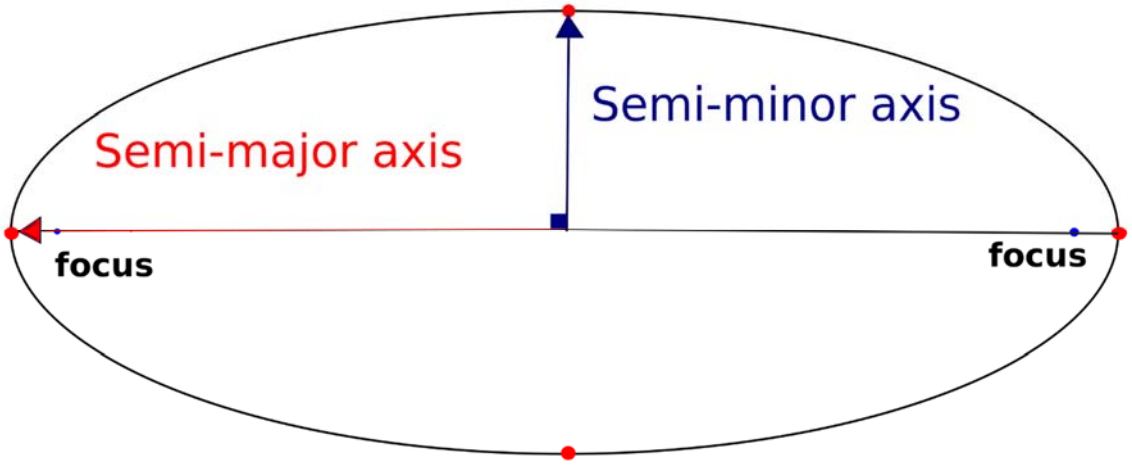

Figure 9. Semi-major Axis. Source: [19].

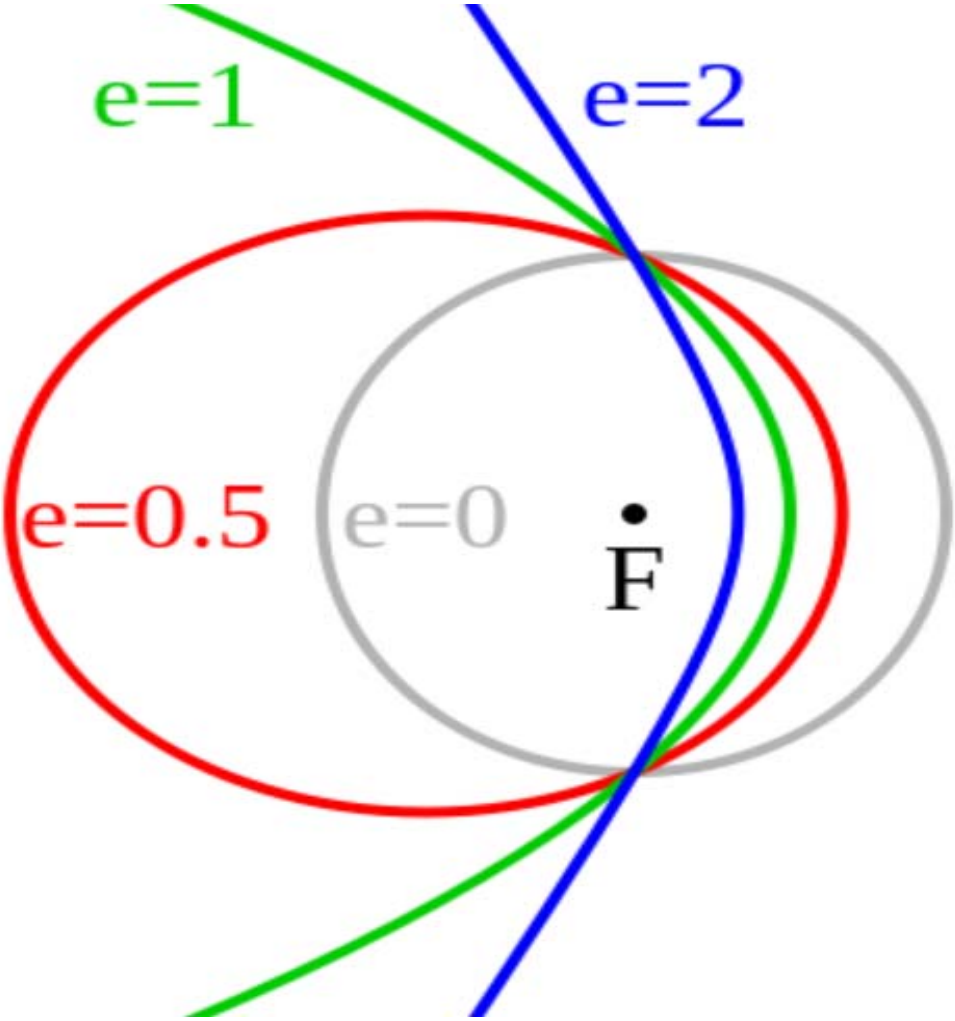

Figure 10. Eccentricity. Source: [20].

An industry standard textbook, *Understanding Space: An Introduction to Astronautics* [14], explains that inclination describes the tilt of the orbital plane with regard to the equator. The longitude of the ascending node is measured by the RAAN. The RAAN angle describes the swivel angle of the orbital plane with regard to the direction of travel. The swivel is the angle over the equator between the direction of travel and the point where the plane crosses over the equator from south to north, also known as the ascending node, measured moving eastward. Argument of periapsis, or argument of perigee, is the angle that explains orbital orientation within its orbital plane. This is the angle between perigee and the ascending node, measured in the direction of the satellite's (celestial body below)

motion, perigee being the closest approach to Earth and apogee being the furthest. True anomaly identifies the position of an object in an orbit and the angle between the object's position vector and perigee measured in the direction of travel as explained in Figure 11. True anomaly is the only COE of the six that changes with the time in a perfect, two-body system [14]. Of course, because of the earth's oblateness and other influences, the other COEs also change with time for real earth-satellite systems.

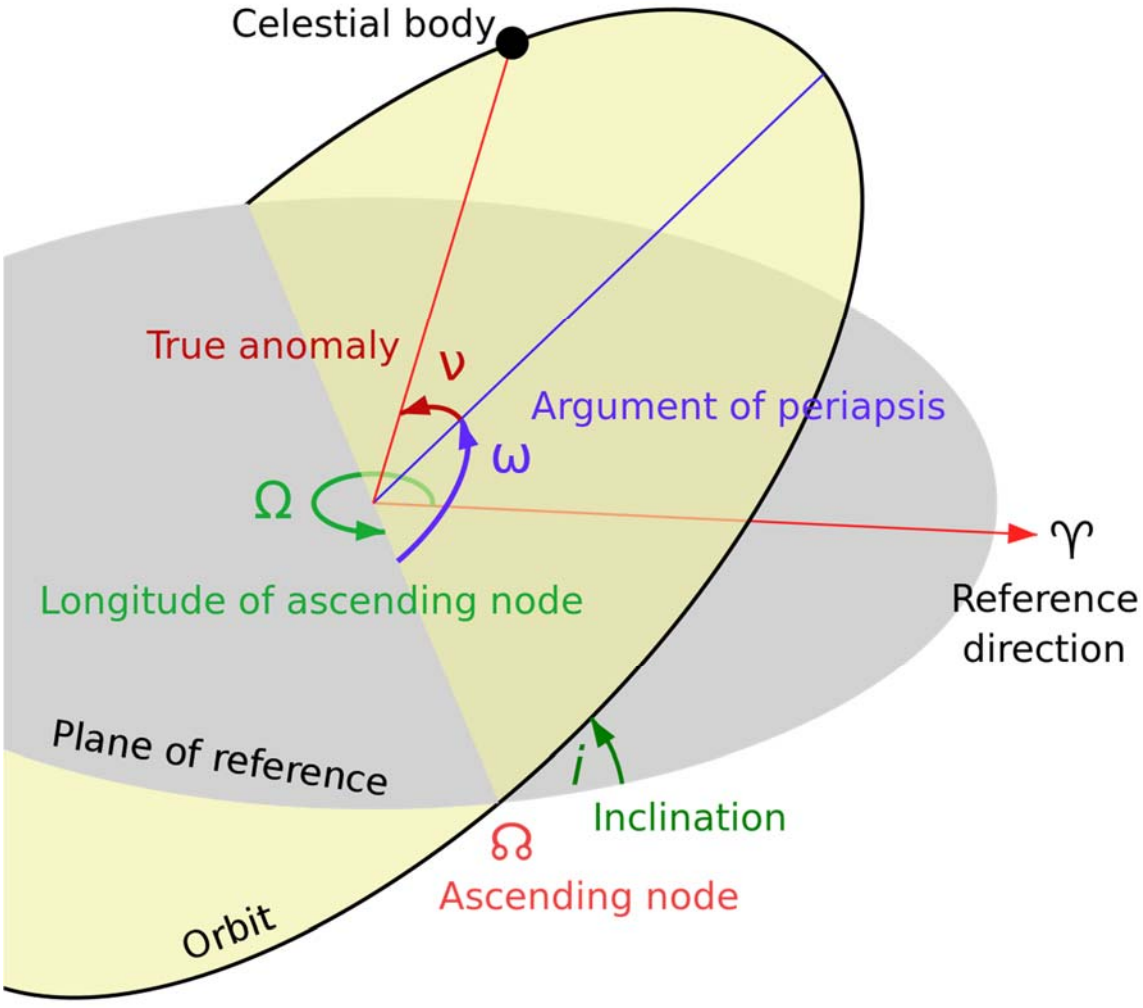

Figure 11. Inclination, ascending node, argument of perigee and true anomaly. Source: [21].

G. THEORETICAL FLIGHT PATTERNS FOR SWARMS

Swarm satellite operations are still theoretical. Along with the swarm concept, several flight patterns have been suggested. These theories form the baseline for the research and modeling as explained in this chapter.

The NASA Jet Propulsion Lab (JPL) Lead/Follow (L/F) (Figure 12) flight architecture is a flight pattern where the follower satellites maintain position with respect to the leader satellite. It is a hierarchical architectural theory that provides stability to the swarm [9]. The stability comes from the ability of the satellites to quickly adjust to any fluctuations in the flight pattern.

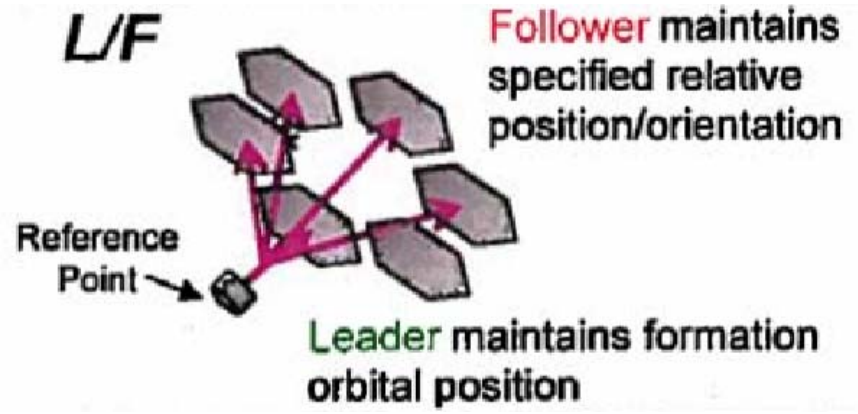

Figure 12. Lead/Follow (L/F) flight architecture. Source: [9].

Another NASA JPL flight pattern is called the Center of Formation (COF) architecture (Figure 13). This formation focuses spacecraft control on the geometric center of the formation, not a specific satellite. Theoretically, COF is more fuel efficient than L/F but the formation is less architecturally stable. The command and control design considerations are more complex as well [9].

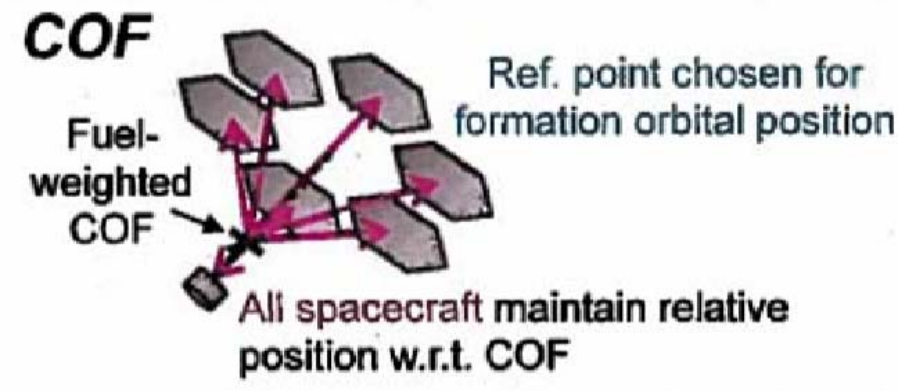

Figure 13. Center of Formation (COF) architecture. Source: [9].

The third flight architecture in this series by NASA JPL is called the Hybrid. It is a fusion of the best aspects of the L/F and COF architectures (Figure 14). The primary segments use the COF concept by focusing their positioning on the geometric center of the formation. The once leader satellite now follows the swarm using the L/F concept to provide support rather than lead the formation [9].

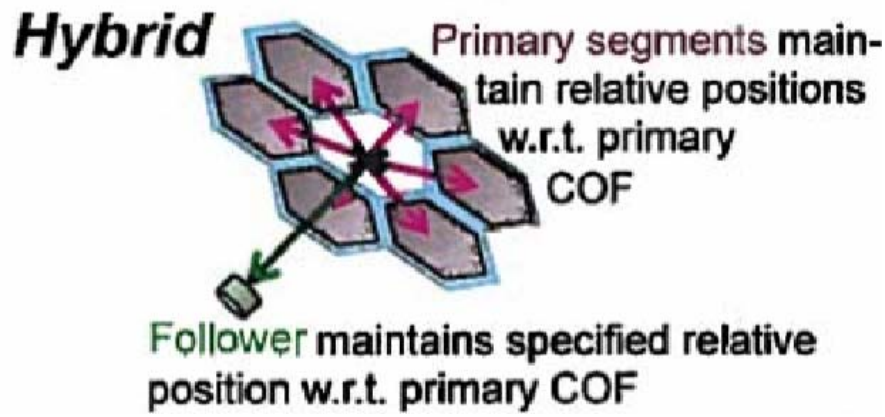

Figure 14. Hybrid L/F and COF architecture. Source: [9].

H. THEORETICAL ORBIT PATTERNS FOR SWARMS

The inline formation, shown below in Figure 15, is a proven flight pattern that simply has one satellite follow another in the same flight path. In the case of the German radar satellite pair of TerraSAR-X and TanDEM-X, they are separated by 500 meters [22].

Figure 15. Two satellite inline architecture. Source: [23].

The two satellite pendulum formation, as demonstrated in Figure 16, is designed to offset the inline concept by using "horizontal cross-track separation along the equator by different ascending nodes," [6] which is further defined in Chapter III. Pendulum formations require "along-track displacement to avoid satellite collision at polar crossing points" [6]. The two satellite pendulum formation is significant because it reduces the aliasing errors created by a lack of Doppler Effect differentials for data collection, which is common with inline formations. Simply, a slightly different angle of radar collection provides more accuracy to the image configuration.

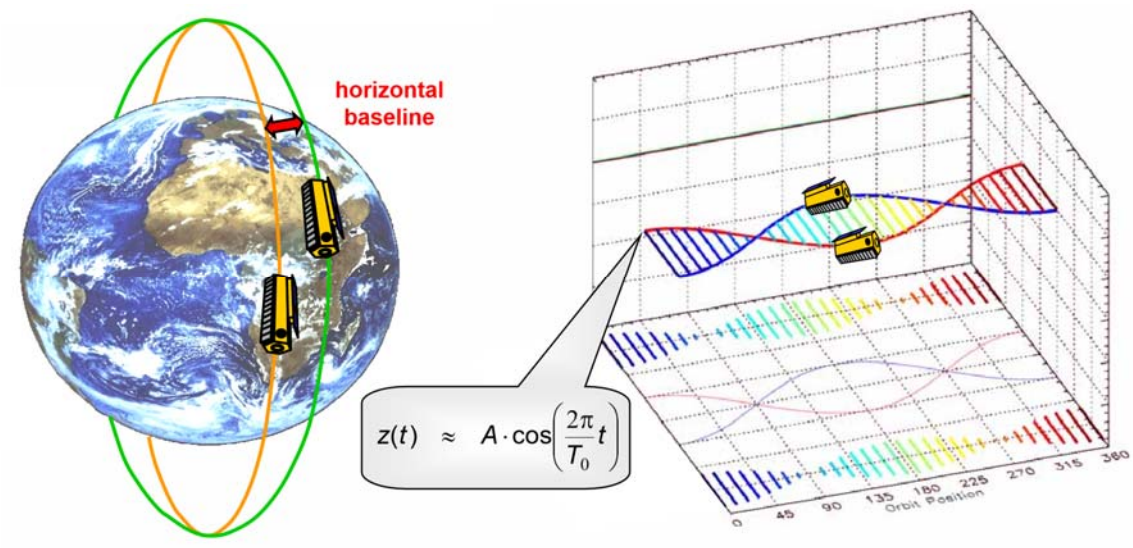

Figure 16. Two satellite pendulum architecture. Source: [6].

The HELIX satellite formation in Figure 17 is a continuation of the two prior formations. HELIX satellite formations enable safer operations because of the "horizontal cross-track separation at equator by different ascending nodes and the vertical (radial) separation at the poles by orbits with different eccentricity vectors (periodic motion of liberation has to be compensated by regular maneuvers)" [6].

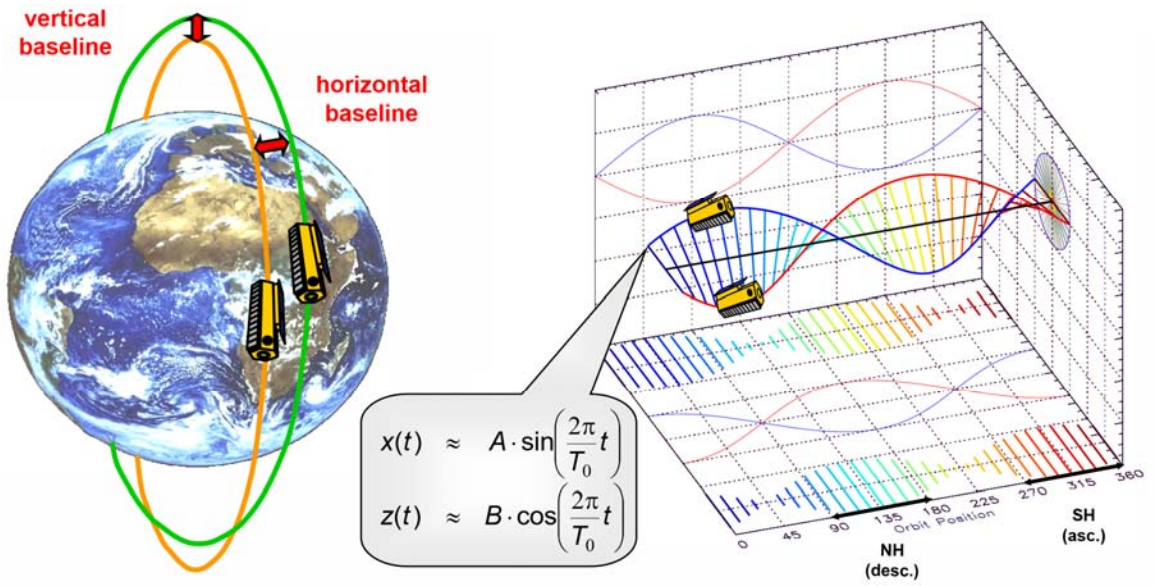

Figure 17. HELIX satellite architecture. Source: [6].

The interferometric cartwheel (Figure 18) is an adaptation of the three architectures above and can be used to accommodate many, perhaps a swarm, of satellites. All satellites share the same inclination with some changes to the individual satellite orbital parameters. The interferometric cartwheel provides a stabilizing vertical baseline for each satellite's orbital position [6].

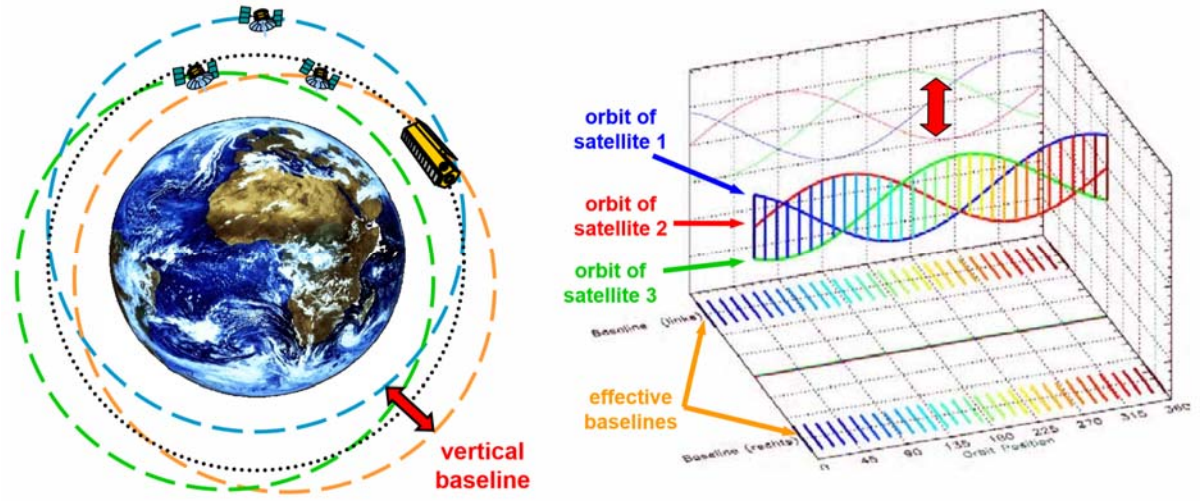

Figure 18. Interferometric cartwheel. Source: [6].

I. SPARSE APERTURE AFFECT ON RESOLUTION

Resolution is directly affected by the dispersal pattern of the swarm. "Ground resolution is defined as the minimum distance on the ground at which two object points can be imaged separately [7]." For SAR, resolution is based on several different aspects to include the pulse duration and power of the emitted microwaves, the frequency and wavelength of the signal, SNR, distance between emitter and target, size and shape of the emitter, distance the emitter travels before receiving the return signal, material that the transmitter and receivers are made of and many other engineering details. For simplicity, we will use a very basic equation known as Rayleigh's criterion. Of the effects on SAR listed above, Rayleigh's criterion focuses only on the wavelength of the signal emitted, distance between emitter and target, and size/shape of a real aperture in the visible spectrum. It also includes a constant of 1.22, which defines the intensity of diffracted light for a visible spectrum aperture. Rayleigh's criterion states that

$$\theta r = 1.22\ (\lambda / a)\ R \tag{1}$$

where θr is the resolution, λ is the wavelength, a is the aperture diameter, and R is the range between emitter and target [24]. Normally, this equation is used for a real aperture and the constant of 1.22 is used to calculate resolution in the visible spectrum. Rayleigh's criterion allows for an approximation of the sparse aperture swarm's resolution as the satellites progress through their orbit, widening the aperture at the equator and narrowing at the poles.

J. THE CHALLENGES OF SPACE DEBRIS

Small satellite swarm technology is still just a theory because the repercussions for failure, such as creating more space debris, can be dangerous for future uses of space. Current space surveillance systems are only able to track items in space larger than about ten centimeters [25]. What we are able to track ranges in the hundreds of thousands of objects and only a few hundred are functioning, controllable satellites. It is estimated that as many as half a million pieces of debris simply too small to track with our current space surveillance capabilities may be in orbit [25]. Something as small as a paint chip striking a

solar panel or transmitter/receiver dish at thousands of miles per hour could render it inoperable and create even more debris.

If a small satellite swarm of only five spacecraft failed to maintain formation, they could be damaged as they bump into each other, adding dozens of pieces of debris to the space environment. Though several companies and nations have been working for years to try and reduce the amount of debris on orbit, no solution is imminent. In the worst of cases, thousands of small satellites could be launched in the next decade and, eventually, the congestion alone would cause an escalating number of collisions possibly creating a barrier of debris preventing continued spaceflight and exploration.

K. SUBJECT MATTER EXPERTS

There are very few subject matter experts in the area of small satellite swarm theory, but one institution provides the majority of scholarly work in the field: Massachusetts Institute of Technology (MIT). MIT, in partnership with JPL, NASA, and Lockheed-Martin, has a faculty and student body that are active and prolific in their pursuit to prove the feasibility of formation flying, ranging in concepts from ultrasonic sensors to electromagnetic collision avoidance measures to maintain flight formations [26]. Much of the background reading for this thesis and many of the citations used come from literature produced by the faculty and students at MIT.

THIS PAGE INTENTIONALLY LEFT BLANK

III. METHODOLOGY

A. INTRODUCTION

This chapter will outline the metrics and methods used in Chapter IV to conduct modeling for a small satellite swarm conducting a SAR mission. This chapter starts by describing the metrics used. Research indicates a need to make assumptions regarding orbits, certain stability capabilities, and some values to highlight imagery resolution patterns. The modeling is done using software called STK developed by AGI. Orbital analysis includes using a program called MATLAB and imaging analysis uses an equation called Rayleigh's criterion.

B. METRICS

The modeling discussed in Chapter IV is based in part on certain "common sense" approaches. To frame the scope and scale of this work to a manageable level, for example, no altitude of orbits higher than Low Earth Orbit (LEO) were modeled due to cost and accessibility of these orbits. Orbits are modeled with the understanding that the satellites will be launched as a secondary payload and therefore will be operating at common inclinations or orbital planes.

The references to the bus and payload are purposely vague, as this body of work focuses on the operation of the satellites and not the engineering aspects. A nonrestrictive approach also allows future work flexibility in design.

All measurements of distance are in the metric system. All measurements of time are in hours and seconds. Discussion of the mathematics and physics of space operations is simplified as much as possible without neglecting their relevance in order to reach the largest audience.

Part of our analysis will use Rayleigh's criterion. Even though the calculated resolution will not be completely accurate (as discussed in Chapter II Section I), we will be able to gain an understanding of the changes to resolution as the swarm travels in its orbit.

C. ASSUMPTIONS

In order to manage the problem of modeling a realistic small satellite swarm we are making a few basic assumptions. First, the most likely launch possibility is in a low Earth polar orbit. Because a polar orbit is very common for imaging missions of all kinds, including radar, and items are regularly launched into polar orbit, we assume that is one of the most likely launch options with small satellites as a secondary payload. For this reason, we assume that an altitude of three hundred kilometers will suffice using a ninety-degree inclination or a polar orbit. A three hundred kilometer altitude is preferable because if there is a collision or malfunction, the swarm is so close to Earth that anything without station keeping ability should deorbit in a matter of months. The tradeoff is that the extra drag requires frequent station keeping, or boosts in altitude, to keep a satellite in orbit for more than a few months, likely shortening the useful lifetime of the mission.

The proximity of each of the satellites in the models to each other reflects an assumption that there are formation-stabilizing techniques. These include the ability to orient the satellites, execute major station-keeping maneuvers, and conduct more nuanced stability operations. Sensors and cross-link will be required to monitor and communicate the distances between the individual satellites.

Finally, we assume a few values to use in Rayleigh's criterion. It is assumed that the sparse aperture nature of the swarm acts in a spherical manner and that the frequency of ~35GHz used is in the Ka-band and has a wavelength of 0.86cm. Also assumed is that the sparse aperture will act as a real aperture for purposes of understanding orbital effects on resolution.

D. SYSTEMS TOOL KIT

In order to conduct the modeling required, we used software called STK. As explained on the AGI website, "Systems Tool Kit sets the standard for modeling and analyzing systems in a four-dimensional, interactive globe. The STK modeling environment is used worldwide by hundreds of organizations to model complex land-, sea-, air-, or space-based systems and evaluate their performance in real or simulated time. [27]."

STK Highlights from the AGI webpage:

- Model with an accurate Earth representation in time and space.
- Support cloud and server-based architectures with flexible development kits and components.
- Add streaming imagery and terrain, or any kind of map and GIS data.
- Define realistic and accurate, idealistic, or user-ingested dynamic vehicles.
- Add vehicle orientation, pointing, and sensor fields of view.
- Report or define new points, vectors, angles, axes and coordinate systems.
- Run in real time or simulate in past or future time.
- Analyze complex physical relationships between all the vehicles, sensors and environment.
- Report, graph or export the results.
- Visualize the scenario in any way imaginable in a 3D environment.
- Create videos, custom views or images to clearly convey results.
- Integrate, customize or extend capability with the open API and file formats. [27]

E. MODELING METHODS

To scope the amount of information in Chapter IV to a manageable level, only three models were selected to highlight. The three models were selected as because each one has a different concept for flight operations and because of the interesting findings during modeling and analysis.

1. Pendulum and Inline Hybrid Model

The pendulum and inline hybrid model in Figure 19 is designed with three satellites inline and two satellites that fly one to the left and one to the right of the formation until the formation crosses the poles. As the formation crosses the poles, the satellites to the left and right tuck into the formation and swap sides. All satellites remain at the same altitude. The Lead (leader) satellite is in the center of formation (COF).

As shown in Figure 20, the Lead satellite provides the base of the formation. Satellite one (Sat1) has the same Classical Orbital Elements (COEs), discussed in Chapter II, with the exception of the true anomaly, which is slightly greater placing it ahead of the lead satellite. Sat2 also has the same COEs with the exception of the true anomaly, which is at a slightly lesser angle, placing it behind the lead satellite. For Sat3, the true anomaly angle is greater than the Lead but less than Sat1, allowing it to tuck in between the two as it crosses the poles. Sat3 also has a lesser RAAN than the Lead which allows it to fly to the right of the formation as it approaches the North Pole and to the left as it approaches the South Pole. Sat4 has a true anomaly angle less than the Lead but greater than Sat2, allowing it to tuck in between the two as it crosses the poles. Sat4 also has a greater RAAN than the Lead which allows it to fly to the left of the formation as it approaches the North Pole and to the right as it approaches the South Pole.

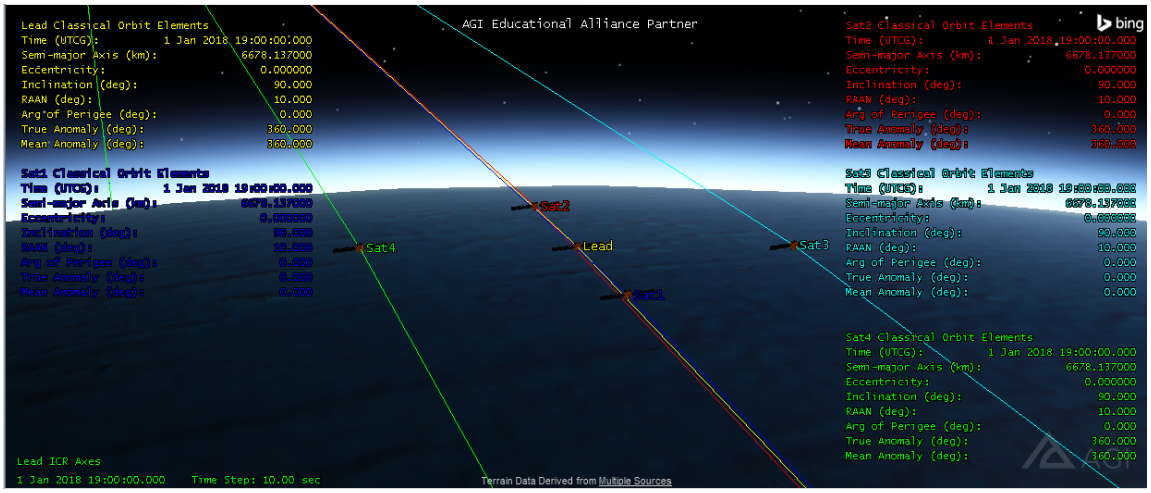

Figure 19. Pendulum and Inline Hybrid_v5

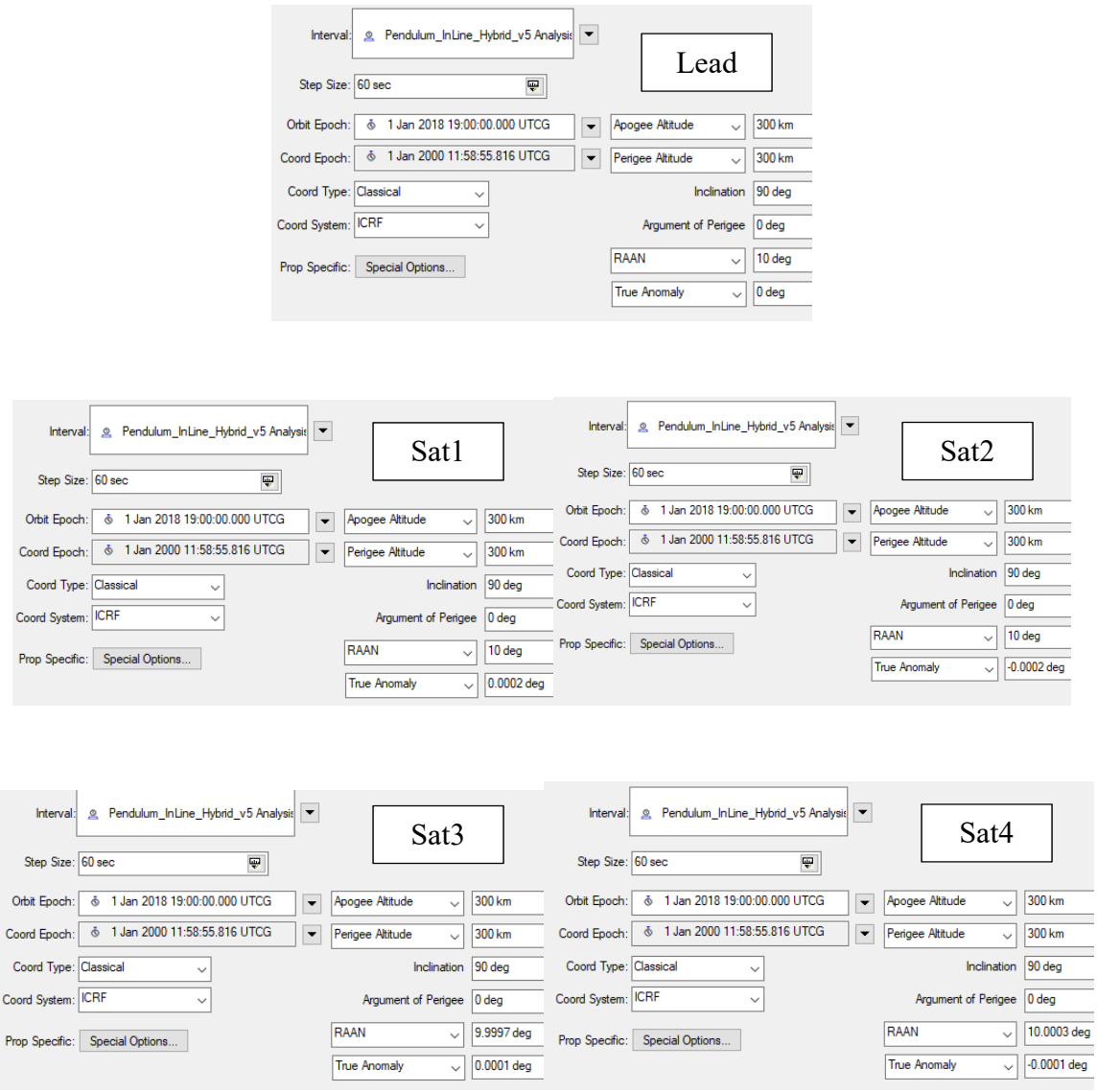

Figure 20. STK Orbital Parameters for Pendulum and Hybrid_v5. Adapted from: [27].

2. Helix and Inline Hybrid Model

The helix and inline hybrid model in Figure 21 is designed with three satellites inline and two satellites that fly one to the left and below and one to the right and above the formation until the formation crosses the poles at offsetting altitudes to each other and the inline satellites. As the formation crosses the poles, the satellites to the left and right

tuck in above and below the formation. Only the inline satellites remain at the same altitude. The Lead (leader) satellite is in the center of formation.

As the orbital elements shown in Figure 22, the Lead satellite provides the base of the formation. Satellite one (Sat1) has the same COEs with the exception of the true anomaly, which is slightly greater placing it behind the lead satellite. Sat2 also has the same orbital parameters with the exception of the true anomaly, which is at a slightly lesser angle, placing it in front of the lead satellite.

For Sat3, the true anomaly angle is greater than the Lead but less than Sat1. Additionally, giving Sat3 a bit of eccentricity by adding to the apogee and subtracting the same from perigee allows the spacecraft to offset its altitude from the three inline satellites throughout a good part of the orbit. Sat3 flies at a higher altitude than the inline satellites moving toward the North Pole and lower moving toward the South Pole. Sat3 also has a lesser RAAN than the Lead which allows it to fly to the right of the formation as it approaches the North Pole and to the left as it approaches the South Pole. As the argument of perigee was kept at 0 degrees for Sat3 and Sat4, the greatest difference in altitude will be when the swarm is at the equator.

Sat4 has a true anomaly angle less than the Lead but greater than Sat2. As with Sat3, adding to the apogee and subtracting the same from perigee allows the spacecraft to offset its altitude from the three inline satellites at the poles. Simply, this is a manipulation of the eccentricity orbital parameter because Sat3 and Sat4 have a ninety degree inclination with a circular orbit. In this case however, to have a second satellite fly above and below the Lead satellite but opposite of Sat3, the argument of perigee must be flipped 180 degrees as apogee is always higher than perigee. Sat4 flies at a lower altitude than the inline satellites moving toward the North Pole and higher moving toward over the South Pole. Sat4 also has a greater RAAN than the Lead which allows it to fly to the left of the formation as it approaches the North Pole and to the right as it approaches the South Pole.

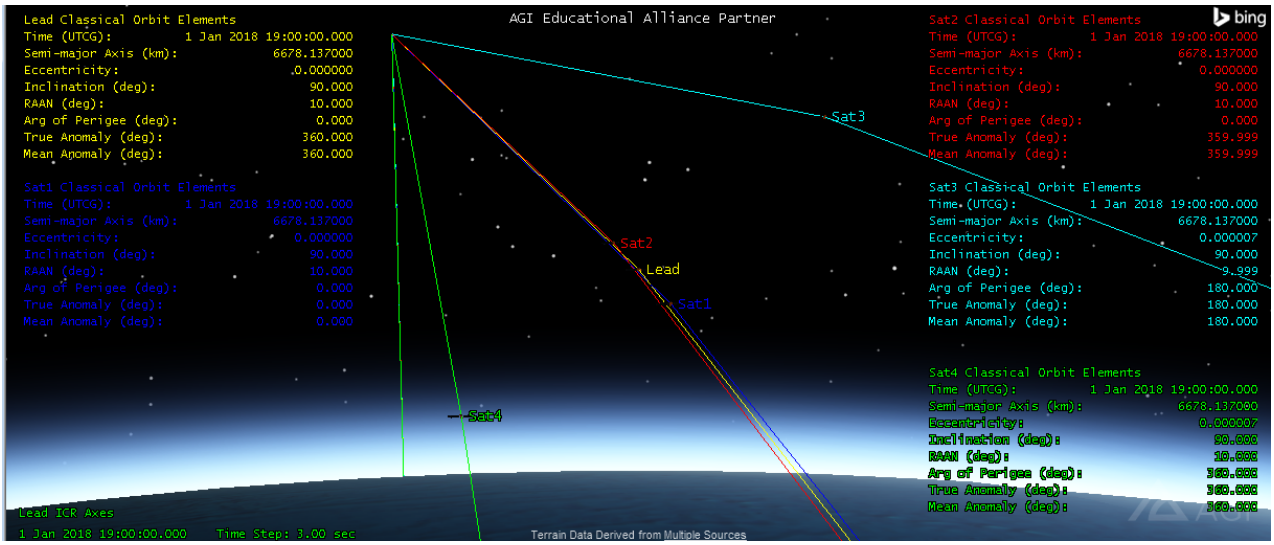

Figure 21. Helix and Inline Hybrid_v3

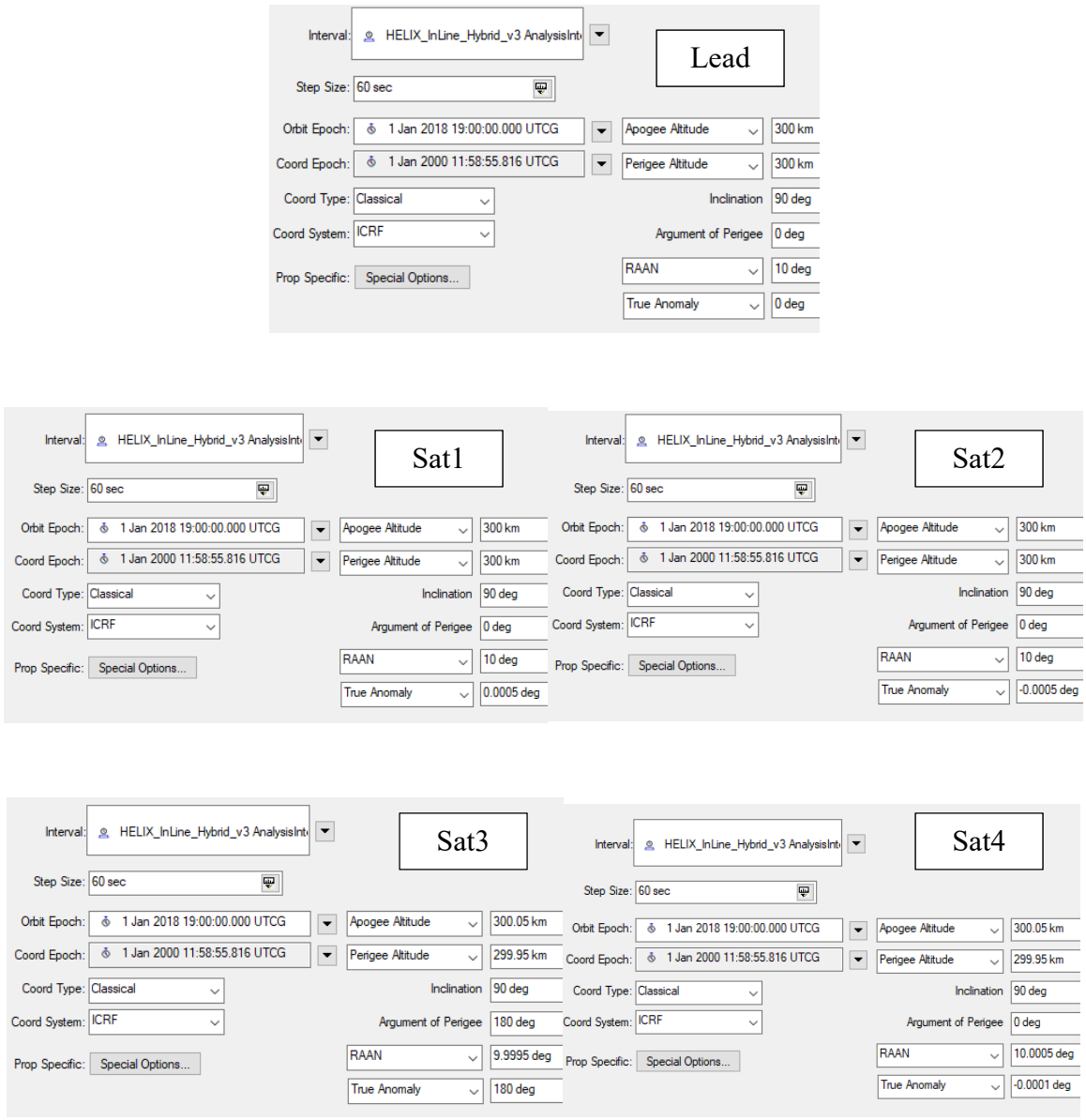

Figure 22. STK Orbital Parameters for Helix Hybrid_v3. Adapted from: [27].

3. Cartwheel Hybrid Model

The cartwheel hybrid model, as shown in Figure 23, is different from the pendulum hybrid and the helix hybrid because we did away with the inline concept. The Lead (leader) satellite remains in the center of formation. The follower satellites fly one to the left and one to the right of the formation at different altitudes. Another flies to the front right and

the last one flies to the left rear of the formation. They also have offsetting altitudes. As the formation crosses the poles, the satellites fall into a line separated in altitude by only a few meters. This formation is the most complicated of the three highlighted in this thesis.

The orbital elements in Figure 24 show the Lead (leader) satellite is in the center of formation setting the baseline and the other four rotate around it as the swarm orbit progresses. Sat1 has an eccentricity change so that it flies higher than the rest of the swarm over the South Pole and lower over the North Pole. As a result, the argument of perigee is opposite (180 degrees) from the Lead satellite. The RAAN is increased to have the satellite fly on the left side of the formation while moving toward the North Pole and on the right side as it travels from the north to the south.

Sat2 has an eccentricity change so that it flies higher than the rest of the swarm over the North Pole and lower over the South Pole and the argument of perigee remains at 0 degrees. The RAAN is decreased to have the satellite fly on the right side of the formation while moving toward the North Pole and on the left side as it travels from the north to the south. Sat2 has a true anomaly angle less than the other satellites so that at it flies in the rear.

Sat3 has an eccentricity change so that it flies higher than the rest of the swarm over the South Pole and lower over the North Pole. As a result, the argument of perigee is opposite (180 degrees) from the Lead satellite. The RAAN is decreased to have the satellite fly on the right side of the formation while moving toward the North Pole and on the left side as it travels from the north to the south.

Sat4 has an eccentricity change so that it flies higher than the rest of the swarm over the North Pole and lower over the South Pole and the argument of perigee remains at zero degrees. The RAAN is increased to have the satellite fly on the left side of the formation while moving toward the North Pole and on the right side as it travels from the north to the south. Sat4 has a true anomaly angle less than the other satellites except Sat2 so that it flies next to last in the swarm.

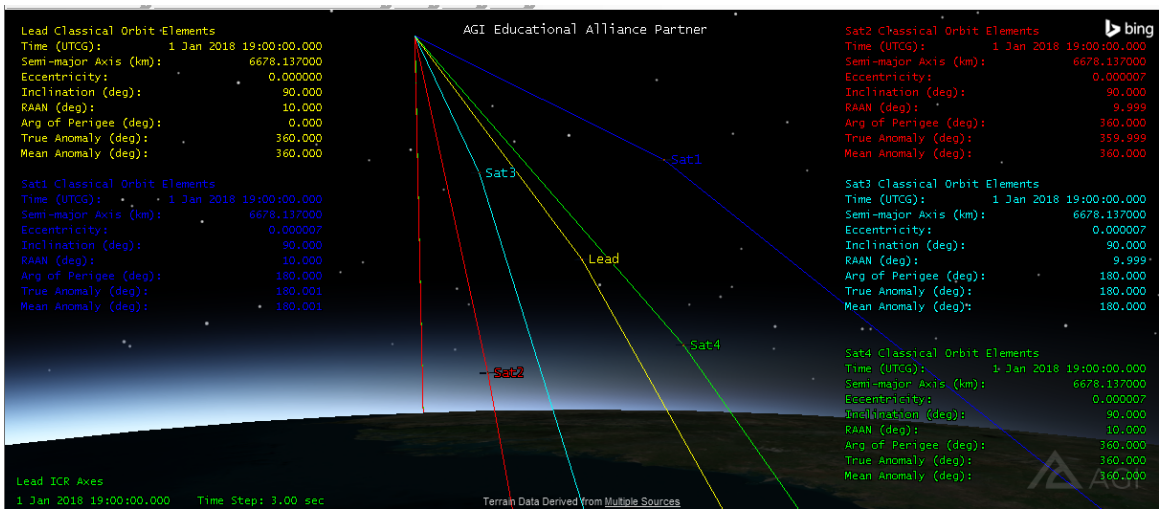

Figure 23. Cartwheel Hybrid_v9

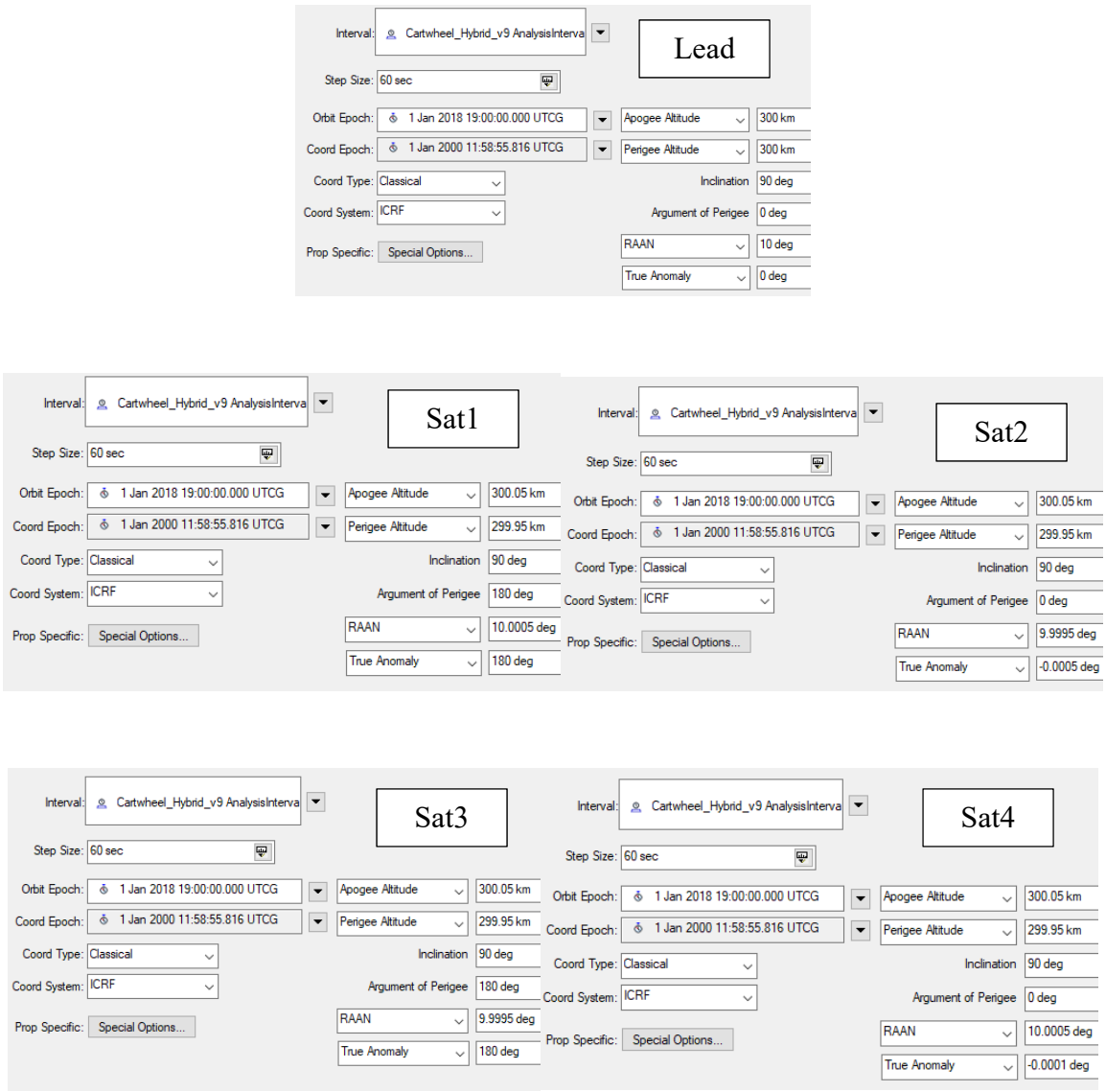

Figure 24. STK Orbital Parameters for Cartwheel Hybrid_v9. Adapted from: [27].

F. MATLAB

To analyze the data modeled from STK and compare imaging capabilities of each model, a program developed by MathWorks called MATLAB was used. As described on their website, "MATLAB combines a desktop environment tuned for iterative analysis and design processes with a programming language that expresses matrix and array mathematics directly. [28]."

G. ANALYSIS METHODS

The MATLAB scripts for the pendulum and hybrid model are in Appendix A, the MATLAB scripts for the helix and hybrid model are in Appendix B, and the MATLAB scripts for the cartwheel hybrid model are in Appendix C. Using the inertial positioning vectors report from STK, the report is converted to a .csv file and imported into MATLAB script over the course of just over one orbit. Each orbit is ninety minutes. Points are sampled at one minute, or four-degree, intervals and we use one-hundred points on each chart. From this sampling we can identify if the swarm formation is stable, convergent, or divergent. A stable swarm occurs when the satellites maintain their respective distances without constant station keeping. Convergence is when the swarm begins to collapse in on itself while divergence describes what happens when the swarm disperses.

When referencing the direction of travel, this is the in-plane view relative to the swarm using the velocity vector. When referencing the horizontal direction or view, this refers to the out of plane vector relative to the swarm in a 2D view and which is perpendicular to the direction of travel. When referencing the vertical direction or view, it is a radial direction that is dorsal to the swarm and adds a third dimensional representation.

Next, the inertial positioning vectors report is used to determine the distances between satellites and construct a notional nadir-facing sparse aperture radar in order to compute real aperture resolution as a function of the orbital position. The Earth-centered inertial (ECI) reference frame is the primary coordinate system used for this analysis. To emphasize the differences in resolution, as applied to just three STK models, we have exaggerated the distances between satellites in each simulation. The MATLAB scripts with detailed descriptions and calculation explanations used for conducting the highlighted sampling in Chapter IV are in the appendices.

SAR resolution relies on several different variables, a complete description of which is outside of the scope of this thesis. These variables include, but are not limited to, the pulse duration and power of the emitted microwaves, the frequency and wavelength of the signal, SNR, distance between emitter and target, size and shape of the emitter, distance the emitter travels before receiving the return signal, material that the transmitter and

receivers are made of and many other engineering details. By manipulating these variables, it is possible to greatly increase and more accurately estimate resolution. However, to analyze resolution within the scope of this thesis, we will use Rayleigh's criterion, as described previously. Of the effects on SAR listed above, Rayleigh's criterion focuses only on the wavelength of the signal emitted, distance between emitter and target, and size/shape of the array for a real aperture resolution [24].

THIS PAGE INTENTIONALLY LEFT BLANK

IV. ANALYSIS

A. INTRODUCTION

This chapter outlines the analysis conducted during modeling for a small satellite swarm conducting a synthetic aperture radar mission. STK was used for modeling the three different swarm patterns. The swarm flight pattern and effect on imaging is discussed at latitude intervals of 30 degrees from the equator to the North Pole. Each swarm is analyzed for a single orbit in MATLAB at the end of each section to assess the stability and an approximate resolution. At the end of Chapter IV, the real aperture resolution for all three models is analyzed.

It is important to point out that when the swarm passes over the poles with all satellites inline and the aperture dispersal pattern collapses, Rayleigh's criterion becomes inadequate to approximate resolution. For a few seconds over the poles, Rayleigh's criterion identifies the resolution as an infinite number. When this occurs, the sparse aperture reverts to a standard SAR aperture as detailed in Chapter II. Because this occurs very briefly, a matter of seconds, Chapter IV identifies the event but does not analyze it in detail.

B. PENDULUM AND INLINE HYBRID MODEL

The pendulum and inline hybrid model was selected for the simplicity of flight operations because of the inline nature and offsetting satellites to the left and right. The most significant findings involved minor stability concerns for two of the satellites. The pendulum and inline hybrid is a viable model but provides less flight safety measures than the helix and inline hybrid and cartwheel hybrid. The cartwheel hybrid has more satellite dispersion than the pendulum and inline hybrid which provides better imaging capability.

The pendulum and inline hybrid model is designed with three satellites inline and two satellites that fly one to the left and one to the right of the formation until the formation crosses the poles. As the formation crosses the poles, the satellites to the left and right tuck into the formation. All satellites remain at the same altitude. The Lead (leader) satellite is in the center of formation (COF).

As we can see in the 2D ground track of Figure 25, the swarm is over the equator or at 0 degrees latitude. The direction of travel is toward the North Pole along the green line that illustrates a single orbit.

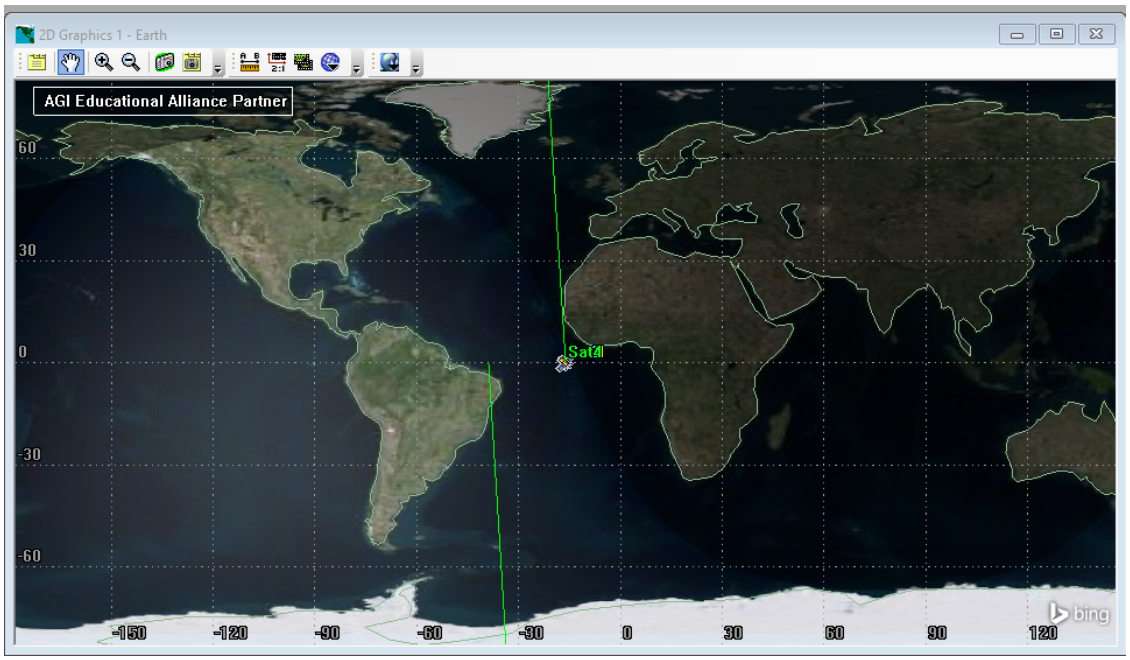

Figure 25. 2D Orbital Positioning for Pendulum Hybrid_v5 at 0 degrees latitude. Adapted from: [27].

Figure 26 shows the formation from above at the equator as the swarm moves to the top of the screen. The formation is spread out to its maximum extent at the equator. Sat3 and Sat4 are offset from the center which will not affect imaging. Using the MATLAB script in Appendix A to determine the distances between the satellites provides a derivation of 46m for the aperture diameter. Using Rayleigh's criterion, Eqn (1), $\theta r = 1.22$ (0.0086m / 46m) 300,000m = 68m resolution. This is an approximate representation of sparse aperture imaging using the method for analyzing a real aperture in the visible spectrum.

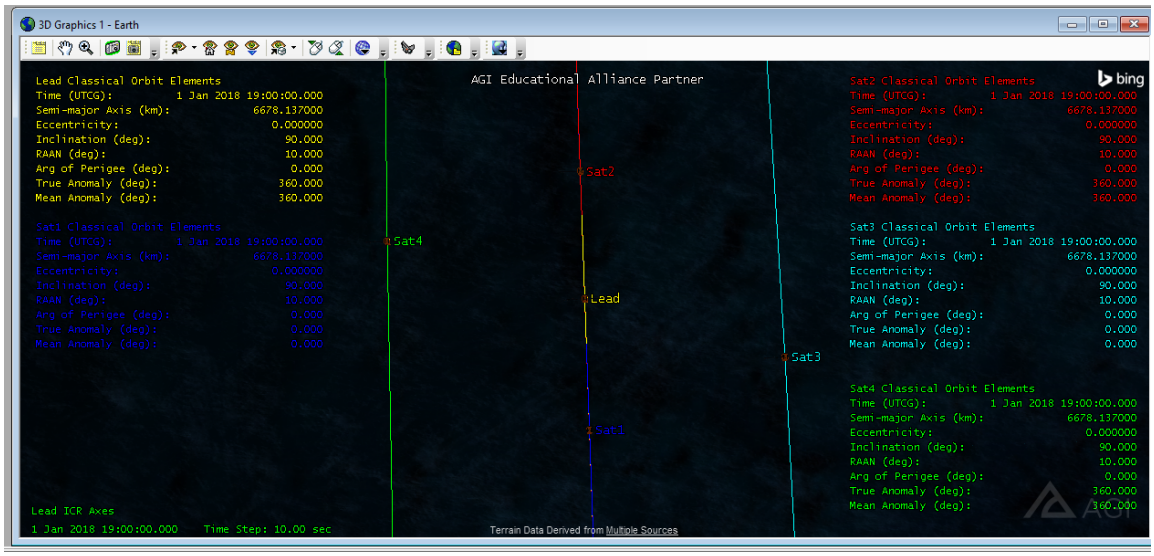

Figure 26. 3D Top View Orbital Positioning for Pendulum Hybrid_v5 at 0 degrees latitude. Adapted from: [27].

Figure 27 shows the swarm from the side at the equator with the direction of travel to the left. This view shows that the formation is flying at the same altitude. The offset of Sat3 and Sat4 show an even distance in plane which allows for greater formation stability.

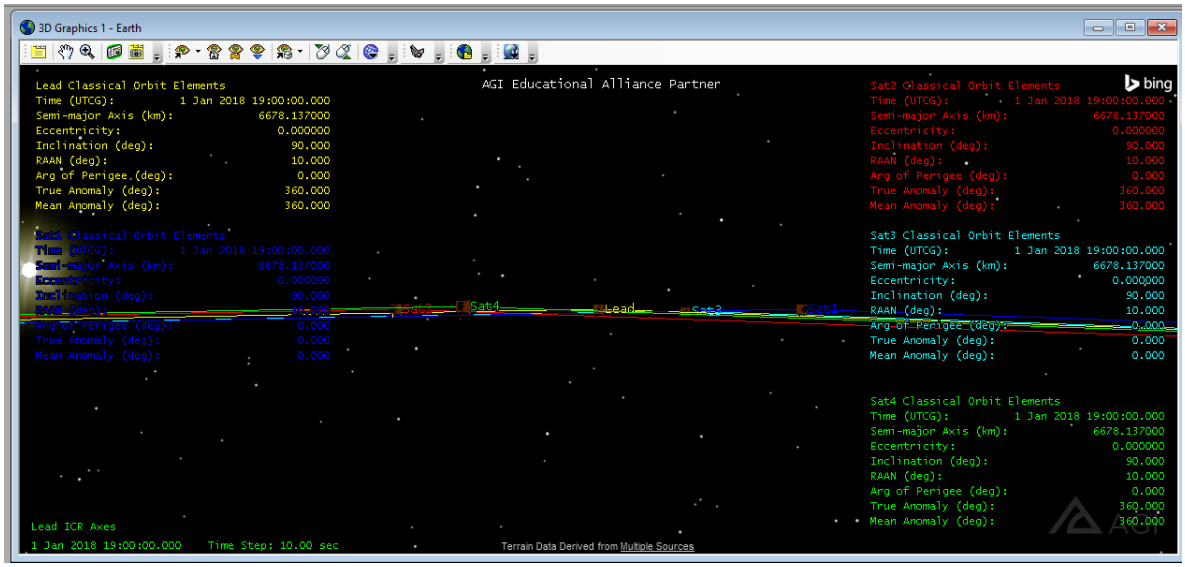

Figure 27. 3D Side View Orbital Positioning for Pendulum Hybrid_v5 at 0 degrees latitude. Adapted from: [27].

Figure 28 shows the 2D ground track of the swarm at thirty degrees latitude. The direction of travel is toward the North Pole.

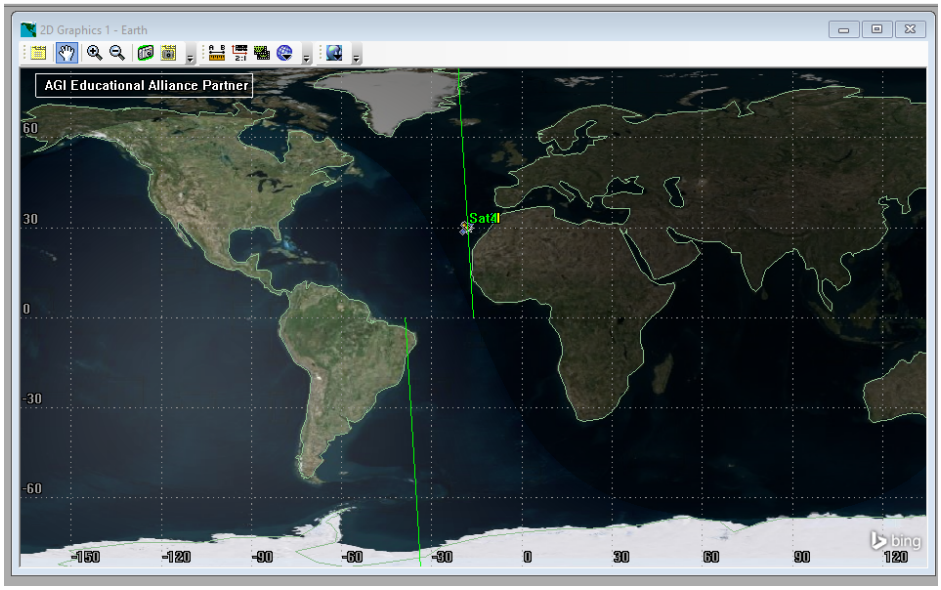

Figure 28. 2D Orbital Positioning for Pendulum Hybrid_v5 at 30 degrees latitude. Adapted from: [27].

Figure 29 represents the swarm at thirty degrees latitude. The direction of flight is to the top of the screen as we view the swarm from the top left and rear. The formation is still spread out but Sat3 and Sat4 are beginning to move toward the rest of the formation. There is still very good dispersion. Using the MATLAB script in Appendix A to determine the distances between the satellites provides a derivation of 44m for the aperture diameter. Using Rayleigh's criterion, Eqn (1), θr = 1.22 (0.0086m / 44m) 300,000m = 71m resolution. This is a very small change from the equatorial resolution.

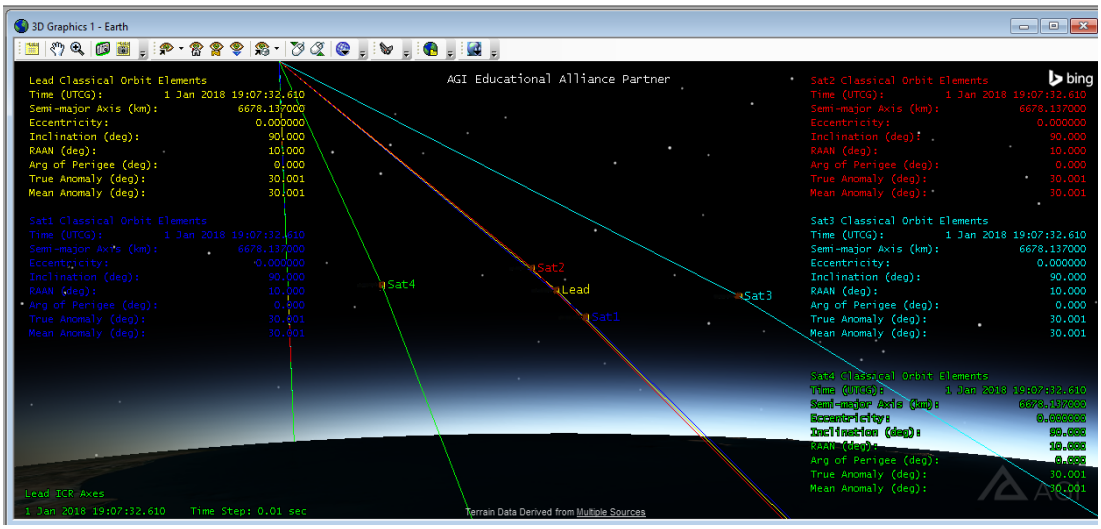

Figure 29. 3D Top View Orbital Positioning for Pendulum Hybrid_v5 at 30 degrees latitude. Adapted from: [27].

In Figure 30, the 2D ground track shows the swarm at sixty degrees latitude. The direction of travel is toward the North Pole.

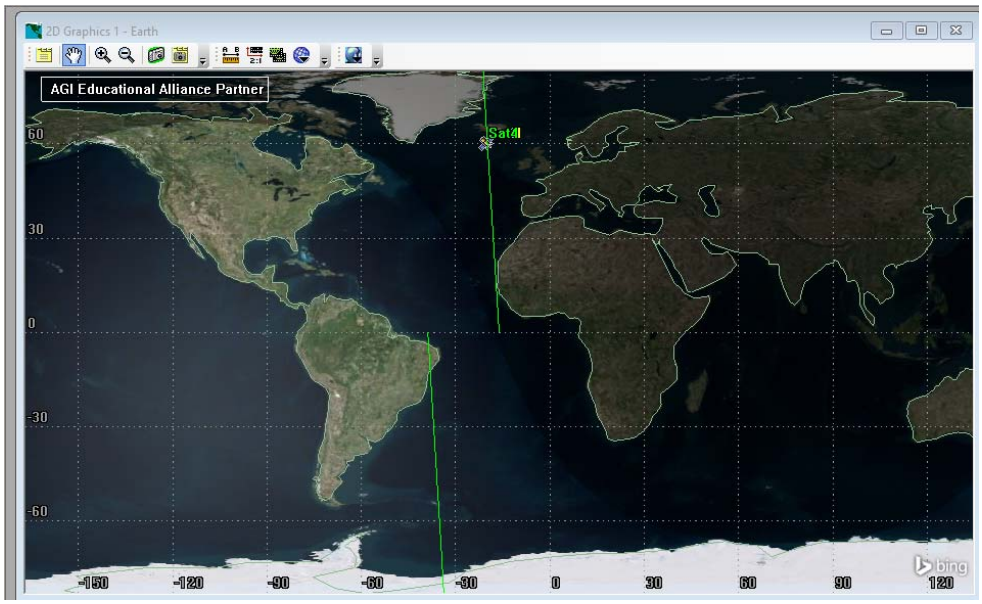

Figure 30. 2D Orbital Positioning for Pendulum Hybrid_v5 at 60 degrees latitude. Adapted from: [27].

Figure 31 views the swarm at 60 degrees latitude. The direction of flight is to the top of the screen as we view the swarm from the top left and rear. The formation remains spread out but the distance of Sat3 and Sat4 has moved much closer to the rest of the formation though dispersion is still acceptable to conduct imaging. The MATLAB script (Appendix A) computed the instantaneous distance between satellites to be 34 meters. Using Rayleigh's criterion, we get $\theta r = 1.22\ (0.0086m / 34m)\ 300{,}000m = 92m$ resolution.

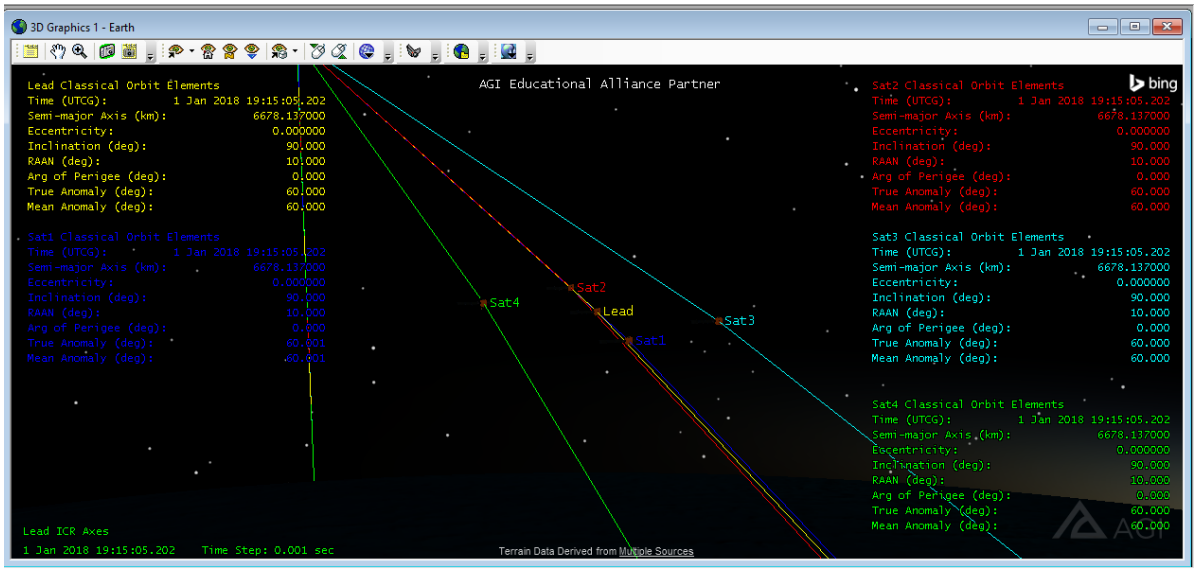

Figure 31. 3D Top View Orbital Positioning for Pendulum Hybrid_v5 at 60 degrees latitude. Adapted from: [27].

Figure 32 is the 2D ground track of the swarm over the North Pole at ninety degrees' latitude.

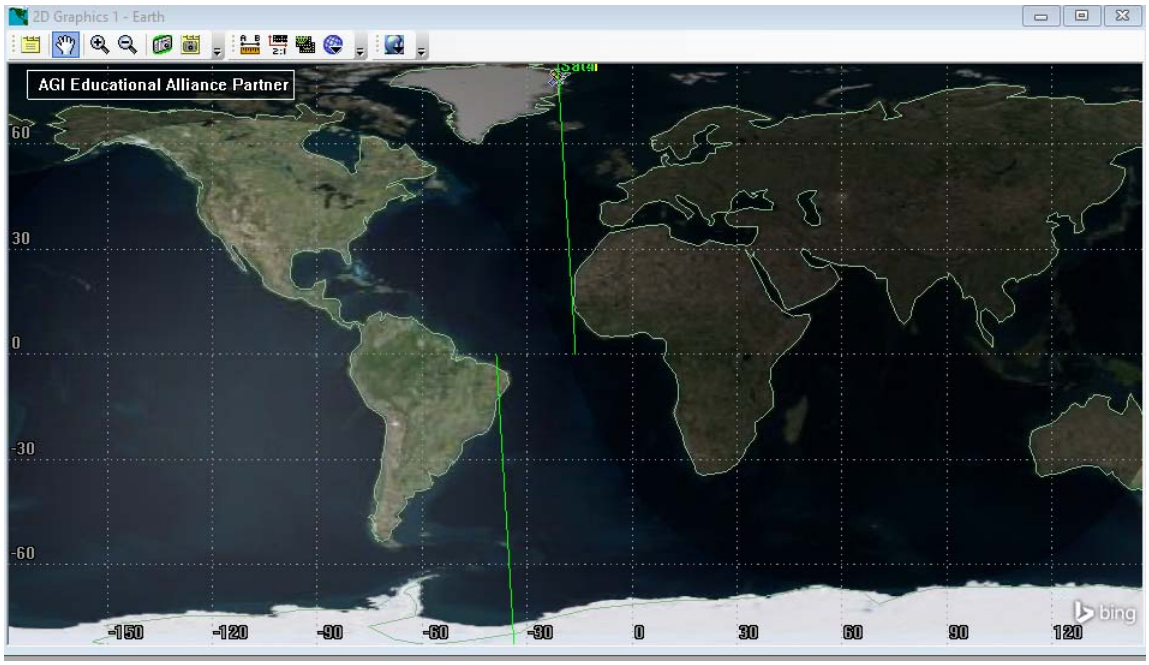

Figure 32. 2D Orbital Positioning for Pendulum Hybrid_v5 at 90 degrees latitude. Adapted from: [27].

Figure 33 represents the swarm over the North Pole with the direction of travel to the top of the screen. Notice that Sat3 and Sat4 are now in line with the other three spacecraft in the swarm. As Sat3 and Sat4 cross the pole, they will switch which side of the formation they flank. A sparse aperture capability is reduced now to a simple SAR ability as discussed in Chapter II, Section E.

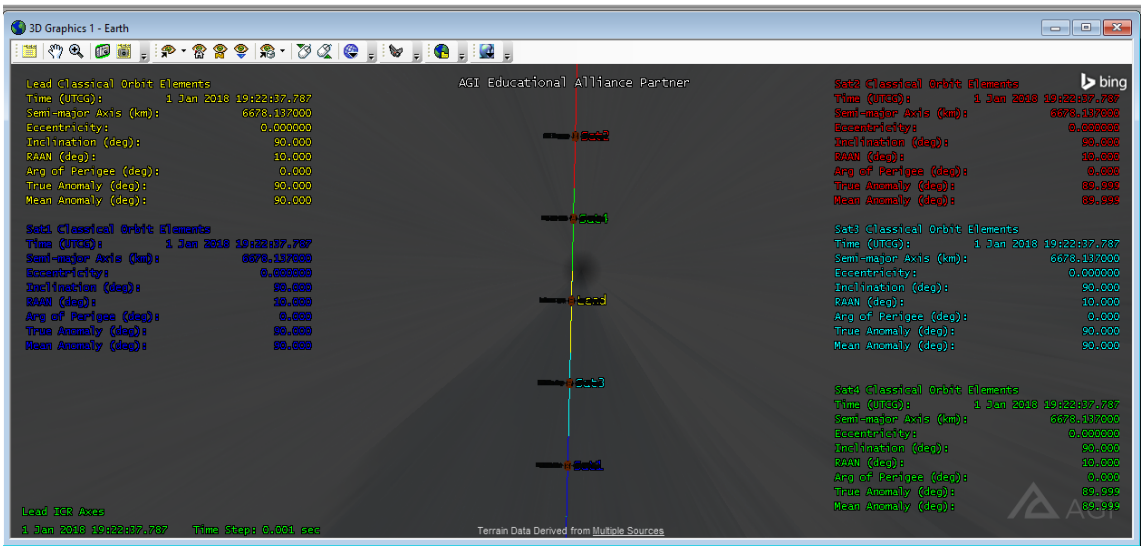

Figure 33. 3D Top View Orbital Positioning for Pendulum Hybrid_v5 at 90 degrees latitude. Adapted from: [27].

From the 3D side view in Figure 34, the direction of travel is to the left of the screen. At the poles, as at the equator, the satellites remain at the same altitude. Though the swarm is stable and there are safe distances between the individual satellites, there is no altitude or lateral separation. Separation inherent from the orbital mechanics of the swarm would provide an additional safety margin from potential collision.

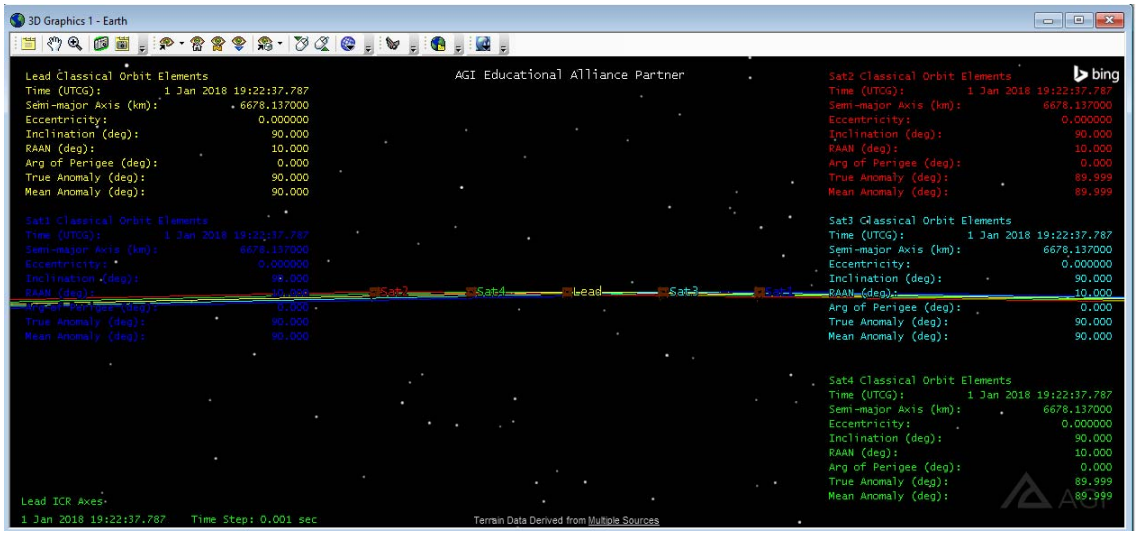

Figure 34. 3D Side View Orbital Positioning for Pendulum Hybrid_v5 at 90 degrees latitude. Adapted from: [27].

Figure 35 is a representation of the horizontal movement of the satellite throughout an entire orbit in MATLAB. The sampling is done at sixty-second intervals which equates to a sampling every four degrees of latitude. There are one hundred samples that overlap the ninety-minute orbit. As is clearly demonstrated, the formation is completely stable. The red (Sat2), black (Lead), and blue (Sat1) dots remain inline without any movement. The teal (Sat3) and green (Sat4) dots move back and forth between the other satellites uniformly and in a straight line without convergence or divergence indicating that the formation is stable.

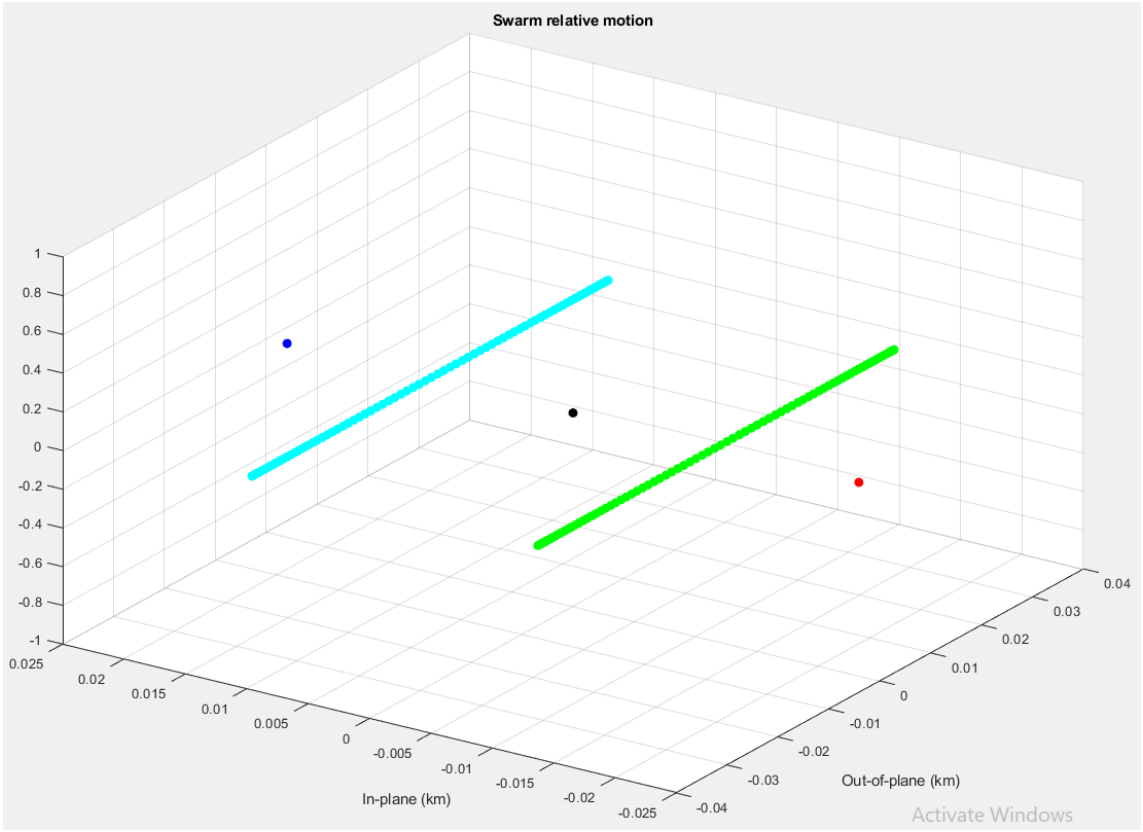

Figure 35. Horizontal Relative Motion for Pendulum Hybrid_v5. Adapted from: [28].

In Figure 36 we see that the black (Lead) dot remains stationary. On the other hand, the red (Sat2), and blue (Sat1) dots indicate movement straight up and down. However, the movement is extremely small, well under a meter in difference. The teal (Sat3) and green (Sat4) dots move back and forth between the other satellites but not as uniformly in a vertical manner as they did in the horizontal. Though the dots appear to be somewhat scattered, the differences are miniscule. Although there is no sign of convergence or divergence indicating that the formation is stable, some sort of continual station keeping methods may be desired to use this formation.

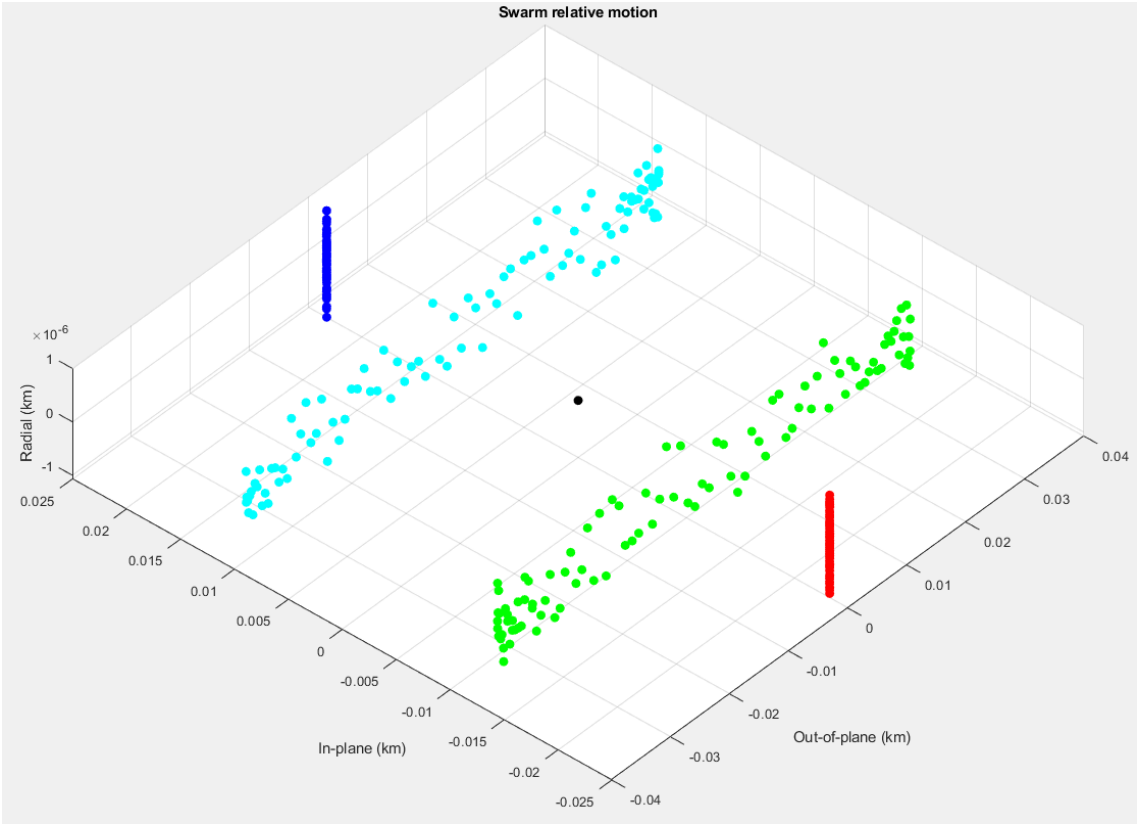

Figure 36. Vertical Relative Motion for Pendulum Hybrid_v5. Adapted from: [28].

In conclusion, the pendulum and inline hybrid formation provides a mostly stable formation with some minor station keeping required, using perhaps an ion thruster. The concept of safe flight operations for this formation may be of some concern. Firstly, all of the satellites are at the same altitude at all times resulting in no redundant safety measures. Proximity sensors and thruster protocols would also be required. The flight paths of all five satellites cross every time the swarm passes over the poles.

C. HELIX AND INLINE HYBRID MODEL

The helix and inline hybrid model was selected because of a combination of simplicity and safety integrated into flight operations. The most significant finding was less radial separation than expected over the poles. The helix and inline hybrid is a viable model and provides more flight safety measures than the pendulum and inline hybrid and

cartwheel hybrid. The cartwheel hybrid has more satellite dispersion than the helix and inline hybrid, which provides better imaging capability.

The helix and inline hybrid model is designed with three satellites inline and two satellites that fly one to the left and one to the right of the formation until the formation crosses the poles at offsetting altitudes to each other and the inline satellites. As the formation crosses the poles, the satellites to the left and right tuck in above and below the formation. Only the inline satellites remain at the same altitude. The Lead (leader) satellite is in the center of formation.

The 2D ground track of Figure 37 depicts the swarm is over the equator. The direction of travel is toward the North Pole.

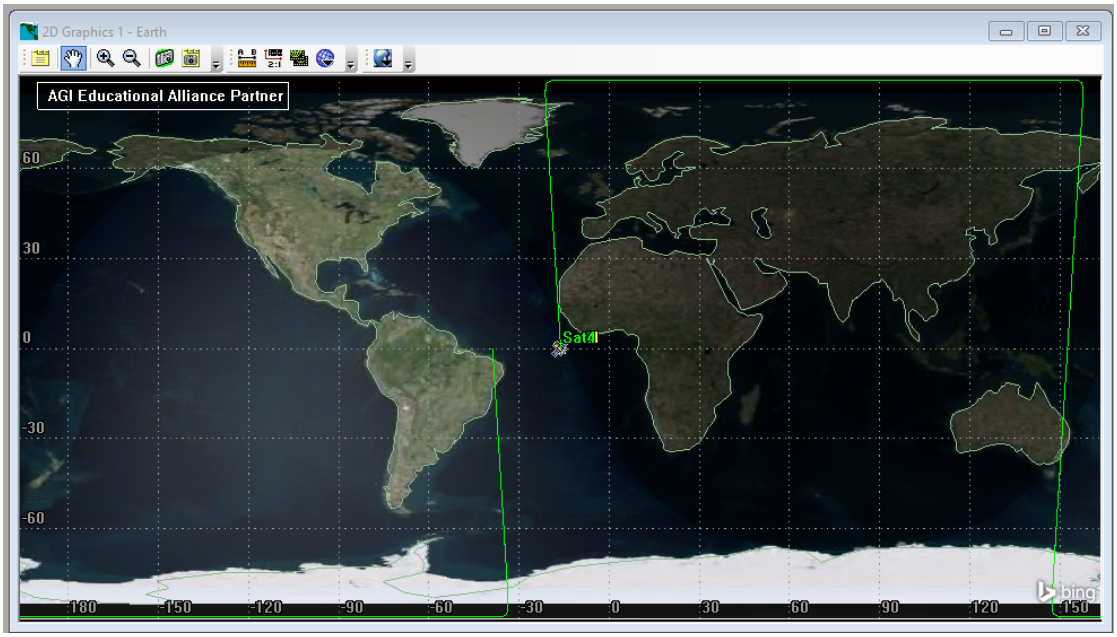

Figure 37. 2D Orbital Positioning for Helix Hybrid_v3 at 0 degrees latitude. Adapted from: [27].

The formation is spread out to its maximum extent at the equator in Figure 38. Sat3 and Sat4 are offset from the center of the inline portion of the swarm. The distance between satellites has been exaggerated to create a sparse aperture. The MATLAB script from

Appendix A computes an instantaneous aperture of 93 m, resulting in a 34m resolution using Eqn (1), $\theta r = 1.22\ (0.0086m / 93m)\ 300{,}000m = 34m$ resolution.

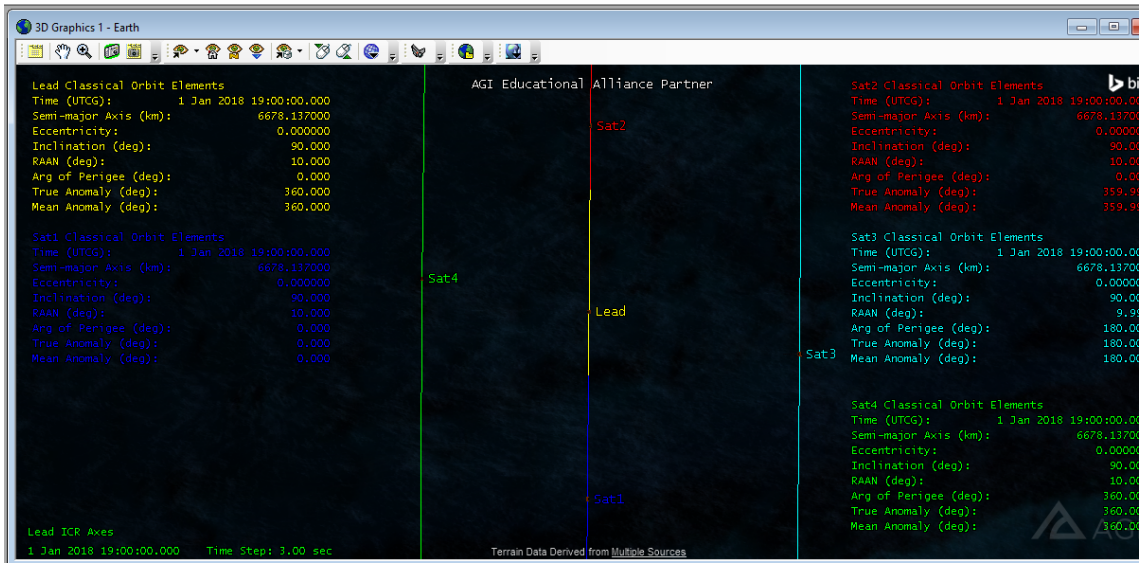

Figure 38. 3D Top View Orbital Positioning for Helix Hybrid_v3 at 0 degrees latitude. Adapted from: [27].

In Figure 39, a side view at the equator, we note that Sat 3 is at a higher altitude and Sat4 is at a lower altitude than the inline Lead, Sat1, and Sat2. The vertical variance provides for greater safety in flight operations for the swarm.

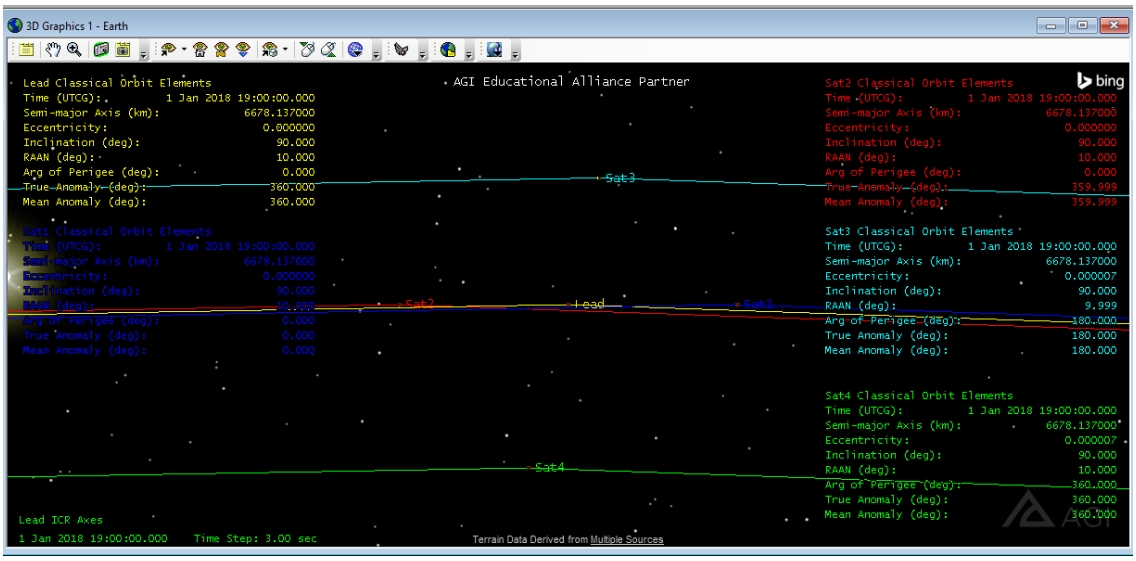

Figure 39. 3D Side View Orbital Positioning for Helix Hybrid_v3 at 0 degrees latitude. Adapted from: [27].

Figure 40 shows the 2D ground track of the swarm at 30 degrees latitude. The direction of travel is toward the North Pole.

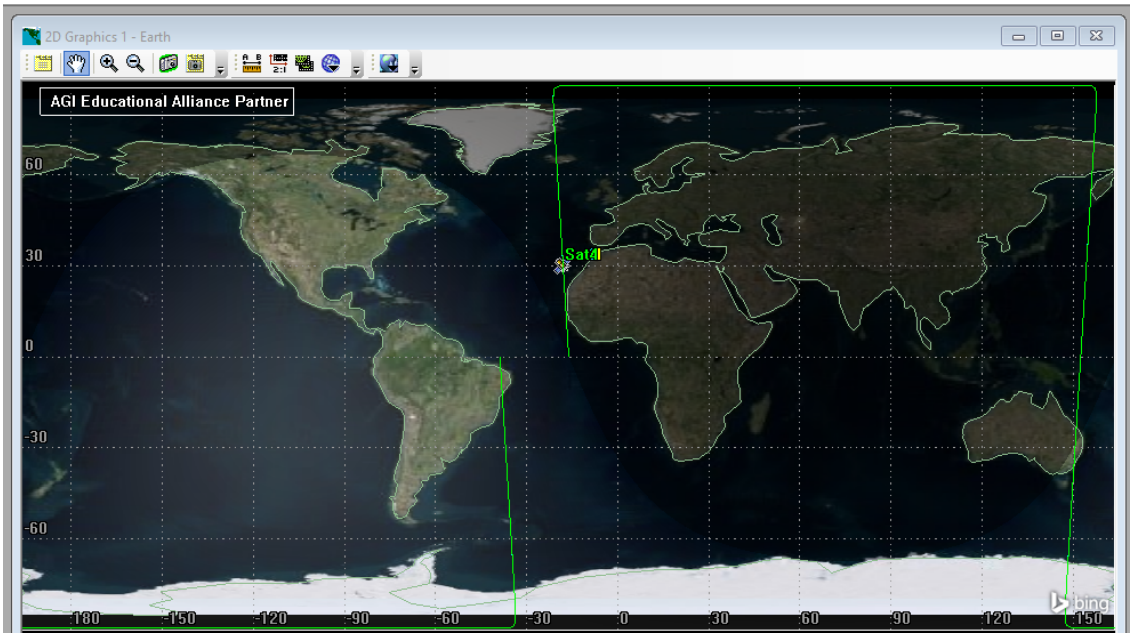

Figure 40. 2D Orbital Positioning for Helix Hybrid_v3 at 30 degrees latitude. Adapted from: [27].

Figure 41 indicates from above that the swarm is at thirty degrees latitude. The direction of flight is to the top of the screen as we view the swarm from the top. The formation is still spread out but Sat3 and Sat4 are beginning to move toward the rest of the formation horizontally. There is still very good dispersion. Using the MATLAB script to determine the distances between the satellites provides a derivation of 87m for the aperture diameter. Using Rayleigh's criterion, Eqn (1), $\theta r = 1.22\ (0.0086m / 87m)\ 300{,}000m = 36m$ resolution again. It is interesting to note that the change in diameter from thirty degrees latitude is six meters.

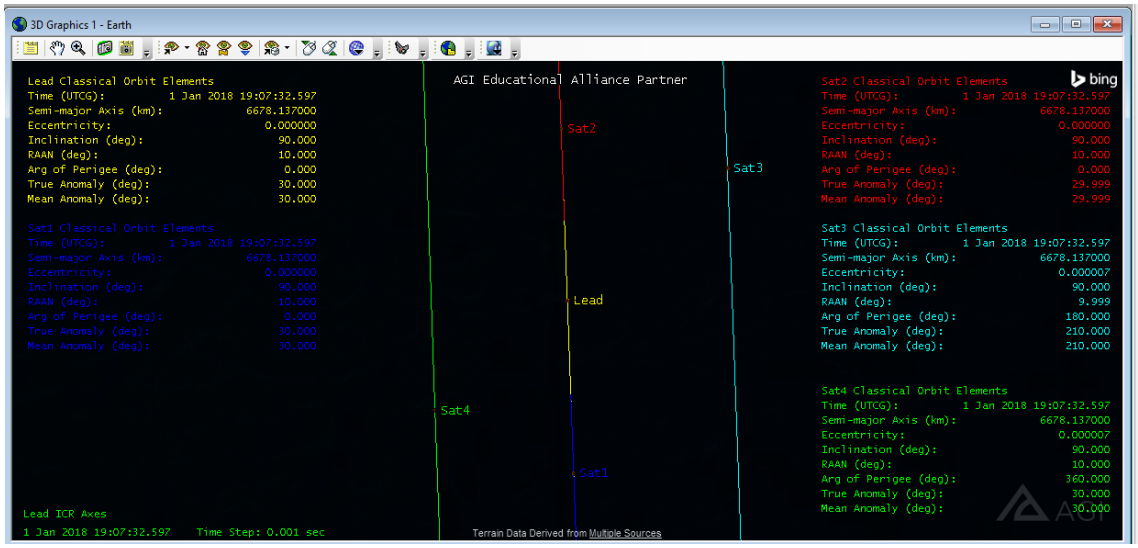

Figure 41. 3D Top View Orbital Positioning for Helix Hybrid_v3 at 30 degrees latitude. Adapted from: [27].

From the side in Figure 42, we see that Sat 3 is still at a higher altitude and Sat4 is at a lower altitude than the inline Lead, Sat1, and Sat2. Sat3 is now ahead of the Lead and Sat4 is behind as the orbit progresses faster than expected.

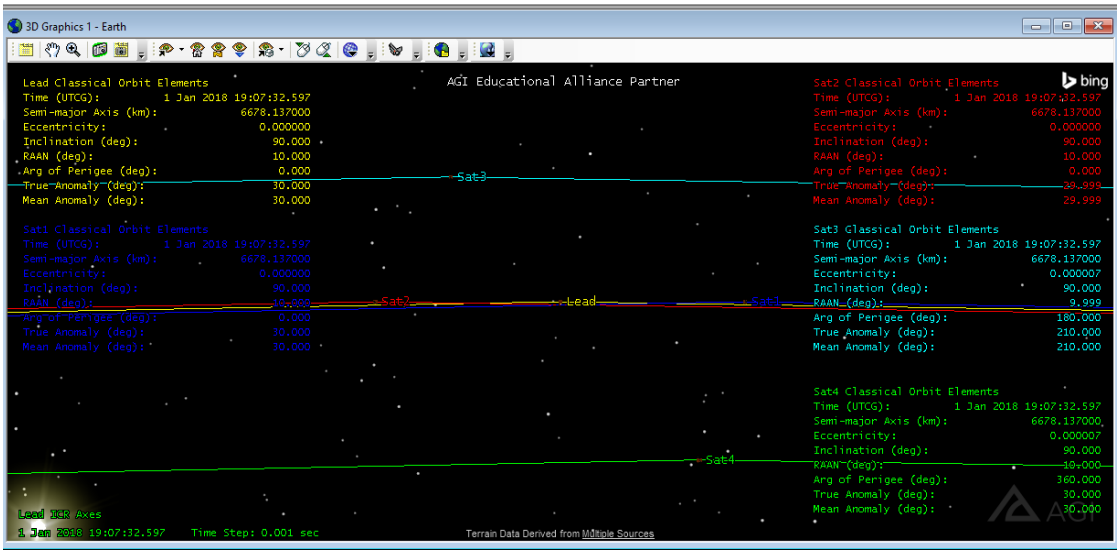

Figure 42. 3D Side View Orbital Positioning for Helix Hybrid_v3 at 30 degrees latitude. Adapted from: [27].

In Figure 43, the 2D ground track shows the swarm at sixty degrees latitude. The direction of travel is toward the North Pole.

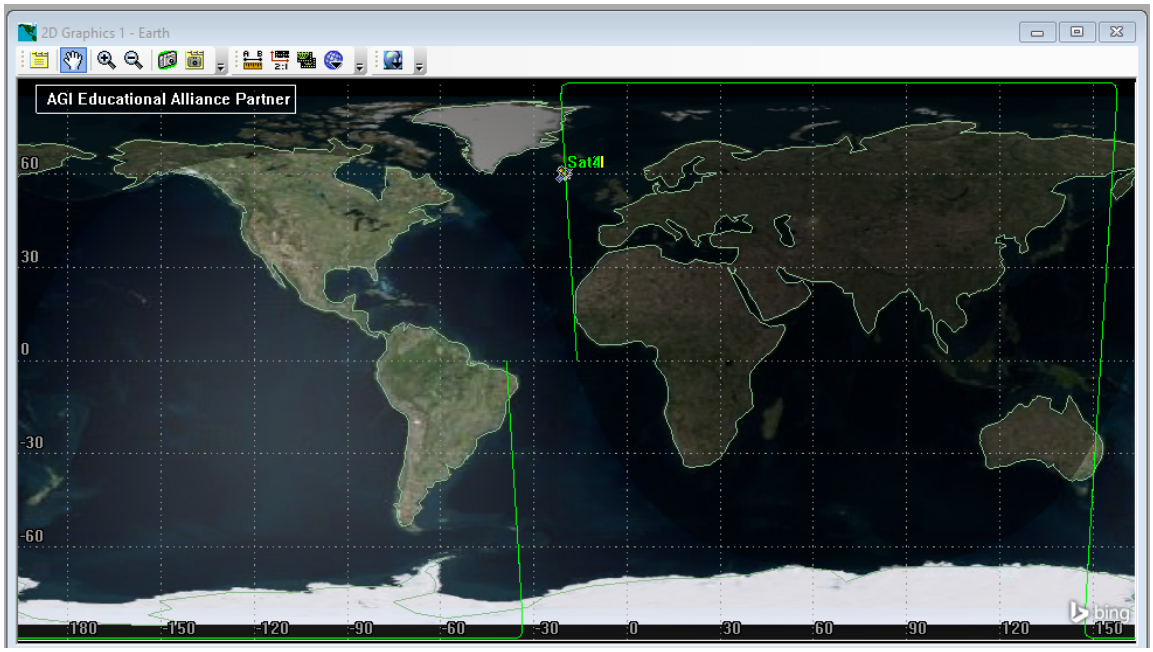

Figure 43. 2D Orbital Positioning for Helix Hybrid_v3 at 60 degrees latitude. Adapted from: [27].

Figure 44 views the swarm at sixty degrees latitude. The direction of flight is to the top of the screen as we view the swarm from the top. The formation remains spread out but the separation between Sat3 and Sat4 has decreased, moving closer to the rest of the center line of the formation. Using the MATLAB script to determine the distances between the satellites provides a derivation of 70m for the aperture diameter. Using Rayleigh's criterion, Eqn (1), $\theta r = 1.22\ (0.0086m / 70m)\ 300{,}000m = 45m$ resolution. It is important to note that the aperture is now elongated and may cause some distortion to the image as noted in Chapter II or allow the image to be viewed as a single aperture SAR satellite. With additional satellites in the swarm, the elongation can be removed.

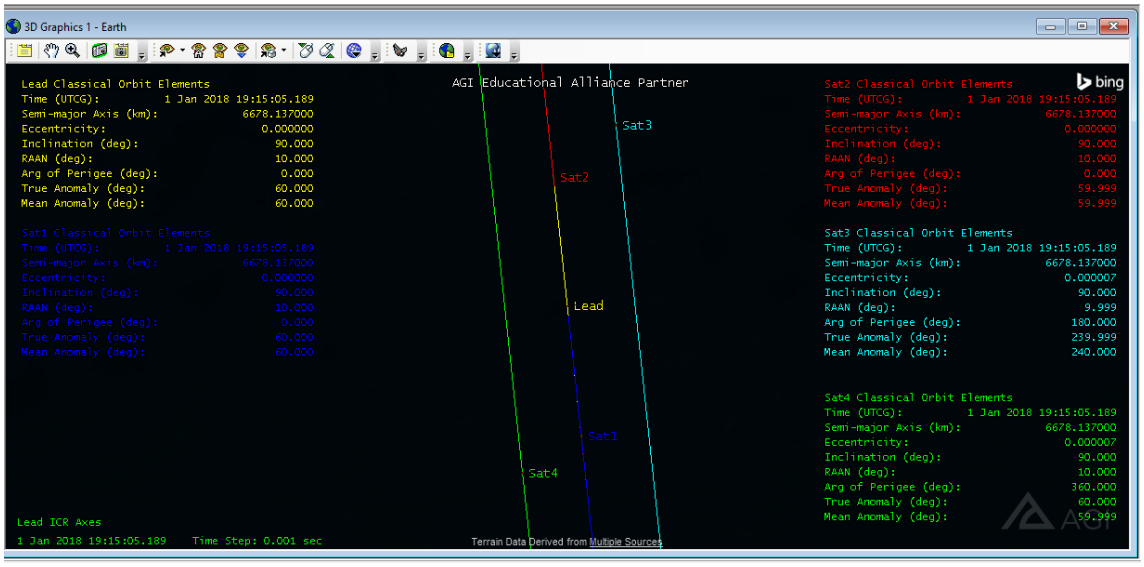

Figure 44. 3D Top View Orbital Positioning for Helix Hybrid_v3 at 60 degrees latitude. Adapted from: [27].

In Figure 45 we see from the side that Sat 3 is still at a higher altitude and Sat4 is at a lower altitude than the inline Lead, Sat1, and Sat2. Sat3 and is now ahead of Sat2 and Sat4 is behind Sat1. Their progressions away from the horizontal centerline have slowed.

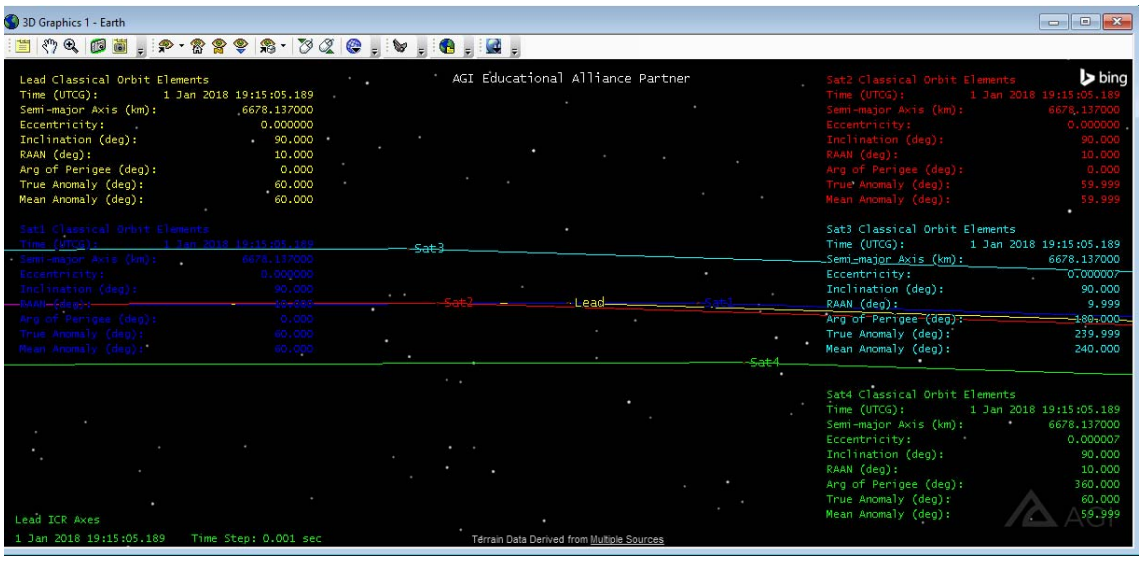

Figure 45. 3D Side View Orbital Positioning for Helix Hybrid_v3 at 60 degrees latitude. Adapted from: [27].

Figures 46 and 47 represent the swarm from above over the North Pole at ninety degrees with the direction of travel to the top of the screen. Notice that Sat3 and Sat4 are now in line with the other three spacecraft in the swarm. As Sat3 and Sat4 cross the pole, they will switch which side of the formation they flank. The sparse aperture capability is again reduced to a simple SAR ability as discussed in Chapter II.

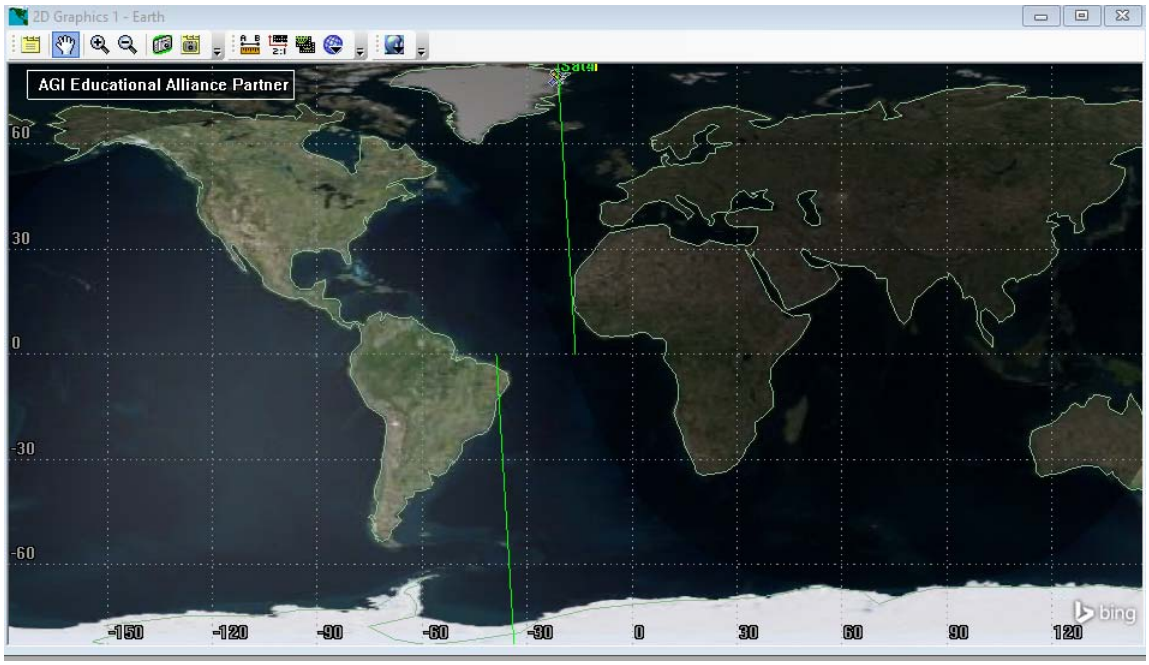

Figure 46. 2D Orbital Positioning for Helix Hybrid_v3 at 90 degrees latitude. Adapted from: [27].

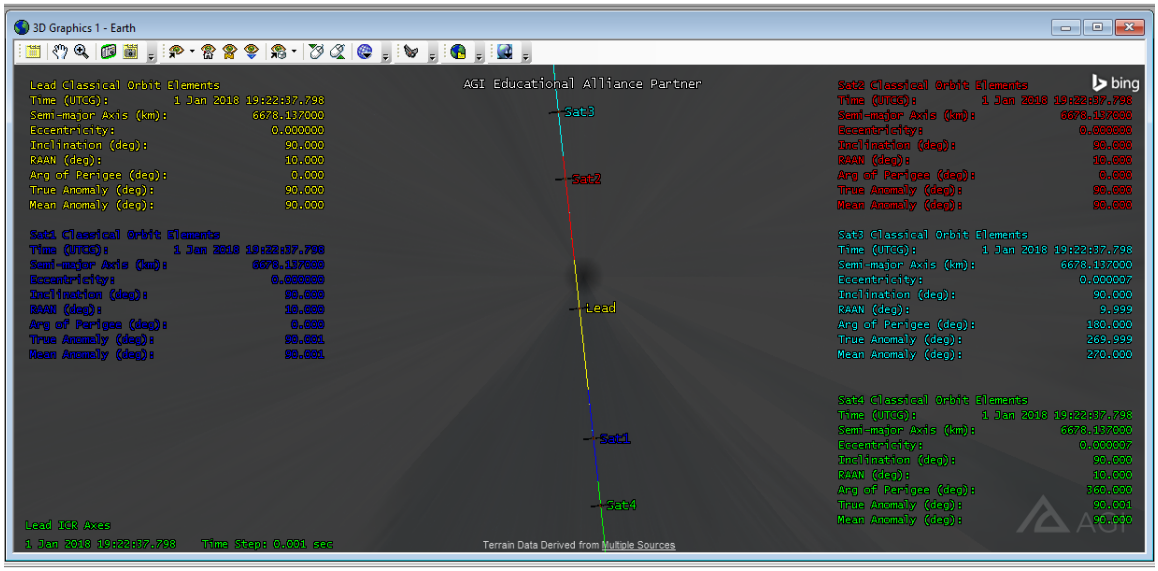

Figure 47. 3D Top View Orbital Positioning for Helix Hybrid_v3 at 90 degrees latitude. Adapted from: [27].

From the 3D side view in Figure 48, the direction of travel is to the left of the screen. It is difficult to see but there is lateral separation of less than ten meters for Sat3 at a higher

altitude and Sat4 at the same altitude but lower than the inline satellites. Though the swarm is stable and there are safe distances between the individual satellites, there is less altitude separation than expected, according to the orbital parameters inserted into STK. These parameters were adjusted in later versions of the helix hybrid simulation but this version was the most interesting in its findings as it led to a better understanding of how eccentricity can impact the spacing between satellites of a swarm.

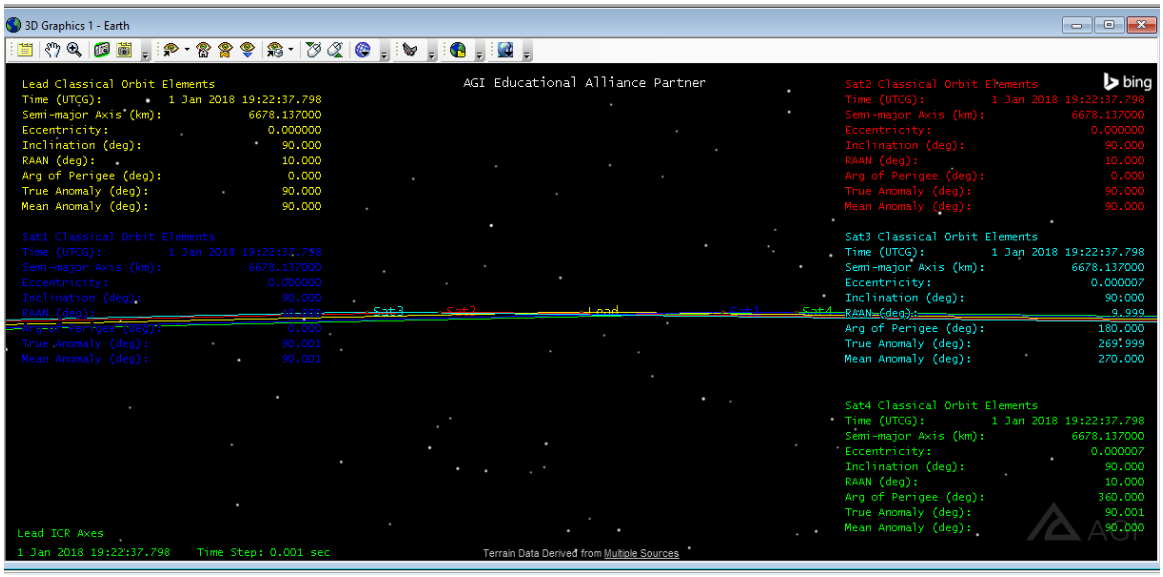

Figure 48. 3D Side View Orbital Positioning for Helix Hybrid_v3 at 90 degrees latitude. Adapted from: [27].

Figure 49 is a representation of the horizontal movement of the satellite throughout an entire orbit in MATLAB. The sampling is done at sixty second intervals which equates to a sampling every four degrees of latitude. There are one hundred samples that overlap the ninety-minute orbit. As is clearly demonstrated, the formation is completely stable. The red (Sat2), black (Lead), and blue (Sat1) dots remain inline without any movement. The teal (Sat3) and green (Sat4) dots move circularly around the other satellites in offset circles without convergence or divergence indicating that the formation is stable.

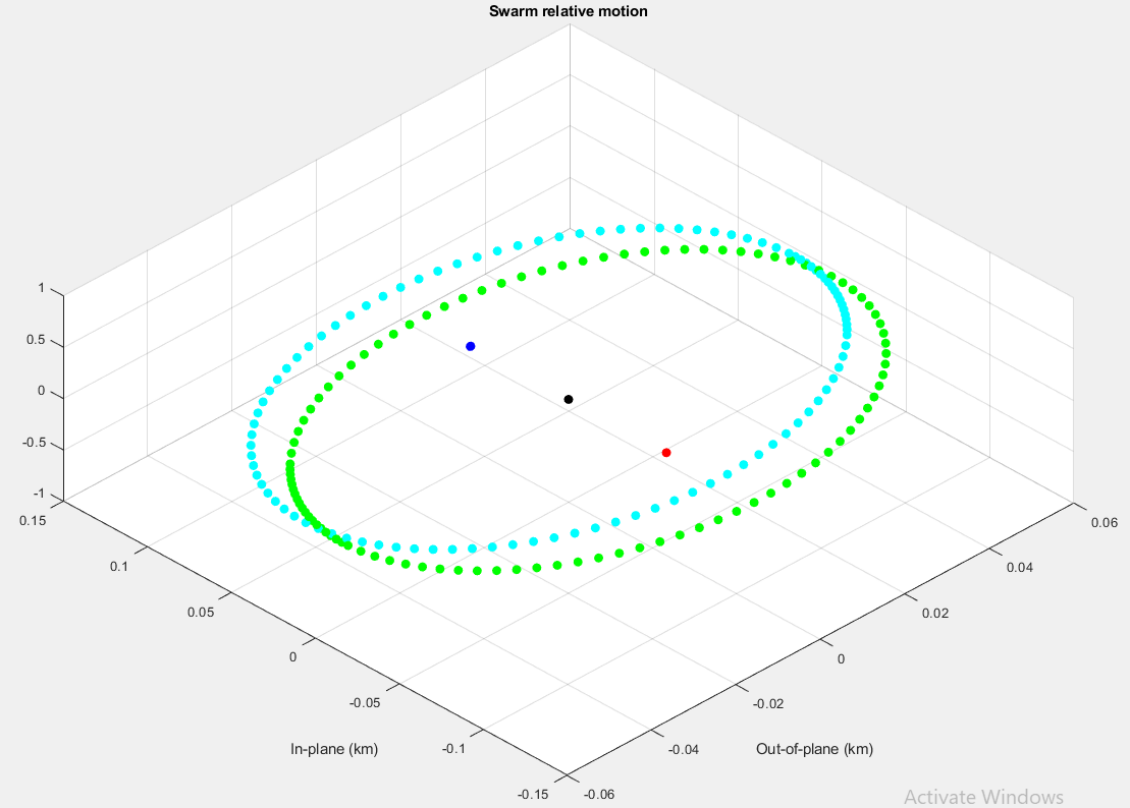

Figure 49. Horizontal Relative Motion for Helix Hybrid_v3. Adapted from: [28].

In Figure 50 we see that the black (Lead) the red (Sat2), and blue (Sat1) dots remain stationary. Again the teal (Sat3) and green (Sat4) dots move in a circle around the other satellites in offset circles without convergence or divergence indicating that the formation is stable vertically. Sat3 and Sat4 fly one to the left and below and one to the right and above the inline satellites until the swarm crosses the poles at different altitudes where Sat3 and Sat4 switch sides and altitude. Sat3 flies at a higher altitude than the inline satellites moving toward the North Pole and lower moving toward the South Pole. Sat4 flies at a lower altitude than the inline satellites moving toward the North Pole and higher moving toward over the South Pole.

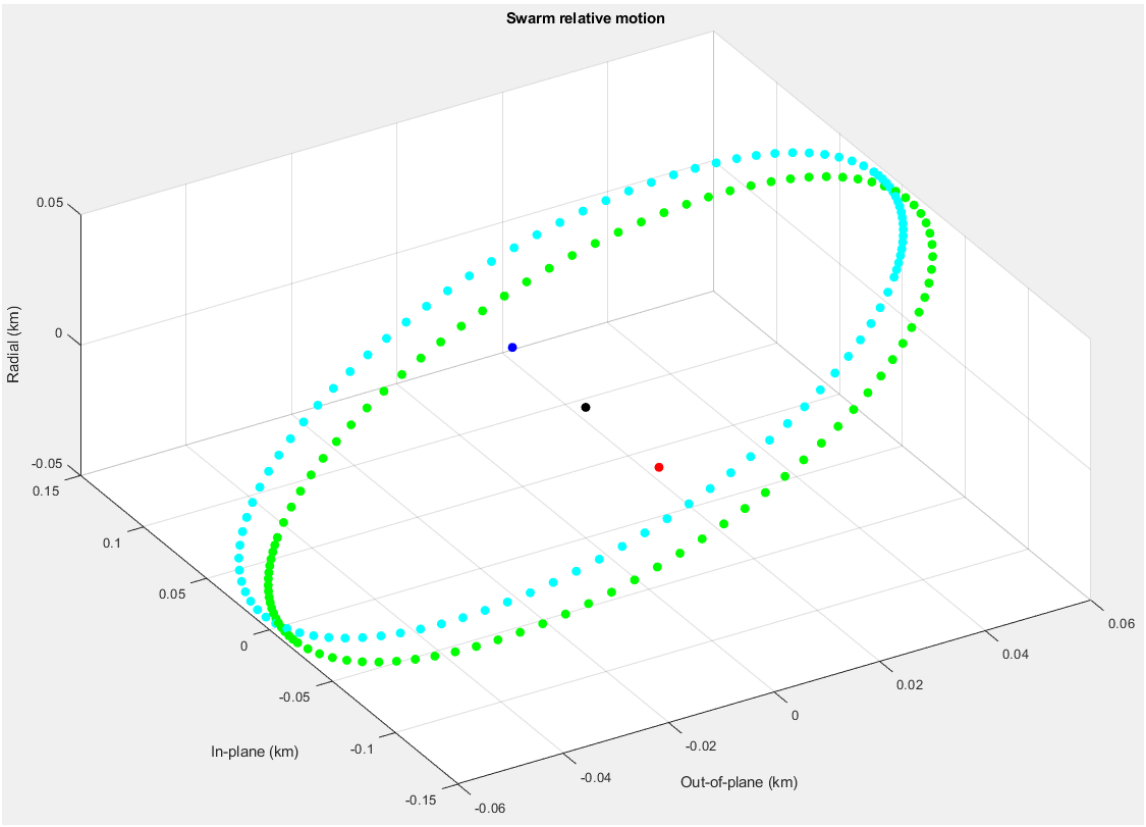

Figure 50. Vertical Relative Motion for Helix Hybrid_v3. Adapted from: [28].

In conclusion, the helix and inline hybrid formation provides a very stable formation. Safe flight operations for this formation are of some concern over the poles but can easily be adjusted by decreasing the eccentricity of Sat3 and increasing the eccentricity of Sat4 over the North. The imaging dispersal pattern of the sparse aperture is good but not great due to elongation as Sat3 and Sat4 move closer to the front and rear of the inline satellites.

D. CARTWHEEL HYBRID MODEL

The cartwheel hybrid model was selected because of the safety measures integrated into flight operations and dispersal patterns of the swarm. The most significant finding was the difference in resolution capabilities in the northern and southern hemispheres. The cartwheel hybrid is a viable model and provides more inherent orbital separation than the

pendulum and inline hybrid but less than the helix and inline hybrid. The cartwheel hybrid has more satellite dispersion than both the pendulum and inline hybrid and the helix and inline hybrid models.

The cartwheel hybrid model is different from the pendulum hybrid and the helix hybrid because we did away with the inline concept. The Lead (leader) satellite remains in the center of formation as the follower satellites fly one to the left and one to the right of the formation at different altitudes. Another flies to the front right and the last one flies to the left rear of the formation. They also have offsetting altitudes. As the formation crosses the poles, the satellites fall into a line separated in altitude by only a few meters. This formation is the most complicated of the three highlighted in this thesis.

The 2D ground track of Figure 51 depicts the swarm is over the equator. The direction of travel is toward the North Pole.

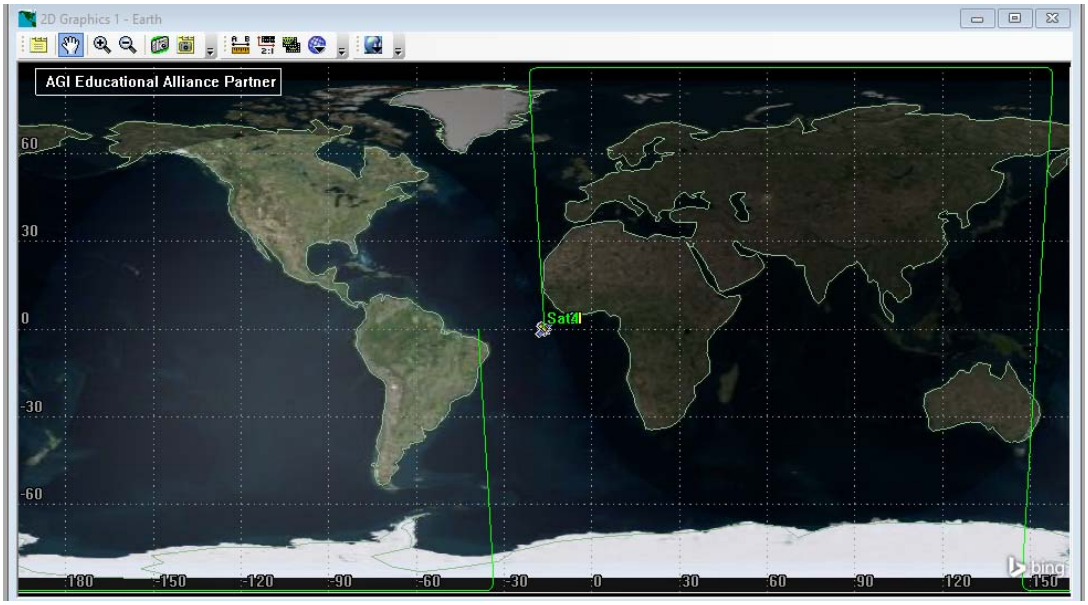

Figure 51. 2D Orbital Positioning for Cartwheel Hybrid_v9 at 0 degrees latitude. Adapted from: [27].

The formation is spread out to its maximum extent at the equator in Figure 52. All satellites are offset from the sole Lead satellite in the center of the formation both

horizontally and laterally. The distance between satellites has been exaggerated to create a large aperture. The MATLAB script of Appendix A computes an instantaneous distance of 105 meters. Using Rayleigh's criterion, Eqn (1), $\theta r = 1.22\ (0.0086m / 105m)\ 300{,}000m = 30m$ resolution. This is much better than both the pendulum hybrid model and the helix hybrid model due to the increased spacing between satellites.

Figure 52. 3D Top View Orbital Positioning for Cartwheel Hybrid_v9 at 0 degrees latitude. Adapted from: [27].

In Figure 53 we note that from the side view, Sat1 and Sat 3 are at a higher, but not the same, altitudes than the Lead. Sat2 and Sat 4 are at a lower, and again offsetting, altitudes than the Lead.

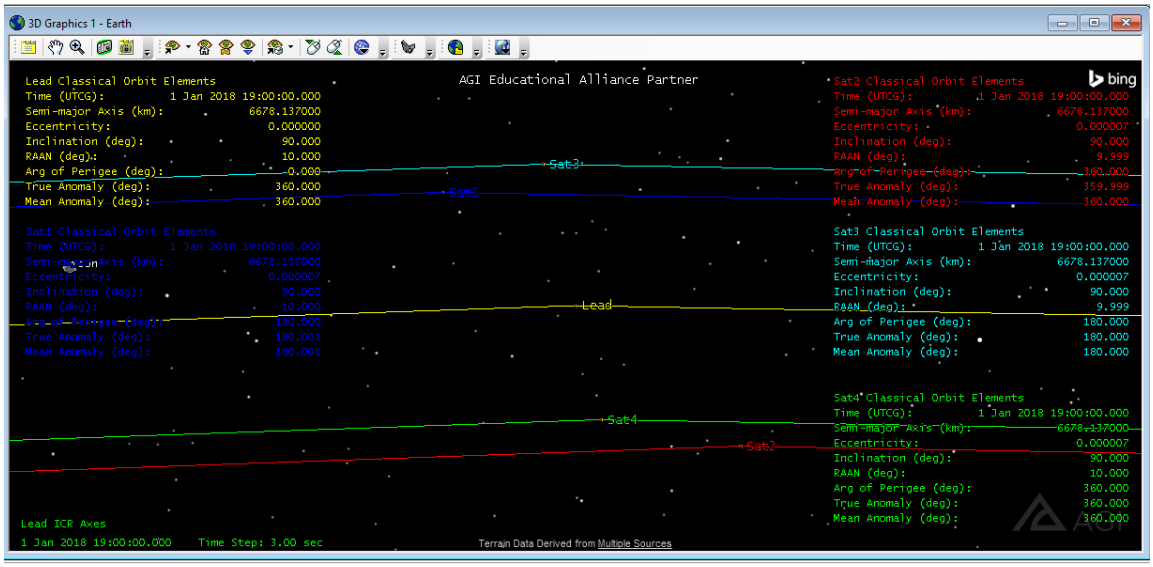

Figure 53. 3D Side View Orbital Positioning for Cartwheel Hybrid_v9 at 0 degrees latitude. Adapted from: [27].

In Figure 54, the 2D ground track shows the swarm at thirty degrees latitude. The direction of travel is toward the North Pole.

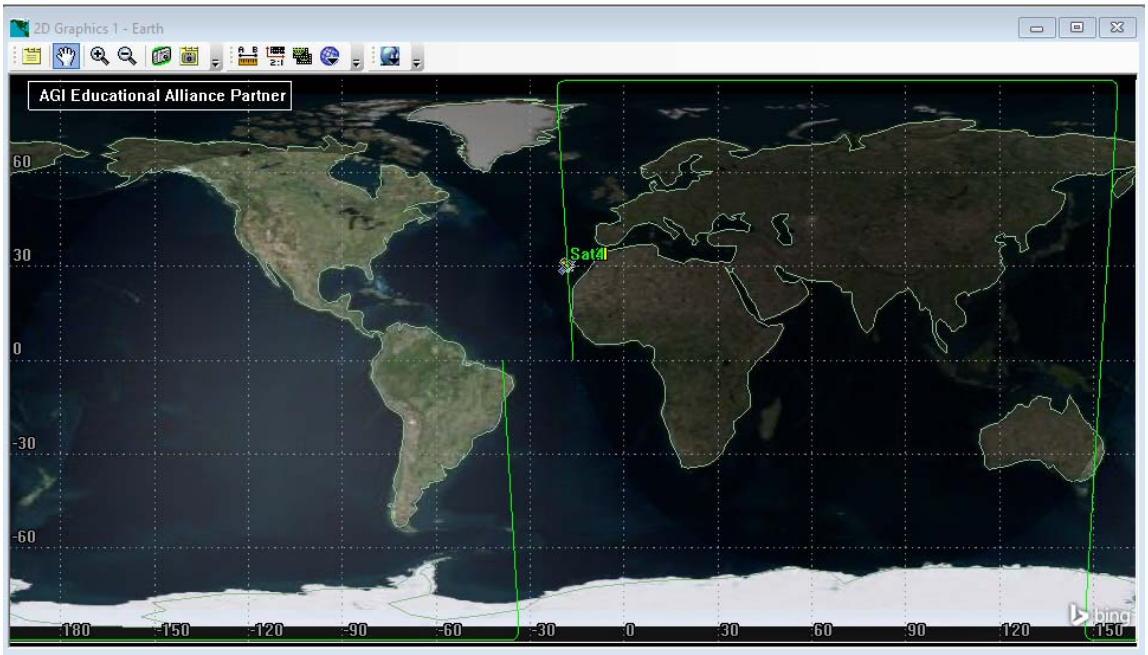

Figure 54. 2D Orbital Positioning for Cartwheel Hybrid_v9 at 30 degrees latitude. Adapted from: [27].

Figure 55 identifies that the swarm is at thirty degrees latitude. The direction of flight is to the top of the screen as we view the swarm from above. The formation is still spread out but Sat1 and Sat4, though at different altitudes, are trading forward and rear positions on the right side. The same is also true of Sat2 and Sat3 on the left of the formation. There is still very good dispersion but, there is more elongation than expected at this latitude The MATLAB script computes a distance of 79 meters for the aperture diameter. Using Rayleigh's criterion, Eqn (1), $\theta r = 1.22\ (0.0086m / 79m)\ 300{,}000m = 40m$ resolution again. It is interesting to note that the cartwheel hybrid at thirty degrees is comparable in resolution to the helix hybrid at the same latitude.

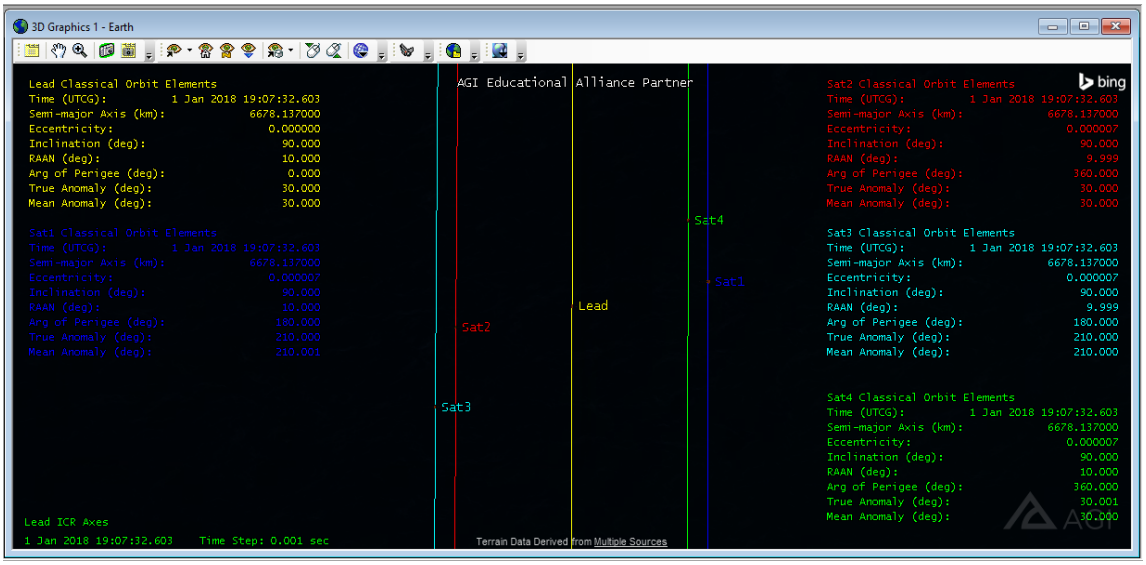

Figure 55. 3D Top View Orbital Positioning for Cartwheel Hybrid_v9 at 30 degrees latitude. Adapted from: [27].

Figure 56 shows the swarm from the side at thirty degrees latitude. Sat1 and Sat 3 are still at higher altitudes than the Lead and Sat2 and Sat4 are at lower altitudes than the Lead.

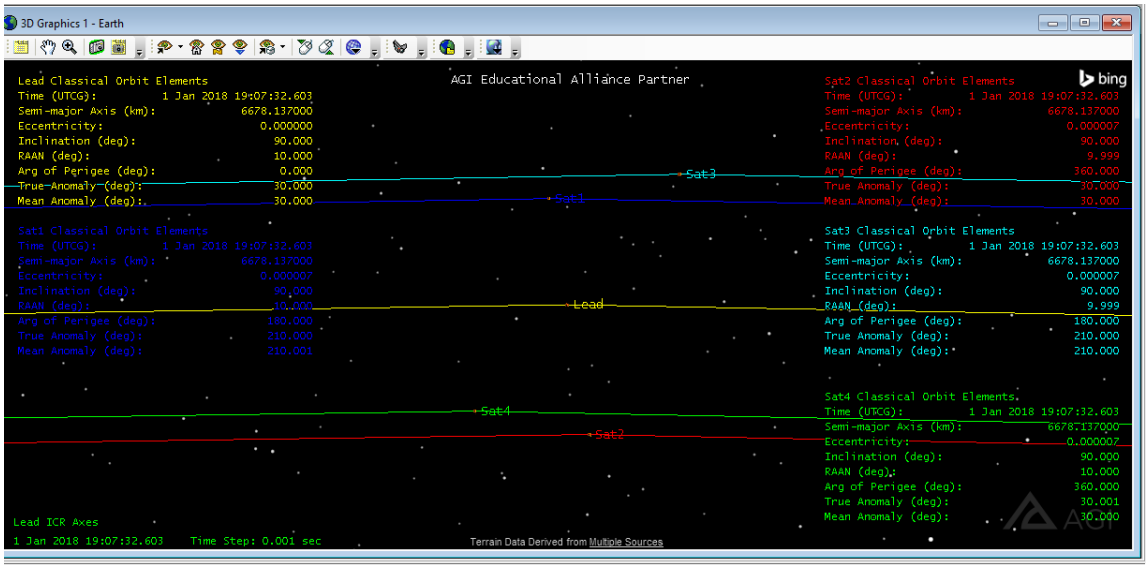

Figure 56. 3D Side View Orbital Positioning for Cartwheel Hybrid_v9 at 30 degrees latitude. Adapted from: [27].

In Figure 57, the 2D ground track shows the swarm at sixty degrees latitude. The direction of travel is toward the North Pole.

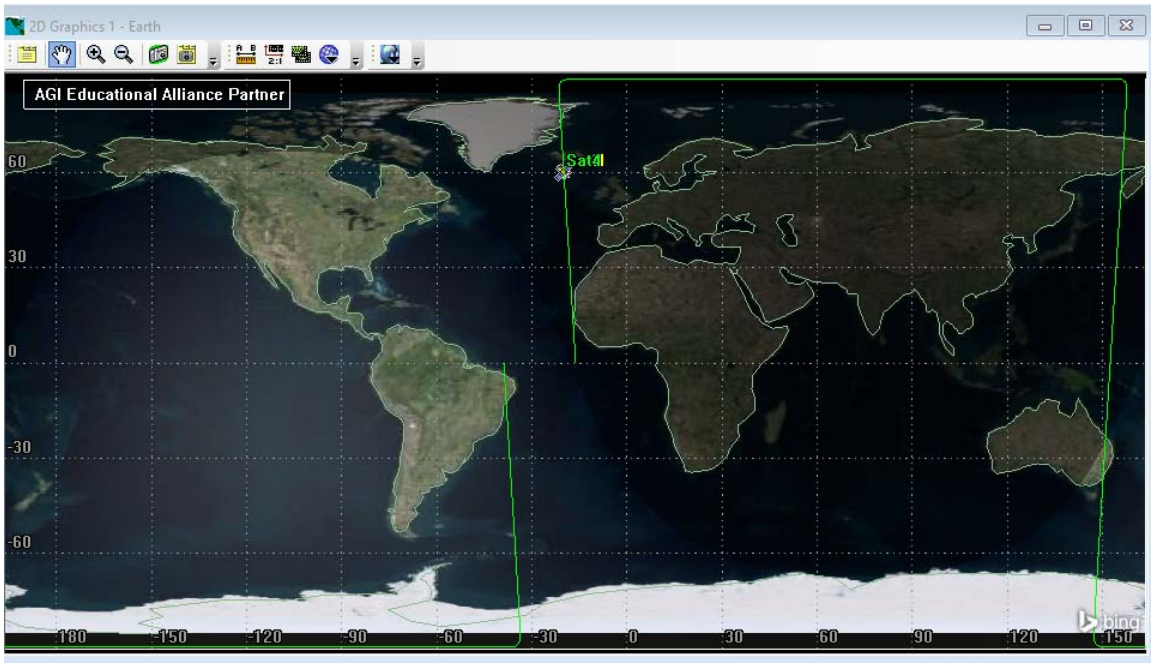

Figure 57. 2D Orbital Positioning for Cartwheel Hybrid_v9 at 60 degrees latitude. Adapted from: [27].

Figure 58 views the swarm at sixty degrees latitude. The direction of flight is to the top of the screen as we view the swarm from the top. The formation remains spread out but the distance of Sat3 and Sat4 have moved closer to the center line of the formation. Dispersion is still rather good for conducting imaging as expected. The MATLAB script computed an instantaneous aperture diameter of 90 meters. Using Rayleigh's criterion, Eqn (1), θr = 1.22 (0.0086m / 90m) 300,000m = 35m resolution. The resolution is reduced by only five meters from 30 degrees to 60 degrees latitude. It is important to note that the aperture is not as elongated as it was at 30 degrees latitude. Also note that the formation is not collapsing into the centerline as much as in the two previous models.

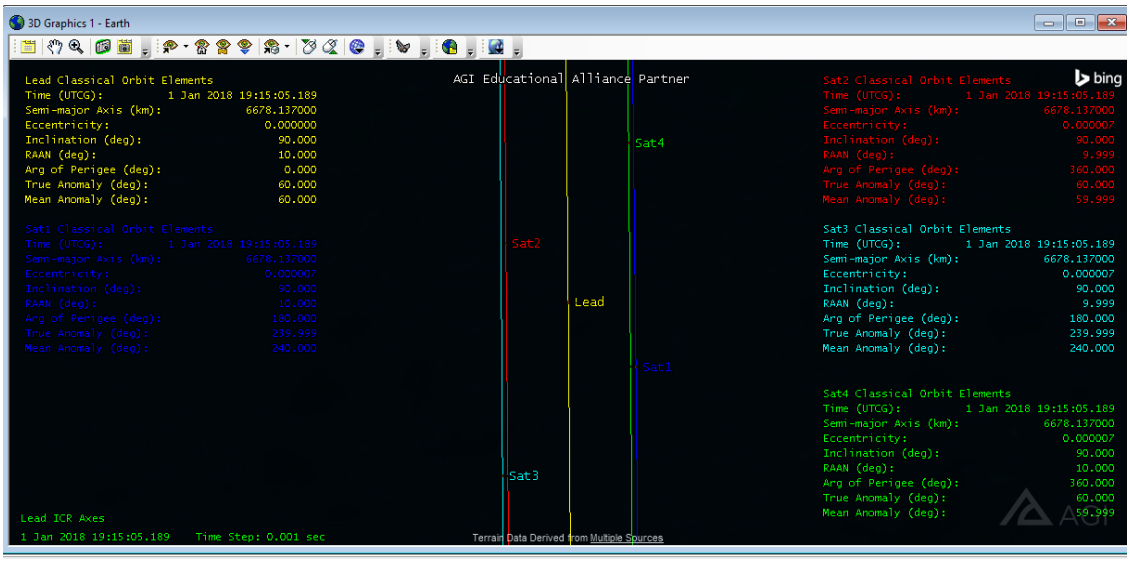

Figure 58. 3D Top View Orbital Positioning for Cartwheel Hybrid_v9 at 60 degrees latitude. Adapted from: [27].

From the side at 60 degrees in Figure 59, we see that Sat1 and Sat 3 are still at higher altitudes than the Lead and Sat2 and Sat4 are at lower altitudes than the Lead.

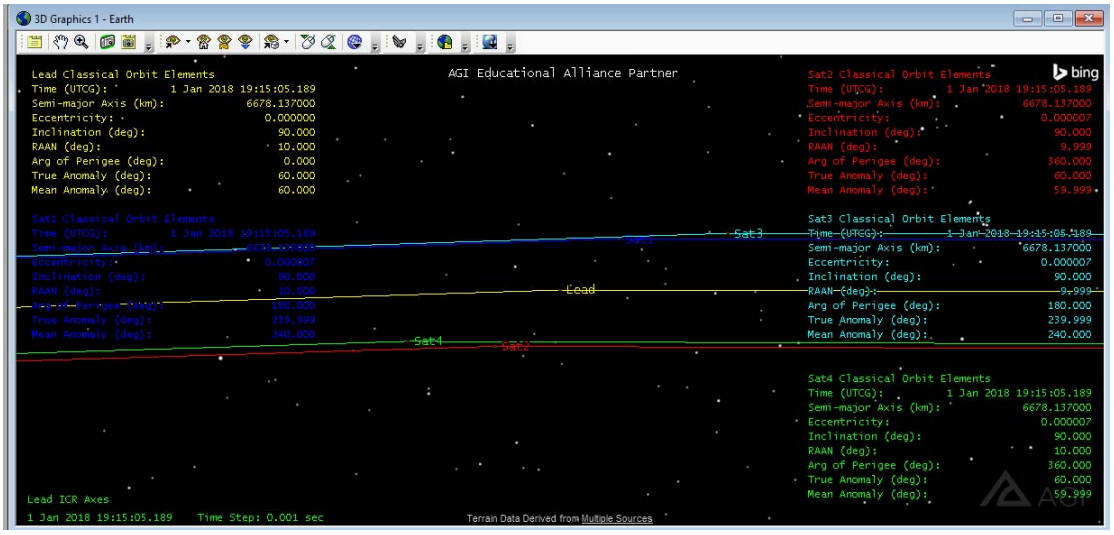

Figure 59. 3D Side View Orbital Positioning for Cartwheel Hybrid_v9 at 60 degrees latitude. Adapted from: [27].

In Figure 60, the 2D ground track shows the swarm at ninety degrees latitude. The direction of travel is toward the North Pole.

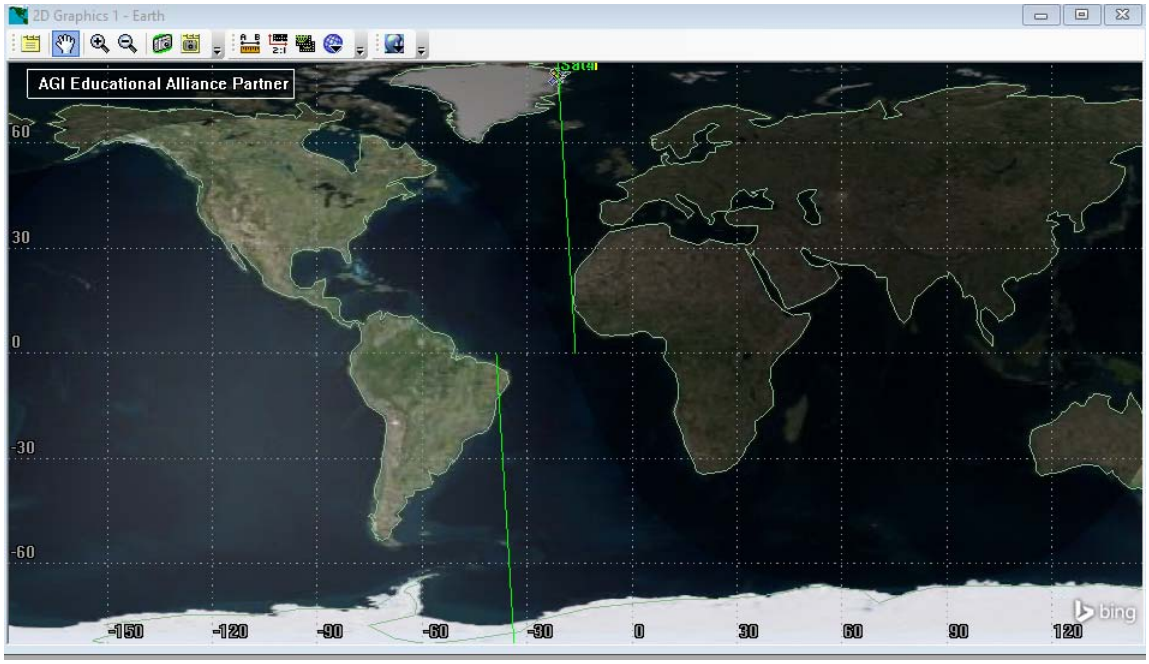

Figure 60. 2D Orbital Positioning for Cartwheel Hybrid_v9 at 90 degrees latitude. Adapted from: [27].

Figure 61 represents the swarm over the North Pole at ninety degrees with the direction of travel to the top of the screen as viewed from above. Notice that all five satellites are now in line at equal distances of separation. As Sat1 and Sat3 cross the pole, they will switch altitudes and sides of the formation with Sat2 and Sat4. The sparse aperture capability is again reduced to a simple SAR ability at the poles due to the inline formation.

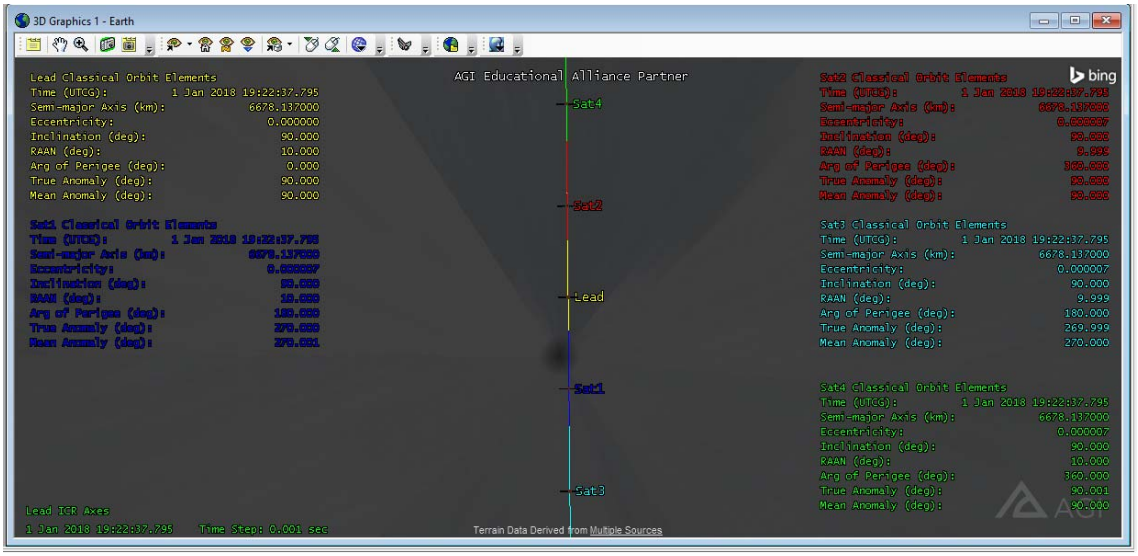

Figure 61. 3D Top View Orbital Positioning for Cartwheel Hybrid_v9 at 90 degrees latitude. Adapted from: [27].

As we view the swarm from the side over the North Pole in Figure 62, it is difficult to see but there is an altitude difference of less than ten meters for all five of the satellites. This provides additional flight safety measures but can be increased by adding eccentricity to Sat2 and Sat4 over the North Pole and increasing eccentricity to Sat1 and Sat3 over the South Pole.

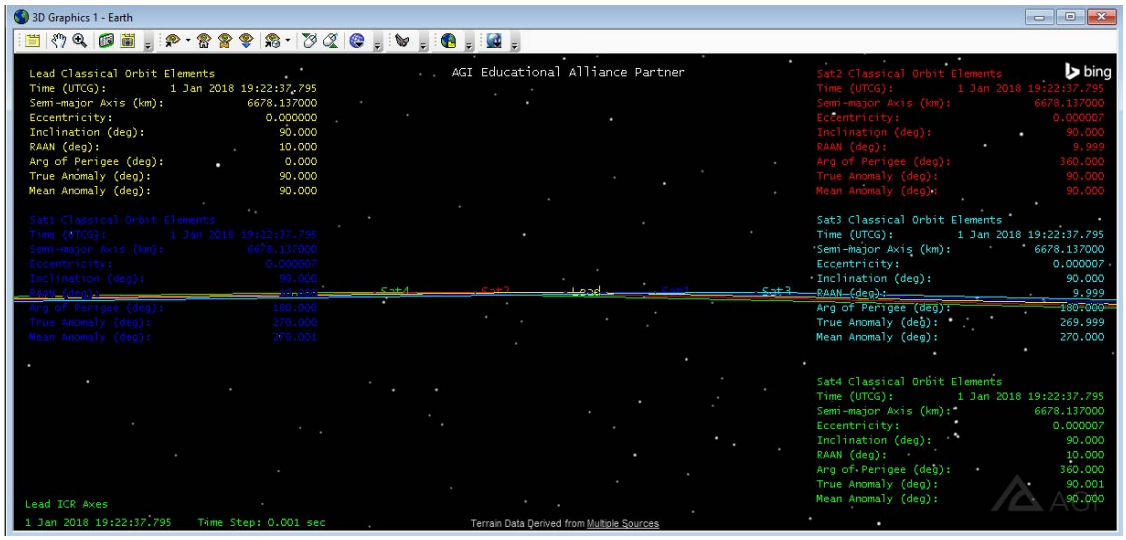

Figure 62. 3D Side View Orbital Positioning for Cartwheel Hybrid_v9 at 60 degrees latitude. Adapted from: [27].

Figure 63 is a representation of the horizontal movement of the cartwheel hybrid swarm throughout an entire orbit in MATLAB. The sampling is done at sixty-second intervals which equates to a sampling of every four degrees of latitude. There are one-hundred samples that overlap the ninety-minute orbit. As is clearly demonstrated, the formation is completely stable. The black (Lead) dot has no movement. The blue (Sat1) red (Sat2), teal (Sat3) and green (Sat4) dots move circularly around the Lead satellite evenly but in offset circles without convergence or divergence indicating that the formation is stable.

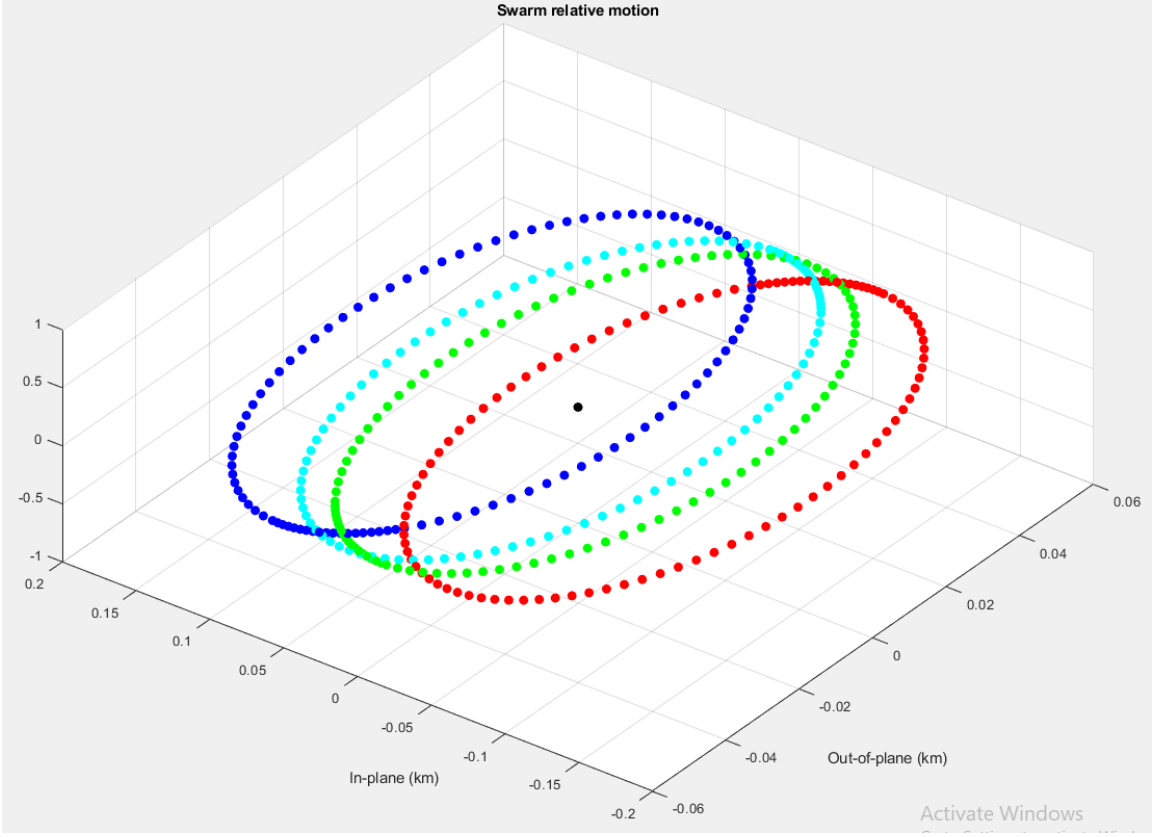

Figure 63. Horizontal Relative Motion for Cartwheel Hybrid_v9. Adapted from: [28].

In Figure 64 we see that the black (Lead) remains unmoved. The blue (Sat1) and red (Sat2) diagonally circle the Lead without crossing each other's paths, providing additional flight safety.

The teal (Sat3) and green (Sat4) dots also diagonally circle the Lead without crossing each other's paths, but opposite Sat1 and Sat2, providing additional flight safety. All five satellites move evenly without convergence or divergence indicating that the formation is stable vertically.

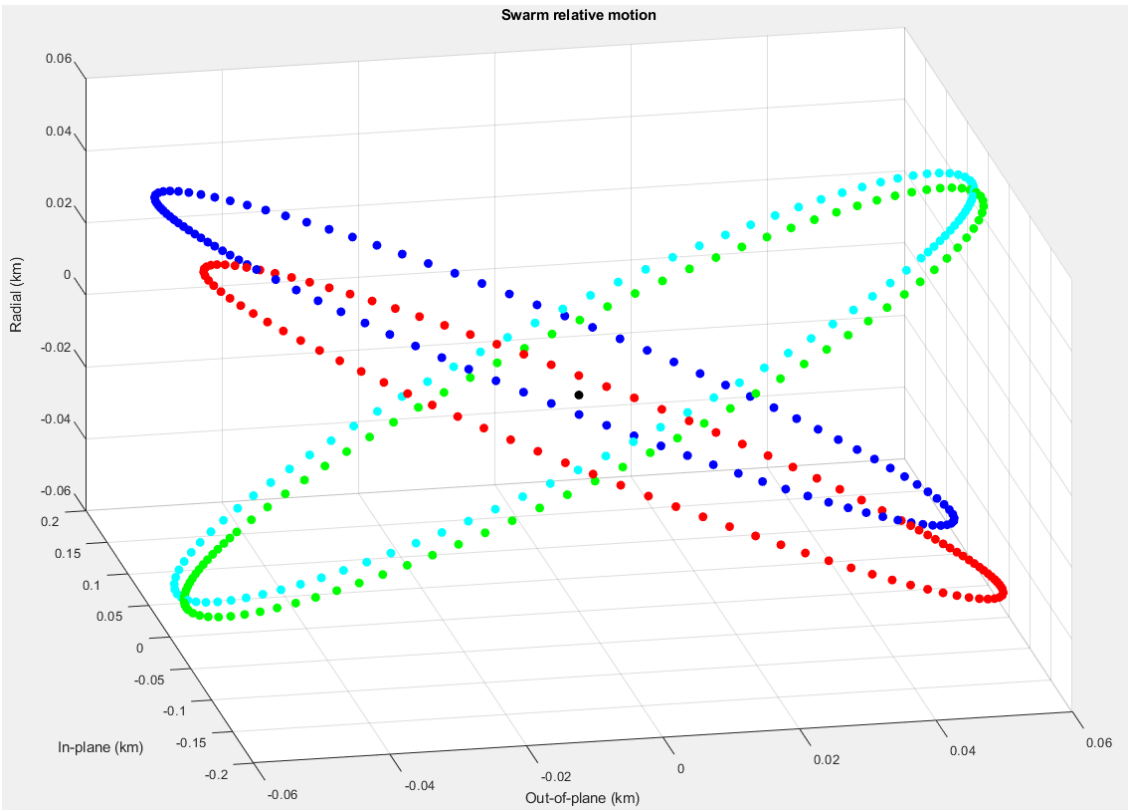

Figure 64. Vertical Relative Motion for Cartwheel Hybrid_v9. Adapted from: [28].

In conclusion, the cartwheel hybrid formation provides a very stable formation. It provides great dispersion techniques for imaging. As none of the flight paths intersect, both laterally and horizontally, the formation's flight safety measures show less likelihood of a conjunction. With some minor adjustments to eccentricity of the follower satellites, flight safety can be improved even more over the poles. However, there is some simplicity of design, engineering and orbital mechanics lost with the three inline satellites that is worth mentioning. The cartwheel hybrid formation is the most interesting formation of the three selected to highlight for this thesis because of the intricate relative motion patterns.

E. RESOLUTION COMPARISONS

The purpose of this sparse aperture swarm is to conduct radar imaging. This section provides an analysis of how the flight operations affect the modified resolution capabilities for each model.

Data from the inertial positioning vectors report from STK can be run through the MATLAB script over the course of just over one orbit. Each orbit is about ninety minutes. The graph is sampled at one minute, or four-degree, intervals and we use one-hundred samples on each chart. From this analysis we can graph the progression of accuracy for a modified resolution through an entire orbit. See Appendices A, B, and C for the MATLAB scripts.

The graph in Figure 65 represents resolution for the pendulum hybrid over the course of an orbit. Each step is a minute and there are one-hundred steps, each representing a change in four degrees of latitude. In the center of the graph, the resolution remains below 200m from thirty minutes (about 120 degrees latitude) to about sixty minutes (240 degrees latitude). Notice the spikes at the poles and how they vary. This is a result of using a sampling size of one minute. If the graph depicted the swarm at the exact time it crossed the poles, the graph would spike to infinity. As the samples were not taken precisely as the swarm passed the poles, the resolution shows the presence of the peak, but not the divergence to infinity.

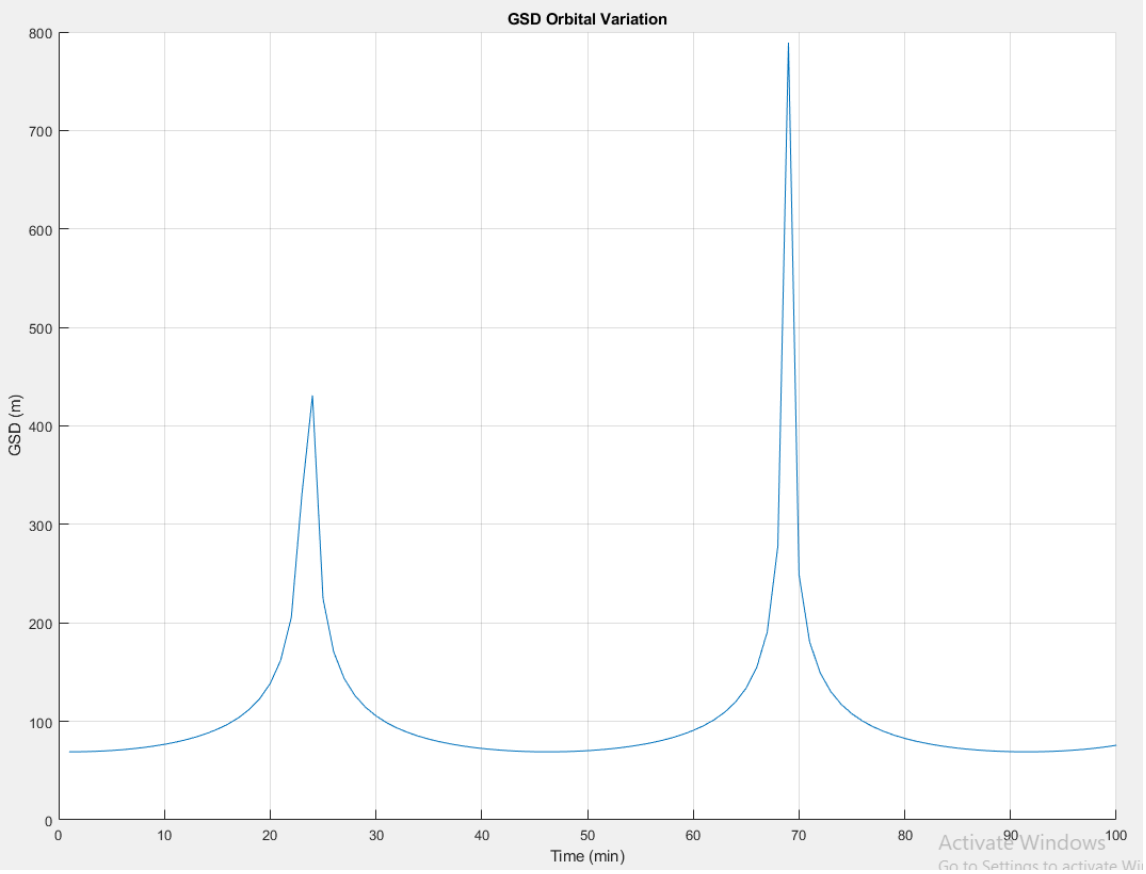

Figure 65. Resolution Variations for Pendulum and Inline Hybrid_v5. Adapted from: [28].

Figure 66 depicts the helix hybrid modified resolution graph and indicates that the pattern of resolution is very similar to the pendulum hybrid resolution graph. The major difference here is the resolution itself. At the equator, the pendulum hybrid resolution is 69m where the helix hybrid resolution is 34m. This is a function of spacing the satellites in the swarm because the pendulum hybrid aperture diameter is 46m and the helix hybrid aperture diameter is 93m.

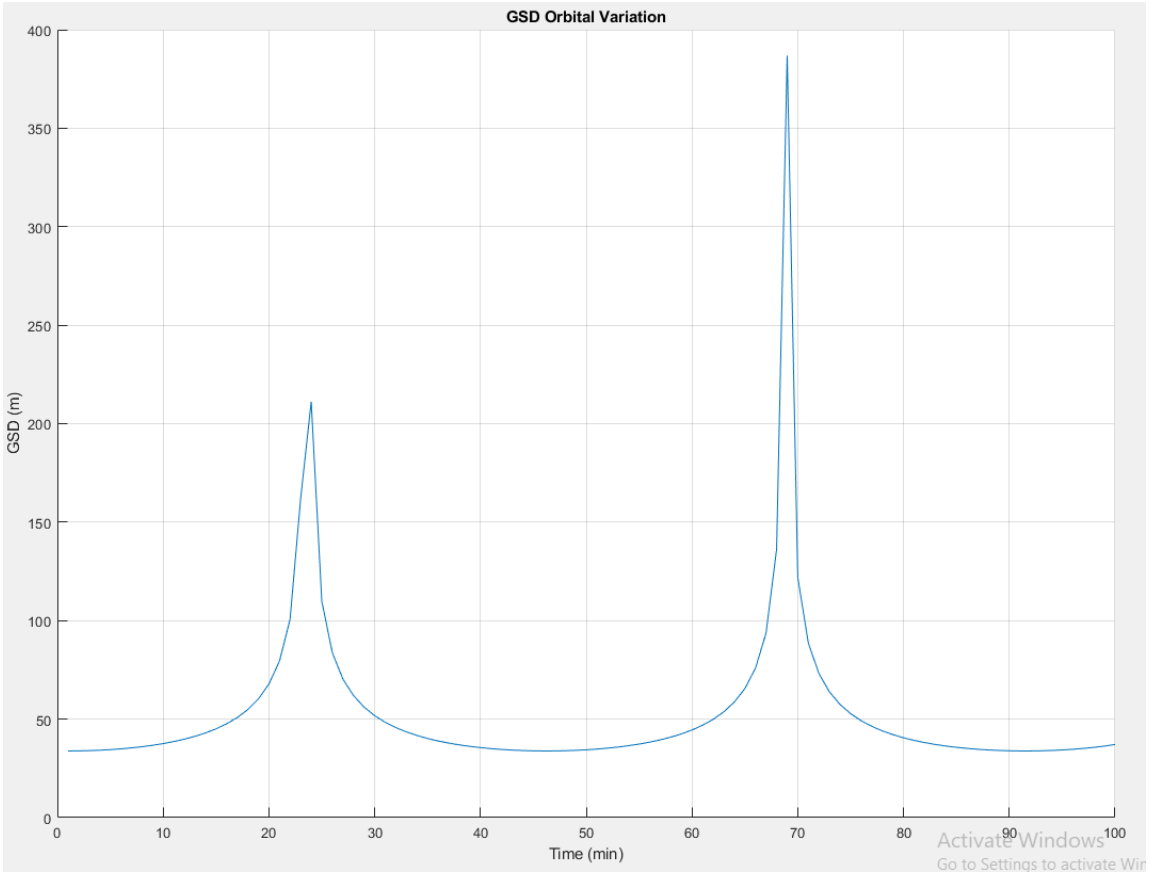

Figure 66. Resolution Variations for Helix and Inline Hybrid_v3. Adapted from: [28].

Figure 67 shows the cartwheel hybrid modified resolution graph and indicates an interesting difference in imaging patterns between the northern and southern hemispheres. This difference occurs because of the way that the swarm formation progresses through an orbit by spreading further forward with Sat3 and to the rear with Sat4 in plane with the swarm in the southern hemispheres and both closer to centerline out of plane as shown in Figure 53 at thirty degrees latitude in the northern hemisphere. This is significant because for successive cartwheel hybrid formations it was preferable to reverse this effect so that resolution is better over the northern hemisphere. Again, it is easy to notice the calculation spikes toward infinity as the swarm crosses the poles in a single line. This is a result of using a sampling size of one minute. If the graph depicted the swarm at the exact time it crossed the poles, the graph would spike to infinity.

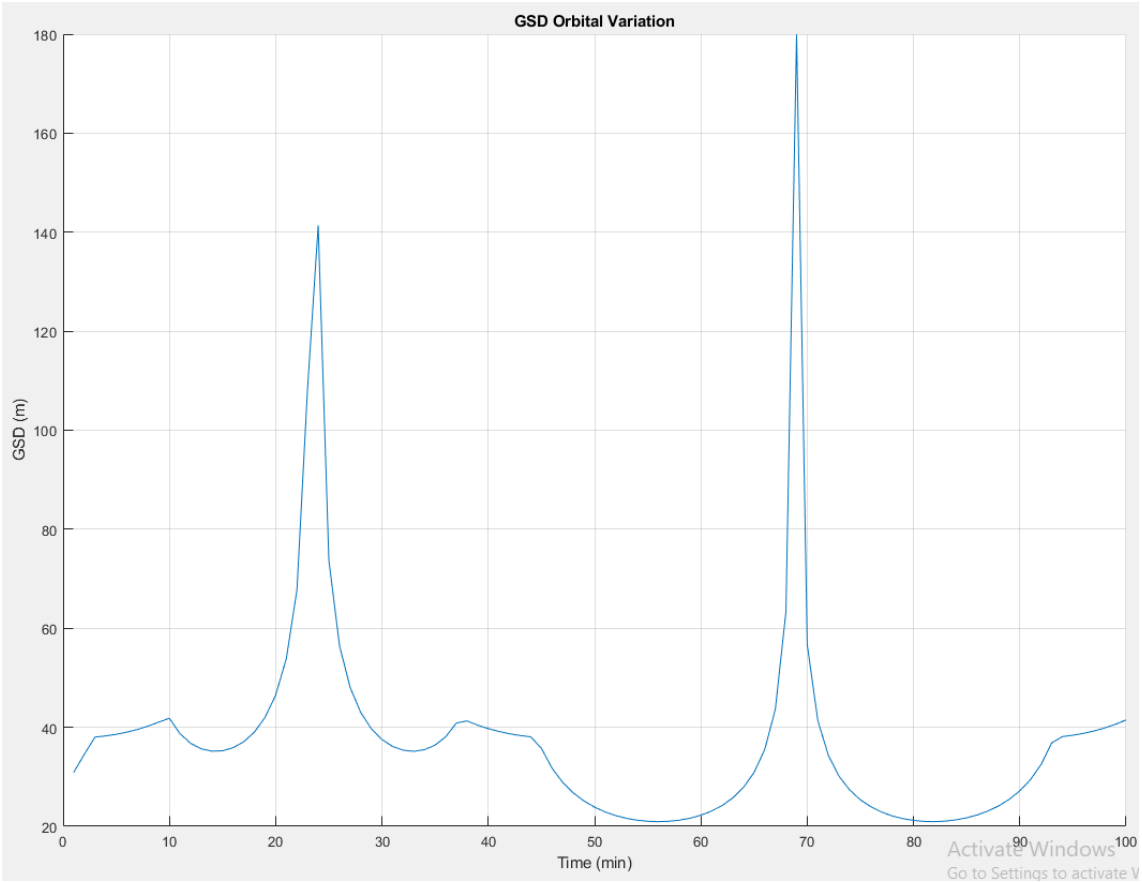

Figure 67. Resolution Variations for Cartwheel Hybrid_v9. Adapted from: [28].

In concluding the modified resolution analysis with Figure 68, both the helix hybrid and cartwheel hybrid seem to provide a better aperture pattern than the pendulum hybrid. However, the cartwheel hybrid provides better resolution over the southern hemisphere than the helix hybrid and about equal resolution capability over the northern hemisphere. Also, the cartwheel hybrid maintains dispersion of the satellites for a longer period before crossing the South Pole. In addition, the helix hybrid provides more imaging consistency than the cartwheel hybrid. This should be considered for any future research into processing data into imagery.

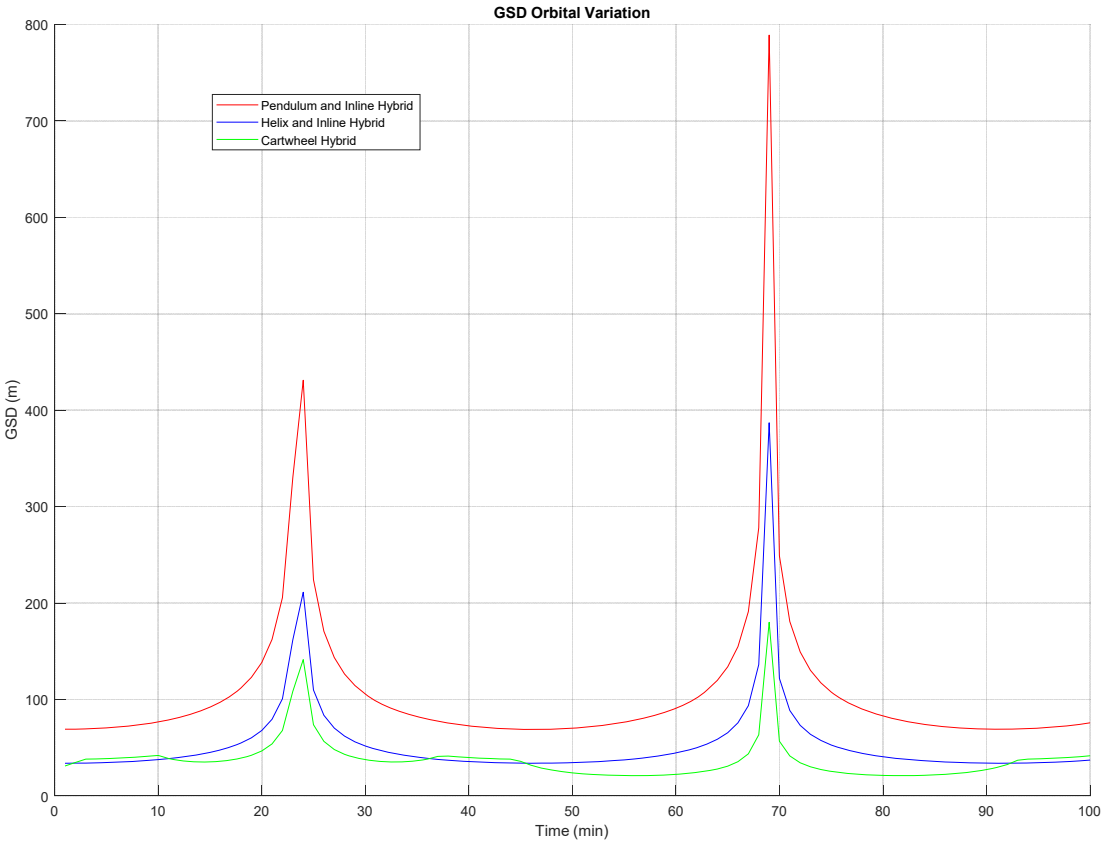

Figure 68. Resolution Variations Combined. Adapted from: [28].

THIS PAGE INTENTIONALLY LEFT BLANK

V. CONCLUSION

A. RECAP

Synthetic aperture radar is an imaging system that does not require imaging to take place in sunlight therefore offers more flexibility than visible light imaging. Small satellites are becoming very common in space and will probably become even more prevalent in the future. In large part this is due to the far lower expense of launching small satellites as a secondary payload. Swarm concepts are still theoretical at this time but there are multiple institutions working on the concept as discussed in Chapter II. This research demonstrates that a stable swarm has the possibility of conducting the same type of SAR mission that a larger and more expensive satellite does by using sparse aperture concepts of a small satellite swarm.

B. FINDINGS

The primary research question answered is: "What is the most effective and efficient formation for a small satellite swarm to support a sparse aperture radar mission with regards to collision avoidance for future NPS satellite operations?" The most effective formation tested in this thesis is the cartwheel hybrid formation using a modified center of formation flight plan. The most efficient formation tested in this thesis with regards to collision avoidance is the helix and inline hybrid formation using a modified COF flight plan. The offsetting and constant alternating motion of all but the Lead satellite provides a continuous near circular sparse aperture that contracts into a line over the poles later than the pendulum and inline hybrid over the poles.

The acceptable balance between effective and efficient can be summed up as achieving a stable dispersion pattern for the satellites to conduct their SAR mission while maintaining safe flight operations. All three formations featured in this thesis provide good satellite dispersal patterns, high levels of stability, and some level of flight path de-confliction. The helix hybrid and cartwheel hybrid provide the best flight path de-confliction. Both also provide very good dispersal patterns for the sparse aperture radar operations as well. The helix hybrid edges the cartwheel hybrid in flight safety but

cartwheel hybrid has considerable improvements over the helix hybrid in regards to conducting the sparse aperture radar mission.

The variables and assumptions we used have firmly scoped the parameters of this research. By assuming the most likely orbit, altitude, and inclination available, we are able to minimize the amount of orbital variations to several dozen rather than several hundred. Station keeping considerations are required to conduct flight operations at very close ranges. Varying orbital parameters ensure additional flight safety measures.

One item that we were not able to explore more fully was an answer to the question: "How long can a small satellite swarm remain stable in each chosen formation before major station keeping operations are required to avoid a collision?" Atmospheric drag and gravitational factors will eventually force station keeping requirements to maintain stability of the swarm. Over time these factors can overwhelm the reaction wheels or require more thrust than what ion thrusters provide, causing the need to use the larger hydrazine type of engines.

C. PROPOSED CONCEPTS FOR FUTURE CONSIDERATION

There were a few concepts not explored during the research, modeling, and analysis of this thesis that are worth mentioning. By bringing these concepts to light, perhaps it will spark thought and ideas for follow on work.

1. Pendulum and Inline Hybrid

The pendulum and inline hybrid formation using a modified center of formation flight is viable as it is stable but not as stable as helix and inline hybrid formation as indicated by the MATLAB analysis. Additionally, the redundant safety measure of offsetting the flight paths using the altitudes of the inline formation, Sat3, and Sat4 over the poles does not exist in a pendulum formation.

A recommended concept of operations for the pendulum and inline hybrid formation using a modified COF leader spacecraft to consider is the idea of a complex lead satellite and less sophisticated follower. Due to the nature of the formation, all spacecraft will require ion thrusters and main (hydrazine) thrusters to conduct station keeping. The

inline Lead, Sat1, and Sat2 should maintain relatively equal spacing using the ion thrusters for months before major station keeping will require boosting their altitude. However, consideration should be made to ensure additional fuel for Sat3 and Sat4.

For telemetry, tracking, and command (TT&C), the lead satellite can conduct all communications with the ground station and act as a relay to the rest of the swarm. A robust cross link system will require both TT&C and imaging data to be passed back and forth between the Lead and follower satellites.

2. Helix and Inline Hybrid

The helix and inline hybrid formation using a modified COF flight plan provides the safest approach and minimal complexity. The inline formation of the Lead, Sat1, and Sat2 spacecraft are very easy to maintain and any deviations can be identified and corrected immediately at any time during the swarm orbit. The apogee and perigee offsets at the poles for Sat3 and Sat4 provides a built in redundant safety measure using orbital mechanics. The flight paths for the inline formation, Sat3, and Sat4 do not cross at any point during their orbit. The helix and inline hybrid formation also provides dispersal of the satellites for sparse aperture imaging at nearly all latitudes except the poles.

A proposed CONOP for the helix and inline hybrid formation using a modified COF leader spacecraft should mirror that of the pendulum and inline hybrid formation for the leader and follower concept. If there is any consideration for a tether between satellites, this is the formation to apply it. A tether can be run from the Lead to Sat1 and from the Lead to Sat2 because they remain in line through their entire orbit. Sat3 and Sat4 do not cross flight paths with the in line satellites avoiding a conjunction with the tether. Using a tether can allow the inline satellites to transfer data without a crosslink and perhaps even share power. Sat3 and Sat4 will still require additional fuel considerations and crosslinks with the Lead for data transfers.

3. Cartwheel Hybrid

The cartwheel hybrid formation using a modified COF flight is a close second choice to the helix and inline hybrid formation. However, the simplicity of a three satellite

inline formation is lost with the cartwheel hybrid formation. When compared to a complex, high speed satellite formation, the simplicity of the Lead satellite, Sat1, and Sat2 is substantially more stable. The cartwheel hybrid formation does ensure that all five satellites do not cross flight paths at the poles and acts as interlocking orbits without flying into the same space at any time.

The cartwheel hybrid formation is the most interesting but also the most complex. The best thing about this formation is the near endless variations of the orbits by altering the orbital mechanics. The leader and follower satellite concept remains applicable however, this is a formation to insert different variations to satellite configurations. Variations can be so divergent as to have five individually different missions conducted from a single swarm.

D. FUTURE WORK AND APPLICATION

Future work to be done includes payload, bus, ground operations, and launch opportunities. The payload that NPS is most interested in is the sparse aperture radar. The sparse aperture concept can include a single emitter of the microwaves from the Lead spacecraft and be received by all satellites in the swarm. The physics involved in a SAR radar can be rather complicated and may be broken down into multiple research projects.

Much work needs to be performed in regards to the equations for sparse aperture radar as discussed by references 7, 10, and 11. When referencing the Rayleigh's criterion where θr is the resolution, λ is the wavelength, a is the aperture diameter, and R is the range between emitter and target [24]. Primarily, the constant of 1.22 defines the intensity of diffracted light for a visible spectrum aperture and not a radar aperture. For radar there does not appear to be such a constant. Rather, complex calculations need to be made constantly as the swarm aperture changes shape [7, 10]. Additionally, a needs to be replaced by the effective diameter of the aperture. The effective diameter calculations will require a very complex examination of differing methods and use of many types of array structures [10].

Another area for future work is in the design of a sustainable bus. If the Lead satellite can be designed to handle the more complicated and expensive aspects of a SAR mission, the follower satellites may be mass produced and the population of the swarm can

be increased. Station keeping will be key to conducting a swarm operation. Research on crosslinks and propulsive maneuvering is perhaps the most vital part of the swarm concept.

Ground station infrastructure requires the following considerations:

- How will the ground station upload commands and how much automation will there be?
- Finally, how will the swarm get into orbit? What launch opportunities are going to be available?
- Will the swarm be launched all at once or will it have to be populated over time?

Using this research, the Space Systems Academic Group and the Small Satellite Laboratory at the Naval Postgraduate School can begin to develop a small satellite swarm to conduct a SAR mission. By focusing solely on the flight operations in this thesis, there are unlimited opportunities to advance the NPS small satellite swarm concept.

THIS PAGE INTENTIONALLY LEFT BLANK

APPENDIX A: MATLAB SCRIPT FOR PENDULUM HYBRID

```
% 2018-05-22 Swarm relative motion visualizer
%
% adapt for determining resolution of SAR swarm

clear
clc
close all       % close old figures
format compact

%load('prime.mat')
load('PIH_v5_IPV')

% Dr. Newman's example for distances to Lead satellite, not used
% MF = sqrt( (xkm-xkm1).^2 + (ykm-ykm1).^2 + (zkm-zkm1).^2 );  % Front
% MB = sqrt( (xkm-xkm2).^2 + (ykm-ykm2).^2 + (zkm-zkm2).^2 );  % Back
% ML = sqrt( (xkm-xkm3).^2 + (ykm-ykm3).^2 + (zkm-zkm3).^2 );  % Left
% MR = sqrt( (xkm-xkm4).^2 + (ykm-ykm4).^2 + (zkm-zkm4).^2 );  % Right

r1 = cat(2,xkm,ykm,zkm);                % Lead
r2 = cat(2,xkm1,ykm1,zkm1);             % Sat1
r3 = cat(2,xkm2,ykm2,zkm2);             % Sat2
r4 = cat(2,xkm3,ykm3,zkm3);             % Sat3
r5 = cat(2,xkm4,ykm4,zkm4);             % Sat4

v1 = cat(2,vxkmsec,vykmsec,vzkmsec);    % Velocity Lead
v2 = cat(2,vxkmsec1,vykmsec1,vzkmsec1); % Velocity Sat1
v3 = cat(2,vxkmsec2,vykmsec2,vzkmsec2); % Velocity Sat2
v4 = cat(2,vxkmsec3,vykmsec3,vzkmsec3); % Velocity Sat3
v5 = cat(2,vxkmsec4,vykmsec4,vzkmsec4); % Velocity Sat4

r21 = r2 - r1;                          % Lead -> Sat1
r31 = r3 - r1;                          % Lead -> Sat2
r41 = r4 - r1;                          % Lead -> Sat3
r51 = r5 - r1;                          % Lead -> Sat4

len = length(xkm);                      % Number of data points (1/min)

% determine the r_rel_in_plane and the r_rel_out_of_plane and plot
for i = 1:len
    % Lead sat, computes unit vectors for formation directions of
flight
    % Establishes coordinate frame
    h1(i,:) = cross(r1(i,:),v1(i,:));               % Angular momentum
vector
    h1_hat(i,:) = h1(i,:) / norm(h1(i,:));          % Unit angular
momentum vector (normal to the orbital plane)
    v1_hat(i,:) = v1(i,:) / norm(v1(i,:));          % Unit velocity
vector (in orbital plane)
    r1_hat(i,:) = r1(i,:) / norm(r1(i,:));          % Unit position
vector (in orbital plane)
```

```
    % Lead to Sat1
    r21_ip(i)  = dot(r21(i,:),v1_hat(i,:));         % Sat1 in-plane
distance
    r21_oop(i) = dot(r21(i,:),h1_hat(i,:));         % Sat1 out-of-plane
distance
    r21_r(i)   = dot(r21(i,:),r1_hat(i,:));         % Sat1 radial
(nadir) distance

    % Lead to Sat2
    r31_ip(i)  = dot(r31(i,:),v1_hat(i,:));         % Sat2 in-plane
distance
    r31_oop(i) = dot(r31(i,:),h1_hat(i,:));         % Sat2 out-of-plane
distance
    r31_r(i)   = dot(r31(i,:),r1_hat(i,:));         % Sat2 radial
(nadir) distance

    % Lead to Sat3
    r41_ip(i)  = dot(r41(i,:),v1_hat(i,:));         % Sat3 in-plane
distance
    r41_oop(i) = dot(r41(i,:),h1_hat(i,:));         % Sat3 out-of-plane
distance
    r41_r(i)   = dot(r41(i,:),r1_hat(i,:));         % Sat3 radial
(nadir) distance

    % Lead to Sat4
    r51_ip(i)  = dot(r51(i,:),v1_hat(i,:));         % Sat4 in-plane
distance
    r51_oop(i) = dot(r51(i,:),h1_hat(i,:));         % Sat4 out-of-plane
distance
    r51_r(i)   = dot(r51(i,:),r1_hat(i,:));         % Sat4 radial
(nadir) distance

end

% Plot two-dimensional swarm relative motion
f1=figure;
hold on
grid on
xlabel('Out-of-plane (km)')
ylabel('In-plane (km)')
title('Swarm relative motion')
plot(0,0,'-o','MarkerFaceColor','k','MarkerEdgeColor','k')  % Plot Lead
sat

for i = 1:len
    plot(r21_oop(i),r21_ip(i),'-
o','MarkerFaceColor','b','MarkerEdgeColor','b')   % Sat1
    plot(r31_oop(i),r31_ip(i),'-
o','MarkerFaceColor','r','MarkerEdgeColor','r')   % Sat2
    plot(r41_oop(i),r41_ip(i),'-
o','MarkerFaceColor','c','MarkerEdgeColor','c')   % Sat3
    plot(r51_oop(i),r51_ip(i),'-
o','MarkerFaceColor','g','MarkerEdgeColor','g')   % Sat4
```

```
    pause(.01)          % slows down plotting to "animate" the
simulation
end

% Plot three-dimensional swarm relative motion
f2=figure;
hold on
grid on
xlabel('Out-of-plane (km)')
ylabel('In-plane (km)')
zlabel('Radial (km)')
title('Swarm relative motion')
plot3(0,0,0,'-o','MarkerFaceColor','k','MarkerEdgeColor','k')  % Plot
Lead sat

% Using plot3 instead of plot to make third dimension
for i = 1:len
    plot3(r21_oop(i),r21_ip(i),r21_r(i),'-
o','MarkerFaceColor','b','MarkerEdgeColor','b')    % Sat1
    plot3(r31_oop(i),r31_ip(i),r31_r(i),'-
o','MarkerFaceColor','r','MarkerEdgeColor','r')    % Sat2
    plot3(r41_oop(i),r41_ip(i),r41_r(i),'-
o','MarkerFaceColor','c','MarkerEdgeColor','c')    % Sat3
    plot3(r51_oop(i),r51_ip(i),r51_r(i),'-
o','MarkerFaceColor','g','MarkerEdgeColor','g')    % Sat4
    pause(.01)                  % slows down plotting to "animate" the
simulation
end


%% Distances across aperture for resolution calculation
% Calculate area of spare aperture with respect to nadir
% Compute effective aperture diameter for resolution calculation

% Find area of parallelogram.  Base is in-plane distance between Sat1
and
% Sat2.  Height is out-of-plane distance of Sat3 and Sat4 (should be
equal)
% Convert from km to meters
for i = 1:len
    height(i) = 1000*(abs(r41_oop(i)) + abs(r51_oop(i))./2;
    base(i) = 1000*(abs(r21_ip(i)) + abs(r31_ip(i)));
    area(i) = base(i)*height(i);
    effective_diameter(i) = sqrt(area(i)*4/pi);  % A = (pi/4) * D^2,
solve for D, in meters
end

lambda = 0.0086;                                        % wavelegnth
meters
altitude = 300000;                                      % meters
theta = 1.22.*(lambda./effective_diameter).*altitude;     % units of
meters

f3=figure;
```

```
hold on
grid on
xlabel('Time (min)')
ylabel('GSD (m)')
title('GSD Orbital Variation')
plot(TimeUTCG, GSD)
hold off
% f2=figure;
% plot(TimeUTCG,MB,TimeUTCG,MR)
% f3=figure;
% hold on
%
% for i = 1:len
%     plot(xkm(i),ykm(i),'-o',xkm1(i),ykm1(i),'-o',xkm2(i),ykm2(i),'-
o',xkm3(i),ykm3(i),'-o',xkm4(i),ykm4(i),'-o')
% end

% f4=figure;
% plot3(r21(:,1), r21(:,2), r21(:,3))
```

APPENDIX B: MATLAB SCRIPT FOR HELIX HYBRID

```
% 2018-05-22 Swarm relative motion visualizer
%
% adapt for determining resolution of SAR swarm

clear
clc
close all       % close old figures
format compact

%load('prime.mat')
load('HIH_v3_IPV')

% Dr. Newman's example for distances to Lead satellite, not used
% MF = sqrt( (xkm-xkm1).^2 + (ykm-ykm1).^2 + (zkm-zkm1).^2 );  % Front
% MB = sqrt( (xkm-xkm2).^2 + (ykm-ykm2).^2 + (zkm-zkm2).^2 );  % Back
% ML = sqrt( (xkm-xkm3).^2 + (ykm-ykm3).^2 + (zkm-zkm3).^2 );  % Left
% MR = sqrt( (xkm-xkm4).^2 + (ykm-ykm4).^2 + (zkm-zkm4).^2 );  % Right

r1 = cat(2,xkm,ykm,zkm);                % Lead
r2 = cat(2,xkm1,ykm1,zkm1);             % Sat1
r3 = cat(2,xkm2,ykm2,zkm2);             % Sat2
r4 = cat(2,xkm3,ykm3,zkm3);             % Sat3
r5 = cat(2,xkm4,ykm4,zkm4);             % Sat4

v1 = cat(2,vxkmsec,vykmsec,vzkmsec);    % Velocity Lead
v2 = cat(2,vxkmsec1,vykmsec1,vzkmsec1); % Velocity Sat1
v3 = cat(2,vxkmsec2,vykmsec2,vzkmsec2); % Velocity Sat2
v4 = cat(2,vxkmsec3,vykmsec3,vzkmsec3); % Velocity Sat3
v5 = cat(2,vxkmsec4,vykmsec4,vzkmsec4); % Velocity Sat4

r21 = r2 - r1;                          % Lead -> Sat1
r31 = r3 - r1;                          % Lead -> Sat2
r41 = r4 - r1;                          % Lead -> Sat3
r51 = r5 - r1;                          % Lead -> Sat4

len = length(xkm);                      % Number of data points (1/min)

% determine the r_rel_in_plane and the r_rel_out_of_plane and plot
for i = 1:len
    % Lead sat, computes unit vectors for formation directions of
flight
    % Establishes coordinate frame
    h1(i,:) = cross(r1(i,:),v1(i,:));               % Angular momentum
vector
    h1_hat(i,:) = h1(i,:) / norm(h1(i,:));          % Unit angular
momentum vector (normal to the orbital plane)
    v1_hat(i,:) = v1(i,:) / norm(v1(i,:));          % Unit velocity
vector (in orbital plane)
    r1_hat(i,:) = r1(i,:) / norm(r1(i,:));          % Unit position
vector (in orbital plane)
```

```
    % Lead to Sat1
    r21_ip(i)  = dot(r21(i,:),v1_hat(i,:));         % Sat1 in-plane
distance
    r21_oop(i) = dot(r21(i,:),h1_hat(i,:));         % Sat1 out-of-plane
distance
    r21_r(i)   = dot(r21(i,:),r1_hat(i,:));         % Sat1 radial
(nadir) distance

    % Lead to Sat2
    r31_ip(i)  = dot(r31(i,:),v1_hat(i,:));         % Sat2 in-plane
distance
    r31_oop(i) = dot(r31(i,:),h1_hat(i,:));         % Sat2 out-of-plane
distance
    r31_r(i)   = dot(r31(i,:),r1_hat(i,:));         % Sat2 radial
(nadir) distance

    % Lead to Sat3
    r41_ip(i)  = dot(r41(i,:),v1_hat(i,:));         % Sat3 in-plane
distance
    r41_oop(i) = dot(r41(i,:),h1_hat(i,:));         % Sat3 out-of-plane
distance
    r41_r(i)   = dot(r41(i,:),r1_hat(i,:));         % Sat3 radial
(nadir) distance

    % Lead to Sat4
    r51_ip(i)  = dot(r51(i,:),v1_hat(i,:));         % Sat4 in-plane
distance
    r51_oop(i) = dot(r51(i,:),h1_hat(i,:));         % Sat4 out-of-plane
distance
    r51_r(i)   = dot(r51(i,:),r1_hat(i,:));         % Sat4 radial
(nadir) distance

end

% Plot two-dimensional swarm relative motion
f1=figure;
hold on
grid on
xlabel('Out-of-plane (km)')
ylabel('In-plane (km)')
title('Swarm relative motion')
plot(0,0,'-o','MarkerFaceColor','k','MarkerEdgeColor','k')  % Plot Lead
sat

for i = 1:len
    plot(r21_oop(i),r21_ip(i),'-
o','MarkerFaceColor','b','MarkerEdgeColor','b')   % Sat1
    plot(r31_oop(i),r31_ip(i),'-
o','MarkerFaceColor','r','MarkerEdgeColor','r')   % Sat2
    plot(r41_oop(i),r41_ip(i),'-
o','MarkerFaceColor','c','MarkerEdgeColor','c')   % Sat3
    plot(r51_oop(i),r51_ip(i),'-
o','MarkerFaceColor','g','MarkerEdgeColor','g')   % Sat4
```

```
    pause(.01)          % slows down plotting to "animate" the
simulation
end

% Plot three-dimensional swarm relative motion
f2=figure;
hold on
grid on
xlabel('Out-of-plane (km)')
ylabel('In-plane (km)')
zlabel('Radial (km)')
title('Swarm relative motion')
plot3(0,0,0,'-o','MarkerFaceColor','k','MarkerEdgeColor','k')  % Plot
Lead sat

% Using plot3 instead of plot to make third dimension
for i = 1:len
    plot3(r21_oop(i),r21_ip(i),r21_r(i),'-
o','MarkerFaceColor','b','MarkerEdgeColor','b')    % Sat1
    plot3(r31_oop(i),r31_ip(i),r31_r(i),'-
o','MarkerFaceColor','r','MarkerEdgeColor','r')    % Sat2
    plot3(r41_oop(i),r41_ip(i),r41_r(i),'-
o','MarkerFaceColor','c','MarkerEdgeColor','c')    % Sat3
    plot3(r51_oop(i),r51_ip(i),r51_r(i),'-
o','MarkerFaceColor','g','MarkerEdgeColor','g')    % Sat4
    pause(.01)                  % slows down plotting to "animate" the
simulation
end


%% Distances across aperture for resolution calculation
% Calculate area of spare aperture with respect to nadir
% Compute effective aperture diameter for resolution calculation

% Find area of parallelogram.  Base is in-plane distance between Sat1
and
% Sat2.  Height is out-of-plane distance of Sat3 and Sat4 (should be
equal)
% Convert from km to meters
for i = 1:len
    height(i) = 1000*(abs(r41_oop(i)) + abs(r51_oop(i))./2;
    base(i) = 1000*(abs(r21_ip(i)) + abs(r31_ip(i)));
    area(i) = base(i)*height(i);
    effective_diameter(i) = sqrt(area(i)*4/pi);  % A = (pi/4) * D^2,
solve for D, in meters
end

lambda = 0.0086;                                        % wavelegnth
meters
altitude = 300000;                                      % meters
theta = 1.22.*(lambda./effective_diameter).*altitude;     % units of
meters

f3=figure;
```

```
hold on
grid on
xlabel('Time (min)')
ylabel('GSD (m)')
title('GSD Orbital Variation')
plot(TimeUTCG, GSD)
hold off
% f2=figure;
% plot(TimeUTCG,MB,TimeUTCG,MR)
% f3=figure;
% hold on
%
% for i = 1:len
%     plot(xkm(i),ykm(i),'-o',xkm1(i),ykm1(i),'-o',xkm2(i),ykm2(i),'-
o',xkm3(i),ykm3(i),'-o',xkm4(i),ykm4(i),'-o')
% end

% f4=figure;
% plot3(r21(:,1), r21(:,2), r21(:,3))
```

APPENDIX C: MATLAB SCRIPT FOR CARTWHEEL HYBRID

```
% 2018-05-22 Swarm relative motion visualizer
%
% adapt for determining resolution of SAR swarm

clear
clc
close all       % close old figures
format compact

%load('prime.mat')
load('CH_v9_IPV.mat')

% Dr. Newman's example for distances to Lead satellite, not used
% MF = sqrt( (xkm-xkm1).^2 + (ykm-ykm1).^2 + (zkm-zkm1).^2 );  % Front
% MB = sqrt( (xkm-xkm2).^2 + (ykm-ykm2).^2 + (zkm-zkm2).^2 );  % Back
% ML = sqrt( (xkm-xkm3).^2 + (ykm-ykm3).^2 + (zkm-zkm3).^2 );  % Left
% MR = sqrt( (xkm-xkm4).^2 + (ykm-ykm4).^2 + (zkm-zkm4).^2 );  % Right

r1 = cat(2,xkm,ykm,zkm);                % Lead
r2 = cat(2,xkm1,ykm1,zkm1);             % Sat1
r3 = cat(2,xkm2,ykm2,zkm2);             % Sat2
r4 = cat(2,xkm3,ykm3,zkm3);             % Sat3
r5 = cat(2,xkm4,ykm4,zkm4);             % Sat4

v1 = cat(2,vxkmsec,vykmsec,vzkmsec);    % Velocity Lead
v2 = cat(2,vxkmsec1,vykmsec1,vzkmsec1); % Velocity Sat1
v3 = cat(2,vxkmsec2,vykmsec2,vzkmsec2); % Velocity Sat2
v4 = cat(2,vxkmsec3,vykmsec3,vzkmsec3); % Velocity Sat3
v5 = cat(2,vxkmsec4,vykmsec4,vzkmsec4); % Velocity Sat4

r21 = r2 - r1;                          % Lead -> Sat1
r31 = r3 - r1;                          % Lead -> Sat2
r41 = r4 - r1;                          % Lead -> Sat3
r51 = r5 - r1;                          % Lead -> Sat4

len = length(xkm);                      % Number of data points (1/min)

% determine the r_rel_in_plane and the r_rel_out_of_plane and plot
for i = 1:len
    % Lead sat, computes unit vectors for formation directions of
flight
    % Establishes coordinate frame
    h1(i,:) = cross(r1(i,:),v1(i,:));               % Angular momentum
vector
    h1_hat(i,:) = h1(i,:) / norm(h1(i,:));          % Unit angular
momentum vector (normal to the orbital plane)
    v1_hat(i,:) = v1(i,:) / norm(v1(i,:));          % Unit velocity
vector (in orbital plane)
    r1_hat(i,:) = r1(i,:) / norm(r1(i,:));          % Unit position
vector (in orbital plane)
```

```
    % Lead to Sat1
    r21_ip(i)  = dot(r21(i,:),v1_hat(i,:));         % Sat1 in-plane
distance
    r21_oop(i) = dot(r21(i,:),h1_hat(i,:));         % Sat1 out-of-plane
distance
    r21_r(i)   = dot(r21(i,:),r1_hat(i,:));         % Sat1 radial
(nadir) distance

    % Lead to Sat2
    r31_ip(i)  = dot(r31(i,:),v1_hat(i,:));         % Sat2 in-plane
distance
    r31_oop(i) = dot(r31(i,:),h1_hat(i,:));         % Sat2 out-of-plane
distance
    r31_r(i)   = dot(r31(i,:),r1_hat(i,:));         % Sat2 radial
(nadir) distance

    % Lead to Sat3
    r41_ip(i)  = dot(r41(i,:),v1_hat(i,:));         % Sat3 in-plane
distance
    r41_oop(i) = dot(r41(i,:),h1_hat(i,:));         % Sat3 out-of-plane
distance
    r41_r(i)   = dot(r41(i,:),r1_hat(i,:));         % Sat3 radial
(nadir) distance

    % Lead to Sat4
    r51_ip(i)  = dot(r51(i,:),v1_hat(i,:));         % Sat4 in-plane
distance
    r51_oop(i) = dot(r51(i,:),h1_hat(i,:));         % Sat4 out-of-plane
distance
    r51_r(i)   = dot(r51(i,:),r1_hat(i,:));         % Sat4 radial
(nadir) distance

end

% Plot two-dimensional swarm relative motion
f1=figure;
hold on
grid on
xlabel('Out-of-plane (km)')
ylabel('In-plane (km)')
title('Swarm relative motion')
plot(0,0,'-o','MarkerFaceColor','k','MarkerEdgeColor','k')  % Plot Lead
sat

for i = 1:len
    plot(r21_oop(i),r21_ip(i),'-
o','MarkerFaceColor','b','MarkerEdgeColor','b')   % Sat1
    plot(r31_oop(i),r31_ip(i),'-
o','MarkerFaceColor','r','MarkerEdgeColor','r')   % Sat2
    plot(r41_oop(i),r41_ip(i),'-
o','MarkerFaceColor','c','MarkerEdgeColor','c')   % Sat3
    plot(r51_oop(i),r51_ip(i),'-
o','MarkerFaceColor','g','MarkerEdgeColor','g')   % Sat4
```

```
    pause(.01)          % slows down plotting to "animate" the
simulation
end

% Plot three-dimensional swarm relative motion
f2=figure;
hold on
grid on
xlabel('Out-of-plane (km)')
ylabel('In-plane (km)')
zlabel('Radial (km)')
title('Swarm relative motion')
plot3(0,0,0,'-o','MarkerFaceColor','k','MarkerEdgeColor','k')  % Plot
Lead sat

% Using plot3 instead of plot to make third dimension
for i = 1:len
    plot3(r21_oop(i),r21_ip(i),r21_r(i),'-
o','MarkerFaceColor','b','MarkerEdgeColor','b')    % Sat1
    plot3(r31_oop(i),r31_ip(i),r31_r(i),'-
o','MarkerFaceColor','r','MarkerEdgeColor','r')    % Sat2
    plot3(r41_oop(i),r41_ip(i),r41_r(i),'-
o','MarkerFaceColor','c','MarkerEdgeColor','c')    % Sat3
    plot3(r51_oop(i),r51_ip(i),r51_r(i),'-
o','MarkerFaceColor','g','MarkerEdgeColor','g')    % Sat4
    pause(.01)                  % slows down plotting to "animate" the
simulation
end

%% Distances across aperture for resolution calculation
% Calculate area of spare aperture with respect to nadir
% Compute effective aperture diameter for resolution calculation

% Find area of parallelogram.  Base is in-plane distance between Sat1
and
% Sat2.  Height is out-of-plane distance of Sat3 and Sat4 (should be
equal)
% Convert from km to meters
for i = 1:len

%     Commented equations generate same result as below
%     height(i) = 1000*((abs(r31_oop(i)) + abs(r51_oop(i))) +
(abs(r41_oop(i)) + abs(r21_oop(i)))./2;
%     base(i) = 1000*((abs(r31_ip(i)) + abs(r41_ip(i))) +
(abs(r51_ip(i)) + abs(r21_ip(i)))./2;
%     area(i) = base(i)*height(i);

%   Single expression, computes areas of two smaller parallelograms and
adds them together.
    area(i) = 1000^2*(abs(r31_oop(i))*(abs(r31_ip(i)) + abs(r41_ip(i)))
+ abs(r51_oop(i))*(abs(r51_ip(i)) + abs(r21_ip(i))); % in meters^2
    effective_diameter(i) = sqrt(area(i)*4/pi);  % A = (pi/4) * D^2,
solve for D, in meters
end
```

```
lambda = 0.0086;                                                % wavelegnth
meters
altitude = 300000;                                              % meters
theta = 1.22.*(lambda./effective_diameter).*altitude;     % units of
meters

f3=figure;
hold on
grid on
xlabel('Time (min)')
ylabel('GSD (m)')
title('GSD Orbital Variation')
plot(TimeUTCG, GSD)
hold off
% f2=figure;
% plot(TimeUTCG,MB,TimeUTCG,MR)
% f3=figure;
% hold on
%
% for i = 1:len
%     plot(xkm(i),ykm(i),'-o',xkm1(i),ykm1(i),'-o',xkm2(i),ykm2(i),'-
o',xkm3(i),ykm3(i),'-o',xkm4(i),ykm4(i),'-o')
% end

% f4=figure;
% plot3(r21(:,1), r21(:,2), r21(:,3))
```

LIST OF REFERENCES

[1] F. Paul, "Theory of Synthetic Aperture Radar." *Atlantis Scientific* (1997).

[2] "New Kids on the Block: How New Start-Up Space Companies Have Influenced the U.S. Supply Chain" Bryce Space and technology, June 2017. [Online]. Accessed March 16, 2018. Available: https://www.nasa.gov/sites/default/files/atoms/files/start_up_space_supply_chain_20170803.pdf

[3] "TerraSAR-X and TanDEM-X Formation Acquires First Bi-static Dataset" Digital Elevation Model of Mount Etna created, Airbus website [Online]. Accessed February 18, 2018 Accessed Available: https://www.intelligence-airbusds.com/en/183-first-bi-static-data-acquired

[4] "Electromagnetic Spectrum," Sapling Learning, McMillan Learning. [Online]. Accessed February 24, 2018 Available: https://sites.google.com/site/chempendix/em-spectrum

[5] R. M. O'Donnell, "Radar Systems Engineering Lecture 18 Synthetic Aperture Radar (SAR)." Slide 28, IEEE New Hampshire Section, 13 February 2016 [Online]. Accessed March 06, 2018 Available: https://www.slideshare.net/Forward2025/radar-2009-a-18-synthetic-aperture-radar

[6] G. Krieger, "Advanced bistatic and multistatic SAR concepts and applications." In European Conference on Synthetic Aperture Radar (EUSAR), pp. 1–101. VDE, 2006.

[7] C. K. Pang, A. Kumar, C. H. Goh, & C. V. Le, "Nano-satellite swarm for SAR applications: Design and robust scheduling." IEEE Transactions on Aerospace and Electronic Systems 51, no. 2 (2015): 853–865.

[8] N. Werth, "Synthetic Aperture Radar Image Formation." PhD diss., Dept. Science, Arizona State University, 2011.

[9] S. Sundey, "Design and Implementation of an Optical Sparse Aperture Testbed for Small Satellite Formation Space-Based Remote Sensing." Naval Postgraduate School, Monterey California, Master's Thesis (2017): Sundey, Sean M. 2017.12_Sundey 2017.12_Sundey.

[10] S. J. Chung, and F. Y. Hadaegh. "Swarms of femtosats for synthetic aperture applications." Cal Tech Library(2011). Accessed February 18, 2018. [Online]. Available: https://authors.library.caltech.edu/74299/

[11] N. J. Miller, M. P. Dierking, and B. D. Duncan. "Optical sparse aperture imaging." Applied Optics 46, no. 23 (2007): 5933–5943.

[12] "What are SmallSats and CubeSats?" National Aviation and Space Agency. [Online]. Accessed February 06, 2018. Available: https://www.nasa.gov/content/what-are-smallsats-and-cubesats

[13] R. Sandau, K. Brieß, and M. D'Errico. "Small satellites for global coverage: Potential and limits." ISPRS Journal of photogrammetry and Remote Sensing 65, no. 6 (2010): 492–504.

[14] J. J. Sellers, W. J. Astore, R. B. Giffen, and W. J. Larson, *Understanding Space: An Introduction to Astronautic*s. Primis, 2000.

[15] G. Templeton, "Geek Answers: What is geostationary orbit, and why is it so important?" Geek.com, December 14, 2013. [Online]. Accessed March 01, 2018. Available: https://www.geek.com/news/geek-answers-what-is-geostationary-orbit-and-why-is-it-so-important-1579225/

[16] "Space Segment," GPS.gov. [Online]. Accessed March 22, 2018. Available: https://www.gps.gov/systems/gps/space/

[17] "Low Earth Orbit (LEO)," NASA.gov [Online]. Accessed March 22, 2018. Available: https://worldwind.arc.nasa.gov/spacebirds/about.html

[18] H. D. Curtis, *Orbital Mechanics for Engineering Students*. Butterworth-Heinemann, 2013.

[19] File: An image describing the semi-major and semi-minor axis of ellipse.svg. (2016, November 17). Wikimedia Commons, the free media repository. Accessed April 22, 2018. [Online]. Available: https://commons.wikimedia.org/w/index.php?title=File:An_image_describing_the_semi-major_and_semi-minor_axis_of_ellipse.svg&oldid=214973865.

[20] "Orbital Eccentricity" Creation Wiki. Accessed May 20, 2018. [Online]. Available: http://creationwiki.org/File:OrbitalEccentricityDemo.png

[21] "Orbital Inclination" Wikipedia. Accessed April 11, 2018. [Online]. Available: https://en.wikipedia.org/wiki/File:Orbit1.svg

[22] E. Maurer, R. Kahle, G. Morfill, B. Schlepp, and S. Zimmermann. "Reversal of TanDEM-X's relative motion from counter-clockwise to clockwise." Accessed March 14, 2018. In *SpaceOps 2014 Conference*, p. 1775. 2014.

[23] B. Elsaka, K. H. Ilk, and A. Alothmani, " Mitigation of Oceanic Tidal Aliasing Errors in Space and Time Simultaneously Using Different Repeat Sub-Satellite Tracks from Pendulum-Type Gravimetric Mission Candidate." Acta Geophysica 63(1):301 - 318 February 2015

[24] Olsen, Richard C., and R. C. Olsen. *Remote Sensing from Air and Space*. 2nd ed. SPIE Press, 2007.

[27] "Engineering Tools" Analytical Graphics, Inc. Accessed April 03, 2018. [Online]. Available: https://www.agi.com/products/engineering-tools

[28] "Products page" MathWorks, Inc. Accessed May 14, 2018. [Online]. https://www.mathworks.com/products/matlab.html

[25] C. Moskowitz, "How Much Junk is in Space?," SPACE.com, May 3, 2010. [Online]. Available: https://www.space.com/8334-junk-space.html

[26] "Electromagnetic Formation Flight (EMFF)," Massachusetts Institute of Technology MIT Space Systems Lab, 2006. [Online]. Accessed March 06, 2018. Available: http://ssl.mit.edu/research/current.html

THIS PAGE INTENTIONALLY LEFT BLANK

INITIAL DISTRIBUTION LIST

1. Defense Technical Information Center
   Ft. Belvoir, Virginia

2. Dudley Knox Library
   Naval Postgraduate School
   Monterey, California